Evaluation and optimisation of RF current-transformer bridges.

By David Knight

A study of the causes of inaccuracy in HF broadband transmission bridges, and a demonstration of the methods that can be used to correct them.

Version 1.01, 10th Feb. 2014.

Please check the author's website to make sure you have the most recent version of this document and the accompanying work files: http://www.g3ynh.info/zdocs/bridges/ .

This article is an updated version of an HTML document that first appeared on the author's website in 2007. Except for minor changes and corrections, the original content and conclusions are unchanged.

Abstract

An impedance monitoring bridge can be characterised by choosing two independent (or nearly independent) circuit parameters related to the magnitude and phase of the load impedance at balance. By adjusting the selected parameters to balance the bridge exactly with a reference load attached, the deviations of the parameters from their target values can be used to compute the bridge error at a given frequency. In a bridge that uses a capacitive potential divider for voltage sampling (Douma's bridge), suitable parameters are the lower voltage-sampling network capacitance and the LF-compensation resistance. The balance point can be located with great precision by using a communications receiver as the detector. Shielding and the use of common-mode chokes in the earth-loop between the signal generator and receiver prevents errors due to spurious signal injection. The optimised system can make relative phase measurements with an RMS uncertainty of about ±0.0075º.

The effect of the series inductance of the lower voltage sampling capacitor is clearly determined by the data. Compensation for this parasitic reactance can be obtained by inserting a small adjustable inductance in series with the upper voltage-sampling arm. Magnitude flatness of around ±0.03% over 5 octaves is possible by this method.

The parallel-equivalent secondary-inductance of the current transformer is a strongly conserved model parameter. The measurement of parallel secondary capacitance is however skewed by through-line mismatch and other parasitic reactances, to the extent that it may appear to be positive, negative, or accidentally zero. A perturbation series is derived to account for the various contributions, and includes a hitherto undocumented effect of Faraday shield displacement current. Control of parasitics is needed if bridges built by different individuals are to give comparable results.

The data show a linear relationship between phase error and frequency except for a small deviation attributable to a dispersion region in the permeability of the ferrite transformer core. This supports the view that the phase error can be considered as a time delay occurring primarily in the transformer.

Various phase compensation schemes are proposed and evaluated. These lead to bridge designs with 2-point frequency tracking that can easily achieve a maximum phase error of better than ±0.2° and a maximum magnitude error of better than ±0.3% over the 1.6 MHz to 30 MHz range. A three-point tracking scheme that gives a maximum phase error of ±0.04° is also demonstrated.

The need for the transformer Faraday shield is investigated. Theory indicates that the effect of the parasitic capacitance from line to detector port is correctable depending on the coupling factor.

An unshielded bridge with 2-point frequency tracking gave a maximum phase error of ±0.05° over the 1.6 MHz to 30 MHz range, close to the ±0.03° limit imposed by dispersion effects in the ferrite used.

Note: Data and mathematical analysis relating to the following discussion is contained in Open Document Spreadsheet (.ods) files. These can be viewed and modified using the Open Office software suite, available without charge from OpenOffice.org.

Table of Contents

1. Bridge parameter perturbation

It is too much to expect that a current-transformer bridge designed using a lumped-element analysis based on simplified component models will give perfect results. Therefore a practical circuit evaluation method is needed, but unfortunately, conventional frequency-response test procedures are not well suited to this task. The problem is that; in order to characterise an imperfect bridge, it is necessary to apply a generator to an input port and then determine the impedance that must be connected to an output port in order to bring the voltage at a detector port to zero. This implies the need for a variable impedance load and an auxiliary bridge or network analyser good enough to resolve small variations, i.e., it seems on first appraisal that bridges cannot be tested without access to extremely accurate test equipment.

There is however, an alternative approach that uses what might reasonably be called a 'perturbation method'. The basic idea here is that, provided that the theoretical model is fairly accurate, it should be possible to make measurements that are related to the extent to which a bridge is out of balance and then use the information to calculate the impedance that must be connected to the load port in order to restore balance.

For a first try at devising a test procedure based on perturbations, we might note that; if a fixed and accurately characterised load (i.e., a UHF coaxial resistor) is connected to the output port, and the degree of imbalance is small; then the actual load required to balance the bridge can be calculated from the phase and magnitude of the error voltage appearing at the detector port. Unfortunately, this requires the use of a sensitive vector voltmeter or a very accurately phase-compensated oscilloscope, and so is neither a low-cost nor a potentially straightforward approach.

There is however a much simpler solution: If a bridge has a minimum of two suitably chosen adjustable components (ideally analogs of R and X or $|\mathbf{Z}|$ and φ), then it can be made to balance exactly at a single frequency when connected to the design load impedance. When the frequency is changed, the bridge, being imperfect, will go out of balance, but the adjustable components can be altered to restore it. If we can measure the changes in the component values, then these perturbations (being hopefully small) can be applied to the circuit model in order to deduce the load-impedance error that would have occurred at the new frequency had the adjustments not been made.

A bridge that uses a potential divider as its voltage-sampling network can be re-balanced; by altering the basic ratio to correct for load-resistance errors, and by adjusting the LF-compensation component to correct for reactance errors. In the case of a bridge with a resistive potential divider, changing the ratio is straightforward; but the LF-compensation component is an inductor, and this presents a serious practical drawback. A significant non-ideality of current-transformers is the propagation-delay or 'self-capacitance' of the secondary winding. At some frequency, the phase-lag due to the delay will cancel the phase-lead due to the secondary inductance. The LF compensation inductance can, in-principle, be adjusted to track the deviation from the 'ideal transformer with secondary inductance' model, but at the phase-crossover (secondary network pseudo-resonance) frequency, the inductance required becomes infinite. Hence, in order to make measurements anywhere near the crossover point, a large variable inductance is required, and to produce such an inductance without introducing further significant non-idealities is all but impossible.

The Douma bridge is a different proposition however. Here the potential divider is a pair of capacitors, and the LF-compensation component is a resistor. Reasonably well-behaved variable capacitors and resistors are realisable, and test-equipment for measuring resistance and capacitance is commonplace. Hence the Douma bridge is the obvious candidate for the perturbation method.

An important aspect of basic experimental design is that of how to find out when the bridge is balanced. The issue here is that the null-point must be located accurately at each measurement frequency in order to minimise the scatter in the data. If a diode detector is used, the null will be difficult to locate because the forward-threshold effect makes such detectors insensitive to small voltages. Running the test with high power levels in an attempt to overcome this limitation will

tend to make the bridge components hot and introduce the problem of thermal drift. The solution is to construct the bridge in such a way that any passive detector can be removed and a radio receiver substituted in its place. A laboratory signal generator or VFO with an output of around 0 dBm (224 mV) can then be used instead of a radio transmitter. In the experiments to be described here, null depths of 80 dB to 120 dB were typical, with the signal at balance falling below the noise floor of a good HF communications receiver (<100 nV).

2. The Douma bridge

Shown below is the circuit of Douma's bridge [**US Pat. No. 2808566**] terminated by its target load resistance R_0. The bridge is balanced when the current analog $\mathbf{V_i}$ is equal in magnitude and phase to the voltage analog $\mathbf{V_v}$, the two voltages being arranged in series opposition. The current transformer is tightly-coupled and is therefore largely described by its turns-ratio N and its secondary inductance L_i. It has a finite insertion impedance $\mathbf{Z_{ii}}$, which causes a voltage-drop $\mathbf{V_{ii}}$ in the path to the primary load. The secondary winding is terminated in a resistance R_i, which serves to damp, but cannot eliminate, the effects of transformer reactance. A component of the transformer output voltage in phase with the primary current is cancelled by choosing an appropriate ratio for the potential-divider capacitors C_1 and C_2. A leading quadrature component in the transformer output, due to the finite secondary inductance, is cancelled by introducing a corresponding quadrature component in the potential-divider output by appropriate choice of the resistor R_v. Also shown is a parasitic capacitance C_i, which notionally represents the transformer propagation-delay and the strays across the secondary winding; but is, as will be shown later, also a composite of the effects of the various parasitic reactances in the system. This capacitance (when positive) produces a lagging quadrature component in the transformer output, which increases in magnitude as the frequency of operation is increased, and will at some point overwhelm the effect of the inductance.

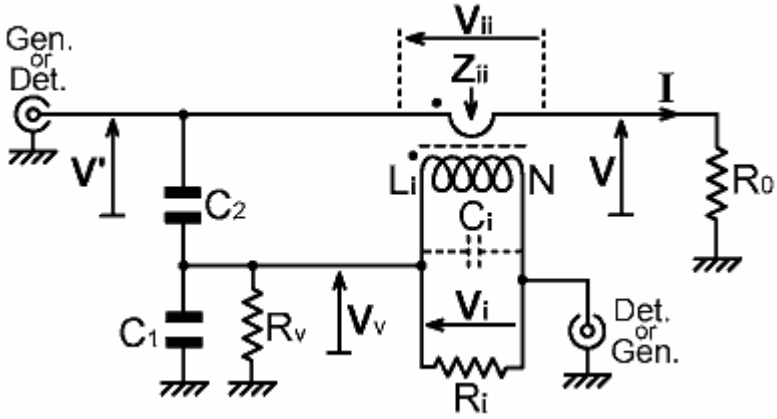

The Douma bridge, as shown, has no means of compensation for the parasitic capacitance C_i, save for the use of a relatively low value of resistance for R_i. Hence the design equations for the bridge have to be derived on the basis that C_i is negligibly small. The procedure is to write dimensionless expressions for the voltage and current analogs and set them to be equal when the bridge is terminated in its target load resistance R_0. The resulting complex expression is then separated into its real and imaginary parts, the real part being the in-phase balance condition, and the imaginary part being the quadrature balance condition. Note that the transformer inefficiency, which can be represented as a resistance[1] (R_k say) in parallel with the secondary winding, has been neglected at this stage of the analysis. The slight shortfall in output can be compensated by a trivial adjustment of the voltage sampling potential-divider ratio, and may be quantified if so desired by replacing R_i with an effective value $R_{ik} = R_i \,//\, R_k$.

The output of the current transformer, by equating primary and secondary ampere-turns, is given by:

$\mathbf{V_i} = \mathbf{I}\,\mathbf{Z_i} / N \quad$ where $\quad \mathbf{Z_i} = (R_i \,//\, \mathbf{j}X_{Li} \,//\, \mathbf{j}X_{Ci})$

1 The input impedance of a tightly-coupled current transformer is too small to allow determination of its leakage inductance in the analysis of this circuit, so the voltage shortfall due to incomplete coupling can also be absorbed into this parameter.

but

$\mathbf{I} = \mathbf{V} / R_0$

hence

$\mathbf{V_i} = \mathbf{V}\, \mathbf{Z_i} / (N\, R_0)$

This gives the dimensionless current transfer function at balance:

$\mathbf{V_i} / \mathbf{V} = \mathbf{Z_i} / (N\, R_\mathbf{0})$

The output of the voltage sampling network is derived as for any potential divider network[2] :

$\mathbf{V_v} = \mathbf{V'}\, (\mathbf{j}X_{C1} \,//\, R_v) / [\, \mathbf{j}X_{C2} + (\mathbf{j}X_{C1} \,//\, R_v)\,]$

and a more convenient form is obtained by multiplying top and bottom of this expression by $\mathbf{j}X_{C2}$:

$\mathbf{V_v} = \mathbf{V'}\, (\mathbf{j}X_{C1} \,//\, \mathbf{j}X_{C2} \,//\, R_v) / \mathbf{j}X_{C2}$

but note that **V'** is not the same as **V**.

$\mathbf{V'} = \mathbf{V} + \mathbf{V_{ii}} = \mathbf{V} + \mathbf{I}\, \mathbf{Z_{ii}} = \mathbf{V} + \mathbf{V}\, \mathbf{Z_{ii}} / R_0 = \mathbf{V}\, (1 + \mathbf{Z_{ii}} / R_0)$

where the insertion impedance $\mathbf{Z_{ii}}$ is the secondary load impedance reflected back into the primary, i.e., it is (to a very good approximation) the secondary load impedance divided by the square of the turns ratio. Hence:

$\mathbf{V'} = \mathbf{V}\, [\, 1 + \mathbf{Z_i} / (R_\mathbf{0}\, N^2)\,]$

and the dimensionless voltage transfer function is:

$\mathbf{V_v} / \mathbf{V} = [\, 1 + \mathbf{Z_i} / (R_0\, N^2)\,]\, (\, \mathbf{j}X_{C1} \,//\, \mathbf{j}X_{C2} \,//\, R_v) / \mathbf{j}X_{C2}$

The overall balance condition is given by equating the voltage and current transfer functions:

$[1 + \mathbf{Z_i} / (R_0\, N^2)\,]\, (\mathbf{j}X_{C1} \,//\, \mathbf{j}X_{C2} \,//\, R_v) / \mathbf{j}X_{C2} = \mathbf{Z_i} / (N\, R_0)$

This can be simplified by dividing both sides by $1 + \mathbf{Z_i} / (R_0\, N^2)$ and inverting the whole expression:

$\mathbf{j}X_{C2} / (\mathbf{j}X_{C1} \,//\, \mathbf{j}X_{C2} \,//\, R_v) = [\, 1 + \mathbf{Z_i} / (R_0\, N^2)\,]\, N\, R_0 / \mathbf{Z_i}$

Multiplying out the right-hand side gives:

$\mathbf{j}X_{C2} / (\mathbf{j}X_{C1} \,//\, \mathbf{j}X_{C2} \,//\, R_v) = (\, N\, R_\mathbf{0} / \mathbf{Z_i}\,) + 1/N$

---

2 See for example: **AC Theory**, by D W Knight (www.g3ynh.info/zdocs/AC_theory/). Section 35.

and noting that $\mathbf{Z_i} = (R_i \,//\, \mathbf{j}X_{Li} \,//\, \mathbf{j}X_{Ci})$:

$\mathbf{j}X_{C2} / (\mathbf{j}X_{C1} \,//\, \mathbf{j}X_{C2} \,//\, R_v) = [\, N\, R_0 / (R_i \,//\, \mathbf{j}X_{Li} \,//\, \mathbf{j}X_{Ci})\,] + 1/N$

This can now be separated into real and imaginary parts by observing that[3]:

$1 / (\mathbf{a} \,//\, \mathbf{b} \,//\, \mathbf{c} \,//\, \ldots) = (1/\mathbf{a}) + (1/\mathbf{b}) + (1/\mathbf{c}) + \ldots$

but before we do that we will combine the transformer reactance into a single quantity, i.e.;

$X_i = X_{Li} \,//\, X_{Ci}$

The reason for so doing is that the circuit has no provision for compensating for the effect of C_i, and so a frequency-independent set of balance conditions can only be obtained insofar as X_i can be treated as a purely inductive reactance (i.e., at low frequencies where $X_{Ci} \rightarrow -\infty$). When X_i is inductive, we can consider it to arise from an inductance L_i' , i.e.:

$X_i = 2\pi f\, L_i'$

and bridge-balance depends on the approximation that L_i' does not vary with frequency. Now the balance identity becomes:

$\mathbf{j}X_{C2} / (\mathbf{j}X_{C1} \,//\, \mathbf{j}X_{C2} \,//\, R_v) = [\, N\, R_0 / (R_i \,//\, \mathbf{j}X_i)\,] + 1/N$

and the reciprocal impedance (admittance) factors separate into arithmetic series:

$\mathbf{j}X_{C2}\,[\,(1/\mathbf{j}X_{C1}) + (1/\mathbf{j}X_{C2}) + (1/R_v)\,] = N\, R_0\,[\,(1/R_i) + (1/\mathbf{j}X_i)\,] + 1/N$

Multiplying out, and noting that $X_C = -1/(2\pi fC)$ gives:

$(C_1/C_2) + 1 + (\mathbf{j}X_{C2} / R_v) = (N\, R_0 / R_i) + (N\, R_0 / \mathbf{j}X_i) + 1/N$

Equating reals:

$(C_1/C_2) + 1 = (N\, R_0 / R_i) + 1/N$

Hence, the in-phase balance condition is:

$C_1 = C_2\,[\,(N\, R_0 / R_i) + (1/N) - 1]$	**2.1**

Equating imaginaries:

$\mathbf{j}X_{C2} / R_v = N\, R_0 / \mathbf{j}X_i$

and noting that capacitive reactance is negative and $1/\mathbf{j} = -\mathbf{j}$:

$-X_{C2} / R_v = N\, R_0 / X_i$

3 See for example, **AC Theory** (already cited) section 17.

Expanding the reactances:

$1 / (2\pi f\, C_2\, R_v) = N\, R_0 / (2\pi f\, L_i')$

which rearranges to give the quadrature balance condition:

$R_v = L_i' / (N\, R_0\, C_2)$	**2.2**

Now notice that both C_1 and R_v depend on the choice of C_2. Consequently, given that N and R_0 are fixed parameters during any test; if C_2 is chosen to be a fixed parameter (ignoring its parasitic inductance for the time being), then C_1 is purely a function of R_i, and R_v is purely a function of L_i'. With C_2 fixed, any adjustments of C_1 and R_v are non-interactive, i.e., data relating to the in-phase and quadrature balance conditions can be separated and analysed independently (at least, to the approximation that C_2 does not change with frequency).

3. Prototype test bridge

On the basis of the preceding discussion, a Douma bridge was constructed in such a way that C_1 and R_v could be both adjusted and measured. The bridge, in its earliest form, is shown in the photograph below. Some important initial considerations were that the transformer Faraday shield should be earthed at the detector socket[4], that the three ports should be reasonably shielded from each other, and that the voltage and current sampling networks should be mounted on opposite sides of a metal bulkhead. Experiments were conducted using a signal generator having an output of about 0 dBm (224 mV), and the detector was a Kenwood TS930s short-wave transceiver used in USB mode (3 kHZ bandwidth, noise floor circa 100 nV) with the AGC set to 'fast' . The basic arrangement proved to be adequate in that the bridge could always be nulled to the point where the detector signal fell below the receiver noise.

In the first version, the resistor R_v was a 500 Ω carbon skeleton potentiometer with a fixed resistor in series; measurement of its value being effected by connecting clip-on probes from a resistance meter across it, with the radio receiver unplugged. The problem of how to measure the capacitance C_1 however, is a little less straightforward. An adjustable capacitance is shown mounted on a plug-in header so that it can be taken away and measured using a laboratory bridge. C_1 however is composed of this capacitance plus strays; and so the plug-in capacitance is designated C_1' . Hence:

$$C_1 = C_1' + C_{1s}$$

C_{1s} is the stray capacitance due to the socket, the wiring, the ceramic insulating pillars, the capacitance of R_v and the capacitance to ground of the Faraday shield. It amounts to several pF and can only be determined by estimation using transformer loss data from other sources[5]. Hence the experiment permits accurate relative measurements of C_1 , but the uncertainty increases somewhat for absolute measurements. This limitation is not serious for the present purpose however, because the measurement of transformer losses is not part of the experimental objective. All capacitors used were either silvered-mica or air-spaced, and had negligible ESR in comparison to external circuit impedances.

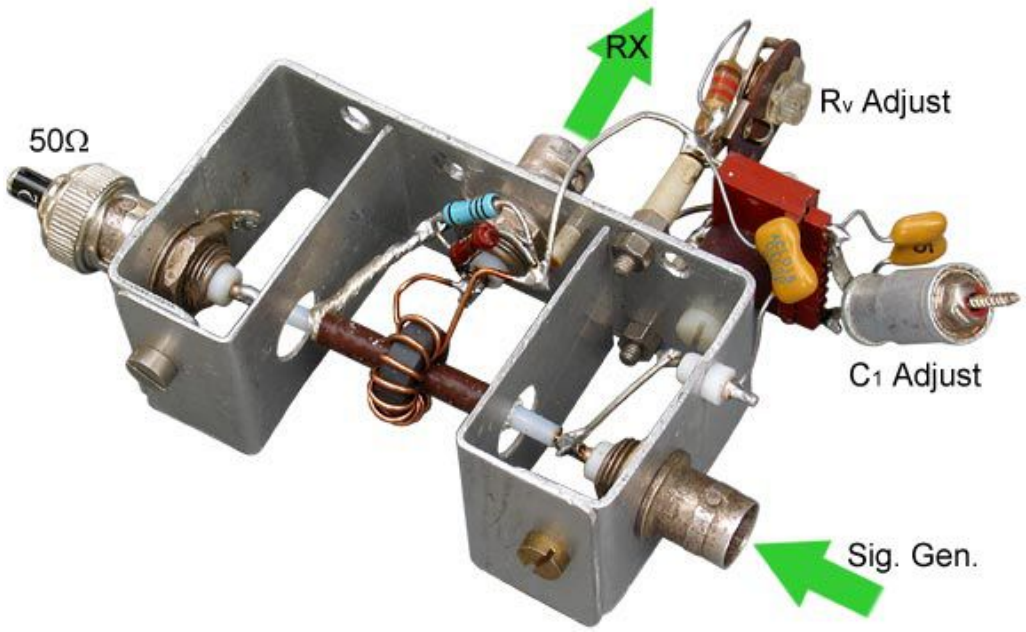

4 See: **Amplitude response of conventional and maximally-flat current transformers**, D W Knight. www.g3ynh.info/zdocs/bridges/appendix/a6-3.html

5 See: **Current transformer efficiency factor**, D W Knight. www.g3ynh.info/zdocs/bridges/appendix/a6-1.html

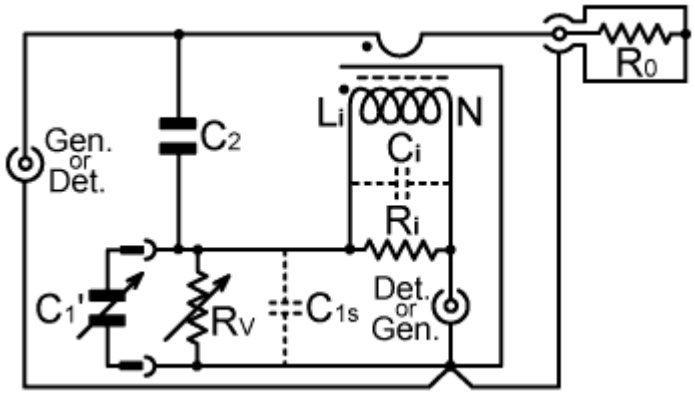

Silver-mica capacitor and
2.5 pF - 30 pF trimmer

To commission the bridge, a current transformer was made using an Amidon FT50-61 ½" ferrite bead (A_L = 68.8 nH/turn² nominal), with 12 turns of 0.9 mm diameter enamelled copper wire for the secondary winding, and a stub of URM108 (Ag-PTFE 50 Ω) cable for the primary. The fixed circuit parameters are listed on the right, where L_{sec} is the measured secondary inductance, expected to be a few % higher than L_i due to leakage inductance and neglect of self-capacitance, but nevertheless providing a first estimate.

N = 12
L_{sec} = 9.25 ±0.23 µH
R_i = 49.80 ±0.06 Ω
R_0 = 49.96 ±0.06 Ω
C_2 = 10.0 ±0.2 pF

Resistances were measured using a Fluke 8060A 4½-digit multimeter. Inductance and capacitance were measured at 1.5915 MHz using a Hatfield LE-300A/1 TRAB[6]. The capacitor C_2 was a silvered-mica type with a nominal tolerance of ±5%, but this was reduced to ±0.2 pF or better by selection of the median sample from a batch of 5.

According to equation **(2.1)**, the expected value for C_1, neglecting transformer losses, is:

$$C_1 = C_2 [(N R_0 / R_i) + (1/N) - 1] = 111.2 \text{ pF}$$

According to equation **(2.2)**, on the basis that L_{sec} is approximately equal to L_i and the secondary capacitance is negligible, an initial estimate for R_v is:

$$R_v = L_{sec} / (N R_0 C_2) = 1543 \ \Omega$$

The first dataset to be acquired is listed and analysed in the spreadsheet **testbrg61-12_1.ods**, measurements being made at points over a range from 1.4 MHz to 15 MHz. The value of R_v required to balance the bridge remained reasonably constant at around 1520 Ω at low frequencies, allowing nulls to be found using a 500 Ω variable in series with a 1.2 kΩ fixed resistor. R_v started to increase rapidly above about 4 MHz however, and at this stage the fixed resistor had to be changed at each new frequency. No resistance measurements were made above 13 MHz because nulls became difficult to locate even with the variable resistor changed to 5 kΩ, and the point at which balance was achieved with R_v disconnected was found to lie somewhere around 14 MHz.

Variation of R_v with frequency is, of course, expected in the event that the parasitic capacitance C_i is finite. C_i adds a lagging component to the transformer output in opposition the leading component associated with the inductance. The result is that the inductance appears to increase with frequency up to the phase crossover point, above which the secondary reactance becomes

6 Manual at http://g3ynh.info/zdocs/bridges/LE300/

capacitive. Allowance for this was made in the initial theoretical considerations, where we allocated the symbol L_i' to the apparent inductance and defined it in the relationship:

$X_i = 2\pi f L_i' = X_{Li} // X_{Ci}$	**3.1**

Experimentally, Li' is obtained from equation **(2.2)** rearranged thus:

$L_i' = N R_0 C_2 R_v$	**3.2**

Spot values of L_i' vs frequency calculated from the experimental data ('observed') are shown below superimposed on a graph obtained by extracting L_i and C_i from a regression analysis ('calculated'). Note that the graph should not be interpreted to mean that the bridge becomes wildly inaccurate as the frequency increases. On the contrary, the phase error due to C_i is only about 3° at 15 MHz, and the graph simply shows that the experiment is very sensitive.

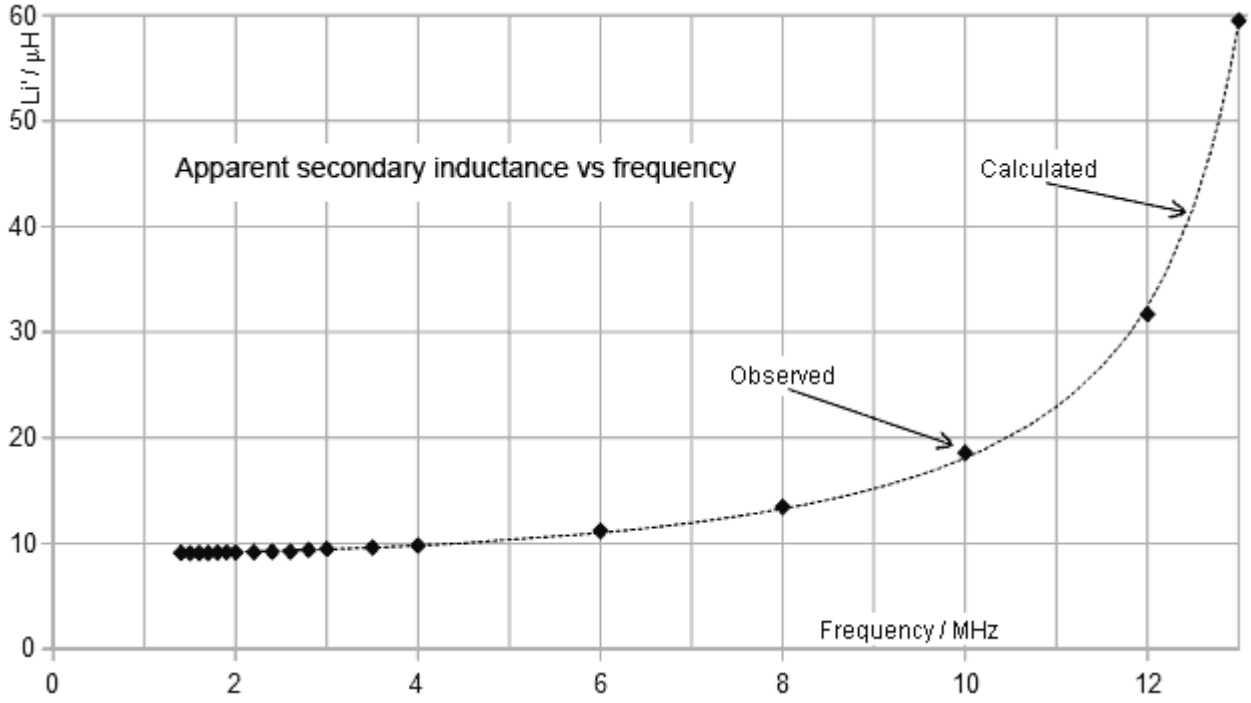

The analysis procedure by which the graph above was produced (see **testbrg61-12_1.ods**) begins with the combination of equations **(3.1)** and **(3.2)**.

$2\pi f \; N R_0 C_2 R_v = X_{Li} // X_{Ci}$

Inverting this expression gives:

$1 / (2\pi f N R_0 C_2 R_v) = [1 / (2\pi f L_i)] - 2\pi f C_i$

Multiplying top and bottom of the right-most term by $2\pi f$ and cancelling through then gives:

$1 / (N R_0 C_2 R_v) = (1 / L_i) - (2\pi f)^2 C_i$	**3.3**

This is in the form $y = a + bx$ and so can be subjected to a linear regression analysis[7]. A suitable breakdown into variables and parameters is:

$y = 1 / (N R_0 C_2 R_v)$, $a = 1 / L_i$, $b = C_i$, and $x = -(2\pi f)^2$.

A weighted linear regression procedure was used in order to allow for the non-linear scaling of the uncertainties in R_v due to its reciprocal relationship with y . The estimated standard deviation (ESD) of a measurement of R_v (σ_{Rv}) was taken to be 1%, not due to the uncertainty in the meter reading but on the basis of repeatability; the issue being that, for this crude early version of the experiment, there was some ambiguity regarding the exact balance point. The figure of 1% was arrived at by repeating a few measurements and noting the scatter of results. Observe also that the fitting weight for a y value is determined only by the effect of R_v on its precision. It does not depend on the overall accuracy of a y value because the uncertainty contributions from R_0 and C_2 are correlated over the whole dataset and so do not contribute to the weight (although they do, of course, contribute to the uncertainties in the derived parameters $L_i = 1/a$ and $C_i = b$). The precision of a y value, σ_y, is given by:

$\sigma_y = |\partial y/\partial Rv| \, \sigma_{Rv}$

where

$\partial y/\partial Rv = -1 / (N R_0 C_2 R_v^2)$

The fitting weight is the reciprocal of the square of the precision:

$w = 1/\sigma_y^2$

The fit gave a reduced χ^2 of 1.3 on 17 degrees of freedom; indicating that, within the precision of the data, the hypothesis that the transformer secondary reactance can be modelled as an inductance in parallel with a capacitance is validated (i.e., the shape of the graph of L_i' vs f given above, is so-far accounted for by the theory). The transformer parameters obtained from the fit were:

$L_i = 9.006 \pm 0.026$ μH , $C_i = 14.11 \pm 0.06$ pF

but note that the uncertainties from the fit represent only the precision of the data. The true uncertainty of a parameter is greater than the precision, because the contributions from to the uncertainties in R_0 and C_2 have not been taken into account; and also because these are the results of an experiment that has yet to be investigated for hidden sources of systematic error. It will transpire that the experiment is in need of improvement, which means that the results obtained at this stage are not trustworthy; but if we treat this as an exercise that serves to establish the basic technique (and the spreadsheet template for the data analysis), then it is sensible to determine the parameter accuracies. To do so analytically is somewhat difficult, because of the various correlations involved, but there is a simple solution to the problem. The spreadsheet (**testbrg61-12_1.ods**) was written in such a way that the input parameters R_0 and C_2 are taken from a single cell in each case. Hence it is possible to shift these parameters, one at a time, to the upper and lower limits of their standard deviations and note the changes in L_i and C_i that occur. The RMS average deviation in (say) L_i, which occurs when (say) R_0 is shifted, is the error contribution to L_i from the uncertainty in R_0, i.e., it is, to a very good approximation, $(\partial L_i/\partial R_0) \, \sigma_{R0}$. The other error terms $(\partial L_i/\partial C_2) \, \sigma_{C2}$, $(\partial C_i/\partial R_0) \, \sigma_{R0}$, and $(\partial C_i/\partial C_2) \, \sigma_{C2}$ are collected in similar fashion. All we need then are the error

7 See, for example, **Scientific Data Analysis**, D W Knight, www.g3ynh.info/zdocs/math/data_analy.pdf

contributions from the experimental uncertainties, i.e., ($(\partial L_i/\partial R_v)\,\sigma_{Rv}$ and $(\partial C_i/\partial R_v)\,\sigma_{Rv}$, but these are already available as the estimated standard deviations (precision) obtained from the fit. The input parameter and fitting uncertainties σ_{R0}, σ_{C2}, and σ_{Rv} are uncorrelated, and so their contributions to σ_{Li} and σ_{Ci} are orthogonal. Hence:

$$\sigma_{Li} = \sqrt{\{ [(\partial L_i/\partial R_0)\,\sigma_{R0}]^2 + [(\partial L_i/\partial C_2)\,\sigma_{C2}]^2 + [(\partial L_i/\partial R_v)\,\sigma_{Rv}]^2 \}}$$

$$\sigma_{Ci} = \sqrt{\{ [(\partial C_i/\partial R_0)\,\sigma_{R0}]^2 + [(\partial C_i/\partial C_2)\,\sigma_{C2}]^2 + [(\partial C_i/\partial R_v)\,\sigma_{Rv}]^2 \}}$$

Using this approach, the determined transformer parameters become:

$L_i = 9.01 \pm 0.18\ \mu H$, $C_i = 14.1 \pm 0.1$ pF

4. Parasitic inductance of the adjustable capacitor

Although the variation of R_v with frequency so-far supports the 'ideal transformer with parallel reactance' model for the transformer under test, the data for the adjustable capacitor C_1' were not so well behaved. Evidence of deviation from the model can be seen in the graph of C_1' vs frequency below (see **testbrg61-12_1.ods, sheet 2**); C_1' in this instance being the value of the detachable part of C_1 as given by measurement on a laboratory bridge operating at 1.5915 MHz.

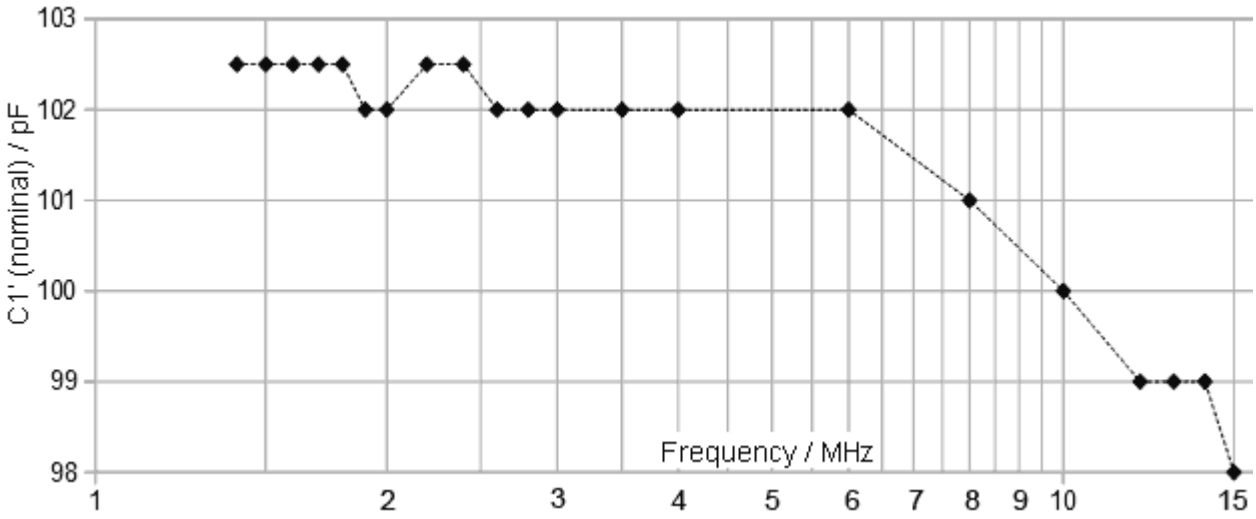

Recall that C_1 is given by equation **(2.1)** as:

$$C_1 = C_2 [(N R_0 / R_i) + (1/N) - 1]$$

It is apparently related only to fixed system parameters and so should not vary with frequency, and yet according to the graph it drops by about 4% over the range covered. One possible but unlikely explanation is that the apparent efficiency of the transformer could be increasing as the frequency rises (Recall from the earlier discussion that R_i can be replaced with $R_{ik} = R_i // R_k$ if efficiency needs to be taken into account). Such an effect is possible in the event of a severe mismatch in the primary transmission line (see **section 14**), but measurements of the relative amplitude vs frequency response of a similar transformer over a 1.6 MHz to 30 MHz frequency range did not show it[8]. Hence that hypothesis has to be rejected. The only sensible conclusion is that the effective value of C_1 (and by inference also C_2) is changing with frequency, i.e., ***the inductance of the potential divider network is not negligible***.

When a capacitor has a significant parasitic series inductance, the inductive reactance cancels some of the capacitance reactance, causing the effective capacitance to increase with frequency. Hence, according to this second hypothesis, the setting of the capacitor designated C_1' has to be backed-off as the frequency is increased, giving the impression that the capacitance required to balance the bridge has fallen. If C_1 varies with frequency, then of course, so must C_2, but there is reason to believe that the variation of C_1 will be substantial, whereas the variation of C_2 will not. The point is that C_2 is a small capacitance (10 pF) and therefore, over the frequency-range of measurement, will always have enough reactance to keep the inductance in its arm of the circuit at bay. An educated guess for the inductance in series with C_2 for the test bridge is that it will be somewhere in the region of 50 nH. At a frequency of 10^8 radians/sec (15.915 MHz) a 10 pF

8 See: **Amplitude response of conventional and maximally-flat current transformers**, D W Knight. www.g3ynh.info/zdocs/bridges/appendix/a6-3.html

capacitance has a reactance of -1000 Ω, whereas an inductance of 50 nH has a reactance of only +5 Ω. Hence the deviation from pure capacitance for C_2 over the range from 0 to 16 MHz is only about 0.5%. C_1 however, is a different matter. A 102 pF capacitance has a reactance of -98 Ω at 10^8 radians/sec, and so a series inductance of 40 nH to 50 nH could well account for the observed 4% to 5% deviation from the model. The test of this reasoning however, is to see how well it agrees with the data; and to this end we must define the problem correctly. We will start by allocating the following symbols:

● C_1' is the value of plug-in capacitance required to balance the bridge, and is assumed not to vary with frequency.

● C_{1m}' is the capacitance of the plug-in capacitor measured at 1.5915 MHz (the raw data).

● C_{10}' is the true capacitance of the plug-in capacitor at zero frequency.

● L_1 is the inductance of the plug-in capacitor and its associated connector and wiring.

Recall that the total capacitance required is defined as:

$$C_1 = C_1' + C_{1s}$$

Here we will make the reasonable assumption that the stray capacitance does not have significant inductance and is therefore constant. Hence if we can prove a condition that makes C_1' invariant, then C_1 is invariant and the transformer model requires no modification.

When the plug-in capacitor is connected to the Douma bridge, its reactance is given by:

$$X_{C1}' = X_{C1'0} + X_{L1}$$

i.e.:

$$-1/(2\pi f C_1') = -[\ 1/(2\pi f C_{10}')\ ] + 2\pi f L_1$$

Multiplying both sides by $-2\pi f$ gives:

$$1/C_1' = (1/C_{10}') - (2\pi f)^2 L_1 \qquad \ldots\ldots \textbf{(4.1)}$$

Similarly, when the plug-in capacitor is mounted on the measuring bridge, which operates at 10^7 radians/sec (1.5915 MHz), we obtain:

$$1/C_{1m}' = (1/C_{10}') - 10^{14} L_1 \qquad \ldots\ldots\ldots \textbf{(4.2)}$$

This assumes that the inductance L_1 does not change when the capacitor is transferred, for which reason the measuring bridge was fitted with a socket identical to the one on the test bridge. Also note that the inductive reactance correction is small at 1.5915 MHz, so that any error in this assumption will have negligible effect. Now, subtracting equation **(4.1)** from equation **(4.2)**:

$$(1/C_{1m}') - (1/C_1') = -10^{14} L_1 + (2\pi f)^2 L_1$$

i.e.:

$(1/C_1'_m) = (1/C_1') + [\,(2\pi f)^2 - 10^{14}\,]\,L_1$

This is in the form y = a+bx , with variables and parameters as follows:

$y = 1 / C_1'_m \quad , \quad a = 1 / C_1' \quad , \quad b = L_1 \quad , \quad x = (2\pi f)^2 - 10^{14}$

As before, a weighted linear regression procedure was used in order to cope with the non-linear scaling of uncertainties when computing y from $C_1'_m$ (see sheet 2 of **testbrg61-12_1.ods**). As may be noted from the data, the $C_1'_m$ values were recorded to the nearest 0.5 pF. Hence, due to the rounding error, this gives the precision of the data as ±0.25 pF, i.e., $\sigma_{C1'_m}$ was taken to be 0.25 pF. σ_y is given by:

$\sigma_y = |dy/dC_1'_m|\ \sigma_{C1'_m}$

where

$dy/dC_1'_m = -(\ 1/C_1'_m)^2$

The fit gave a reduced χ^2 of 1.15 on 19 degrees of freedom, confirming that the apparent variation of C_1' with frequency is an artifact. The graph below illustrates the point by showing the smooth curve underlying the rounded measurements. The derived circuit parameters were:

$C_1' = 102.32 \pm 0.07$ pF , $L_1 = 50 \pm 2$ nH

the quoted uncertainties representing precision, not accuracy.

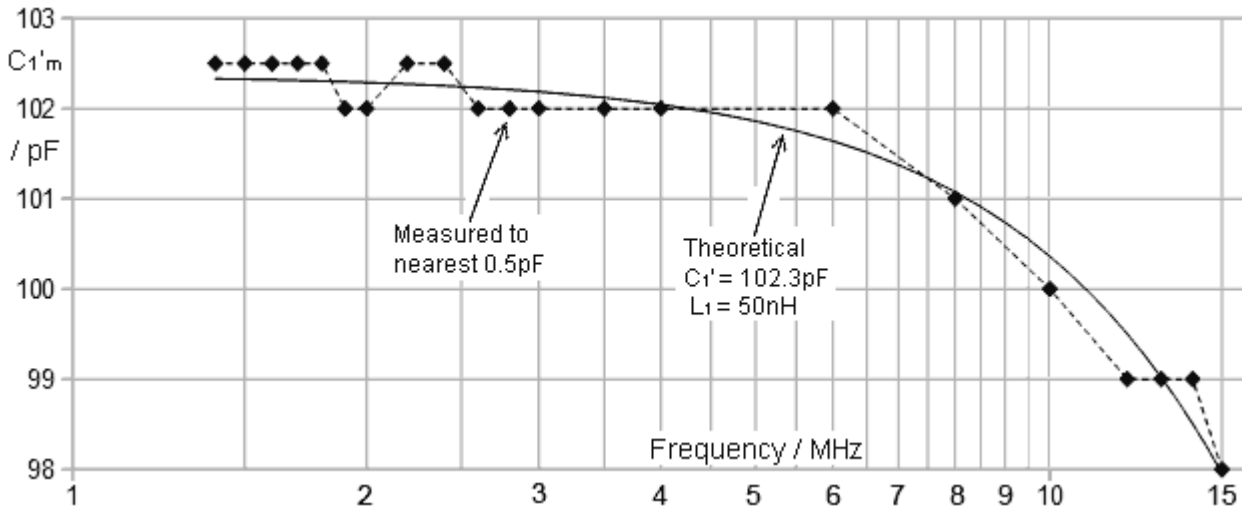

The inductance L_1 obtained from the fit is, incidentally, slightly smaller than the true inductance of the capacitor because the inductance of the upper voltage sampling arm has been neglected.

5. Stray Capacitance

Equation **(2.1)** gives C_1 as:

$$C_1 = C_2 [(N R_0 / R_i) + (1/N) - 1]$$

but if we wish to take transformer voltage-transfer efficiency[9] into account, then R_i can be replaced by:

$$R_{ik} = R_i // R_k = k' R_i$$

Hence a refined prediction for C_1 is given by the expression:

$$C_1 = C_2 [(N R_0 / k' R_i) + (1/N) - 1]$$

with uncertainty

$$\sigma_{C1} = \sqrt{ [(\partial C_1 / \partial C_2) \sigma_{c2}]^2 + [(\partial C_1 / \partial R_0) \sigma_{R0}]^2 + [(\partial C_1 / \partial_k) \sigma_k]^2 + [(\partial C_1 / \partial R_i) \sigma_{Ri}]^2 }$$

where:

$\partial C_1 / \partial C_2 = [(N R_0 / k R_i) + (1/N) - 1]$	[dimensionless]
$\partial C_1 / \partial R_0 = C_2 N / (k R_i)$	[Farads/Ω]
$\partial C_1 / \partial k = -C_2 N R_0 / (k^2 R_i)$	[Farads]
$\partial C_1 / \partial R_i = -C_2 N R_0 / (k R_i^2)$	[Farads/Ω]

An transfer efficiency measurement on a 12-turn current transformer wound on a FT50-61 bead[10] gave k' = 0.959 ±0.011. Hence, using the formulae and derivatives given above, our best prediction for C_1 is:

$$C_1 = 116.4 \pm 2.8 \text{ pF}$$

(for calculation, see sheet 3 of **testbrg61-12_1.ods**).

The previous investigation gave $C_1' = 102.318 \pm 0.07$ pF. The uncertainty in this case is the precision from the fit. A more realistic standard deviation must also take the calibration uncertainty of the measuring bridge into account (about 1%), which gives $C_1' = 102.3 \pm 1.0$ pF. The estimated stray capacitance is the difference between the predicted C_1 and this value, i.e.:

$$C_{1s} = C_1 - C_1'$$

and

9 The k' apparing here is not the same as the transformer coupling factor k, because it includes an element of voltage shortfall due to losses. Numerically however, it is statistically indistinguishable from the coupling factor.

10 **Current transformer efficiency factor**. www.g3ynh.info/zdocs/bridges/appendix/a6-1.html

$\sigma_{C1s} = \sqrt{[\sigma_{C1}^2 + \sigma_{C1'}^2]}$

giving:

$C_{1s} = 14.0 \pm 2.9$ pF

This value appears to be somewhat high in view of the bridge layout, and indicates a possible systematic error.

5a. Transformer constant

The quantity $[(N R_0 / k' R_i) + (1/N) - 1]$ is a circuit constant that defines the ratio C_1/C_2 and also the derivative $\partial C_1/\partial C_2$. As was outlined above, it is used for error analysis and for estimating the stray capacitance C_{1s}. Since it involves only parameters related to the transformer, it will be referred to from here on as the ***transformer constant***.

$K_T = C_1 / C_2 = (N R_0 / k' R_i) + (1/N) - 1$	**5.1**

This version of the transformer constant is correct for Faraday-shielded bridges. A modified version for unshielded bridges is given in **section 19** (equation **19.9a**).

6. Test procedure optimisation

In the matter of demonstrating the feasibility of the proposed bridge evaluation method, the prototype served its purpose. Experimentally however, it left a lot to be desired; and further investigation, triggered by a slightly high value for C_{ls}, uncovered several sources of systematic error. The various problems and their solutions are discussed in **sections 6 to 9**.

The need to change resistors to track the variation of R_v with frequency was both tedious and potentially disruptive to the circuit layout. The solution was to replace the R_v arm with two plastic-bodied 2 W Cermet potentiometers (Vishay 93R1A-R22-xxx) in series, one having a value of 250 Ω (fine) and the other having a value of 25 kΩ (coarse). The potentiometers were initially mounted on a metal plate, screwed to the jig; but it was found that adjustment of the fine control was accompanied by a small change in the capacitance of the arm, making nulls difficult to locate. The solution was to mount the pots away from any conducting surfaces.

The need to disconnect the radio receiver and connect test-leads to measure R_v was once again tedious and potentially disruptive. In looking for a resolution to this issue, it was first noted that the resistance of the transformer secondary-winding is small in comparison to R_v; and so a more reliable connection can be made by fitting the resistance-meter with a BNC to 4 mm adapter, and then connecting it to the detector port via a short length of coaxial cable. A further refinement resulted from the observation that; if the input to the radio receiver could be made a DC open-circuit, then the line to the receiver could be left connected and the resistance measured via a T-piece. The required DC-block was implemented by mounting a capacitor between two BNC connectors, as shown below, and inserting it into the coaxial line.

DC blocking capacitor.
10 nF 1 kV Ceramic.

The BNC connectors are joined using threaded Ni-plated brass pillars. The final assembly is wrapped in aluminium foil and covered with heat-shrink tubing.

Breaking the DC path to the receiver and measuring R_v via a T-piece lead to the discovery that the resistance could be measured continuously, i.e., with the RF on and while searching for nulls. This certainly works when using the Fluke 8060A, and will probably work with other meters. No sign of sampling noise could be heard in the receiver, and the only interference was a pure tone of less than 1 µV at 16.00 MHz and another at 3.20 MHz (presumably sub-multiples of the 8060A's clock oscillator), which could be eliminated by switching the meter off while balancing the bridge at those frequencies. The resistance reading did not change at any of the measurement frequencies when the the signal-generator was switched off and on. The Fluke 8060A did not even care when the generator and receiver connections were swapped to test for bridge reciprocity (but some digital multimeters are known give misleading results when making DC readings in the presence of superimposed RF). There was, furthermore, no change in the balance settings on plugging-in and removing the meter.

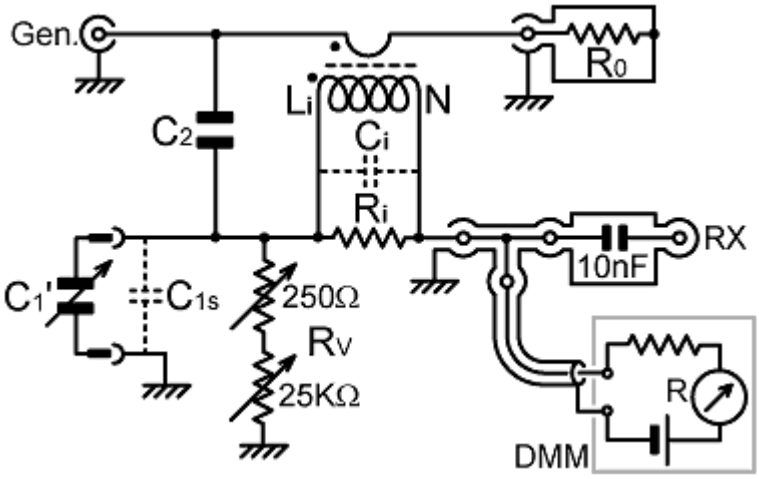

Setup for continuous measurement of R_v

Also tedious, and requiring considerable care, was the business of unplugging the reference capacitor and measuring it on a separate bridge. The solution in this case was to make up an assembly consisting of an air-spaced variable capacitor and a reduction-drive; the control knob and the capacitor being separated by insulating pillars and a non-conductive drive-shaft, so that adjustment could be accomplished without proximity of the operator's hand. The capacitor was fitted with a connector so that it could be taken away and measured as before, but the point in this instance was to take a series of readings of capacitance versus dial-setting and fit them to a regression function. From then on, measuring capacitance became a matter of noting the dial-readings during an experimental run; the nominal (1.5915 MHz) capacitance being obtained later by entering the data into a spreadsheet and applying the formula. Details of the data reduction are given in the spreadsheet file: **capcal_p500.ods** .

One serious problem with early versions of the 500 pF variable capacitor assembly was backlash. The first version had two flexible couplers, but these permitted a twisting motion that made the backlash so severe that accurate capacitance measurement was impossible. The problem was reduced by using one straight coupler and one flexible coupler, but even then, due to the elasticity of the 6 mm diameter plastic drive-shaft fitted at the time, the backlash remained at ±5 divisions of the vernier dial. Finally, the backlash was reduced to ±1 division by using a straight drive-shaft made from solid 19 mm diameter acrylic bar (see photographs below). To allow for the residual backlash, all measurements were made by approaching the null from the clockwise direction of the control knob.

The 500 pF variable capacitor proved useful for tracking the impedance meanderings of uncompensated bridges, but was necessarily limited in resolution on account of its large variation range. A second variable reference capacitor was therefore constructed, this time with a 40 pF range and a 36:1 reduction drive, with a socket for a plug-in padding capacitor. This device fortuitously gave exactly 2.5 pF per turn in its linear region, with a resolution of better than 0.025 pF and no detectable backlash (**capcal_8-48.ods**).

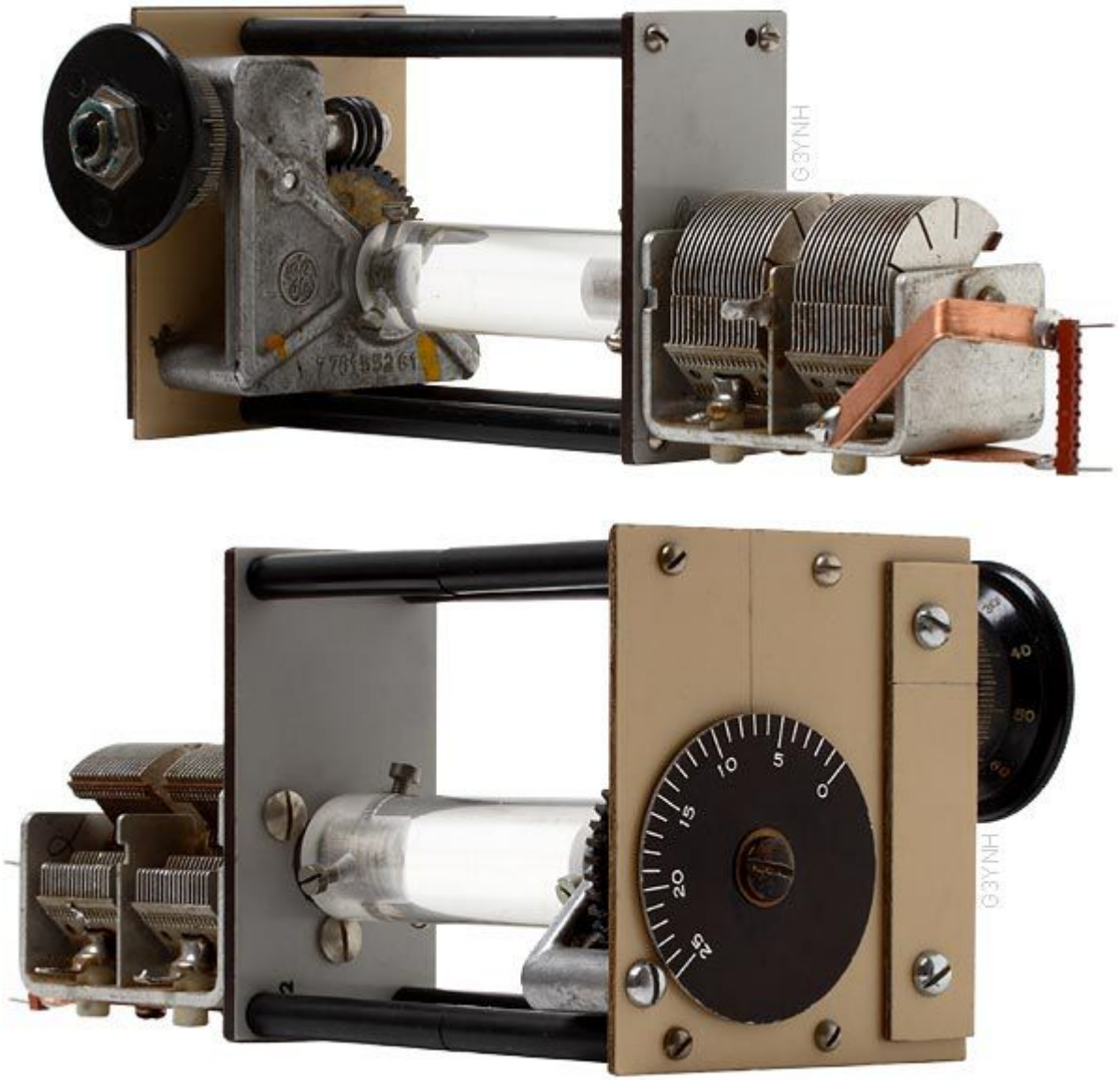

Philips dual-gang 500 pF variable capacitor and General Electric 50:1 anti-backlash worm drive (**capcal_p500.ods**). The drive-shaft is machined from 19 mm diameter acrylic bar for stiffness and the assembly is clamped to a baseboard in use to prevent torsion of the mounting frame. Mounting plates and pillars are made from non-conductive materials. Only one gang of the capacitor is connected, but both can be used if a large capacitance is required. Wiring to the connector is via copper straps to provide rigidity and minimise inductance.

40 pF variable reference capacitor with 36:1 anti-backlash worm drive (**capcal_8-48.ods**). A socket is provided for a parallel padding capacitor

7. Balance disturbances due to common-mode currents

An impedance bridge is a linear reciprocal network. Therefore, if it is configured correctly, the balance condition should not change when the generator and detector are swapped. Note that when the generator is connected to the 'detector' port, it requires a terminating resistor, which can be provided on a T-piece near to the bridge.

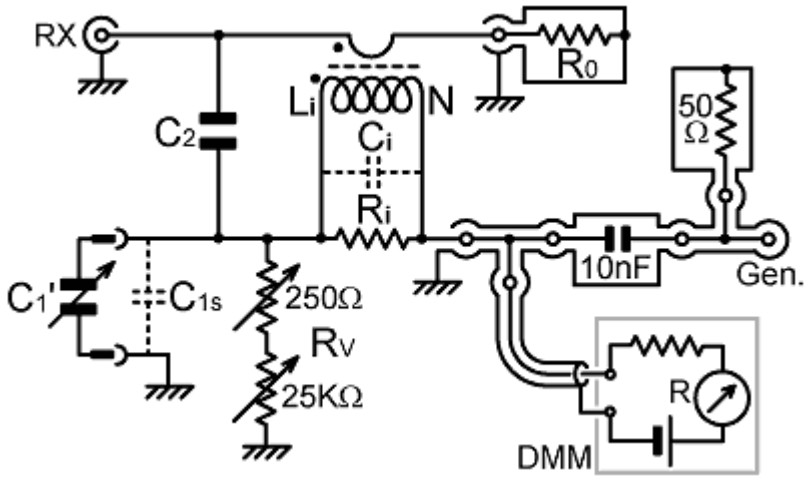

Reciprocity test.
The cable to the DMM is kept short (ca. 100 mm) to avoid excessive mismatch.

It was discovered, during the course of the optimisation work, that the bridge did not behave in an exactly reciprocal fashion. Significantly different results were obtained with the generator and radio-receiver connections swapped, and the results were different again if the generator was left un-terminated. The capacitance setting was seen to change by 3 to 4% ; and the resistance setting changed by about 4% at low frequencies and considerably more around the phase-crossover frequency where R_v is heading for infinity. Such deviations are not acceptable if any physical meanings are to be attached to the derived parameters; and can seriously skew the values obtained for C_i and C_{1s} because these are dependent on small changes in other parameters.

After some deliberation it was concluded that the problem was occurring because the radio receiver did not have infinite common-mode rejection, i.e., it could pick up radio signals travelling on the outside of the antenna cable by virtue of the voltage developed between the antenna socket and the mains wiring. When this problem is related to the situation in which one piece of mains-powered equipment feeds signals into another, it is known, in old parlance, as an "earth loop". The traditional solution, before the invention of 'Health and Safety at Work', was to disconnect the earth-wires from the mains plugs; and although this is unlikely to work, because there is still plenty of capacitance between the chassis and the live and neutral wires, it does add excitement to otherwise dull activities by introducing the risk of lethal electric shock.

The hypothesis for the case of a bridge that fails to obey the reciprocity rule is that the receiver is picking up a small signal from the generator via the common mode. Thus, when a null is obtained, it represents not exact balance, but a situation in which the desired differential-mode output signal is of the correct magnitude and phase to cancel the common-mode signal. The common mode signal changes depending on how the generator is terminated and the bridge connected, and so the balance-condition appears to change according to the external configuration. A test of this hypothesis is to see what happens when the common-mode current is disrupted; not by indulgence in illegal wiring practices, but by the insertion of one or more common-mode chokes into the loop.

Two common-mode chokes (1:1 unun transformers) were constructed as shown below. They were made using ferrite sleeves having an A_L value of 2.5 μH/turn^2, and ferrite rings having an A_L value of 400 nH/turn^2, (inductance factors were measured at 1.5915 MHz). Both chokes have three sections of differing inductance adding up to 47.5 μH (X = +475 Ω at 1.5915 MHz), and were made

deliberately different from each other; the point being that a series resonance in any section can never bring the total reactance to zero.

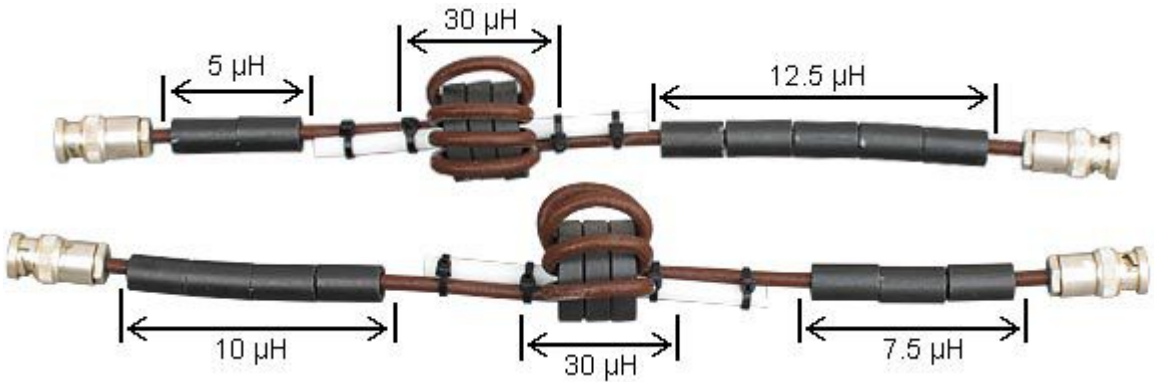

Multi-stage common-mode chokes. The cable is URM108.

It was found that the reciprocity error fell within the measurement repeatability at low frequencies with a single choke in either the lead from the generator or the lead to the receiver. It was also discovered that the balance point could be shifted by connecting a jumper lead across the choke (i.e., by shorting-together the outer bodies of the two BNC plugs), thereby directly confirming the common-mode signal hypothesis. Inserting chokes in both sides gave a lesser but still worthwhile improvement. Note that there is a general point here relating to the extraction of a signal from any bridge for processing by mains powered circuitry, or likewise for feeding a signal into a bridge for purposes such as quiet tuning[11] [12]. If the auxiliary electronics is earthed in any way; then for best accuracy, a common-mode choke should be used to isolate it from the main transmission line.

11 **Simple Quiet Tuning and Matching of Antennas,** M. J. Underhill G3LHZ, Rad Com, May 1981, p420-422.
An antenna can be matched in receive mode by injecting a small signal into a reverse wave directional coupler in the line to the ATU. The antenna is matched when the level of injected signal heard in the receiver is minimised. The injected signal can be from a noise source, or it can be a comb-spectrum from, say, a crystal calibrator. The injected signal is too weak to interfere with other stations, being undetectable at about 1 wavelength from the antenna.

12 **A Quiet Antenna Tuner**, Tony Lymer GM0DHD, QEX May/June 2002, p9-12.
Underhill-Lewis method using a single-core version of the Sontheimer-Fredrick bridge (1.8 - 146 MHz).

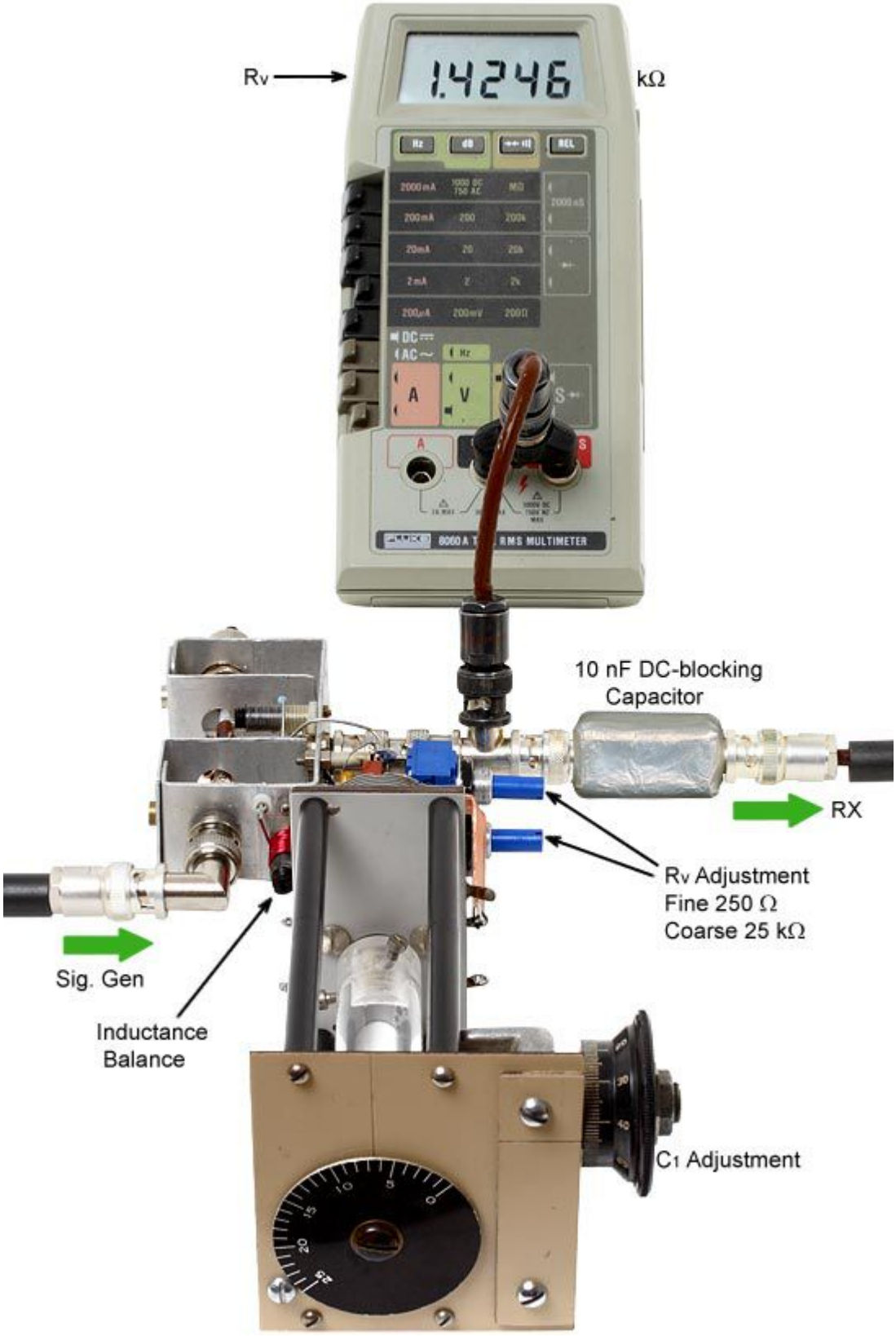

Optimised experimental configuration. Common-mode chokes (47.5 µH each) are connected on both sides. The inductance balance coil (discussed in **Section 17**) is used for bridge optimisation, but not during the determination of basic circuit parameters.

Bridge on baseboard with 40 pF variable capacitor fitted.

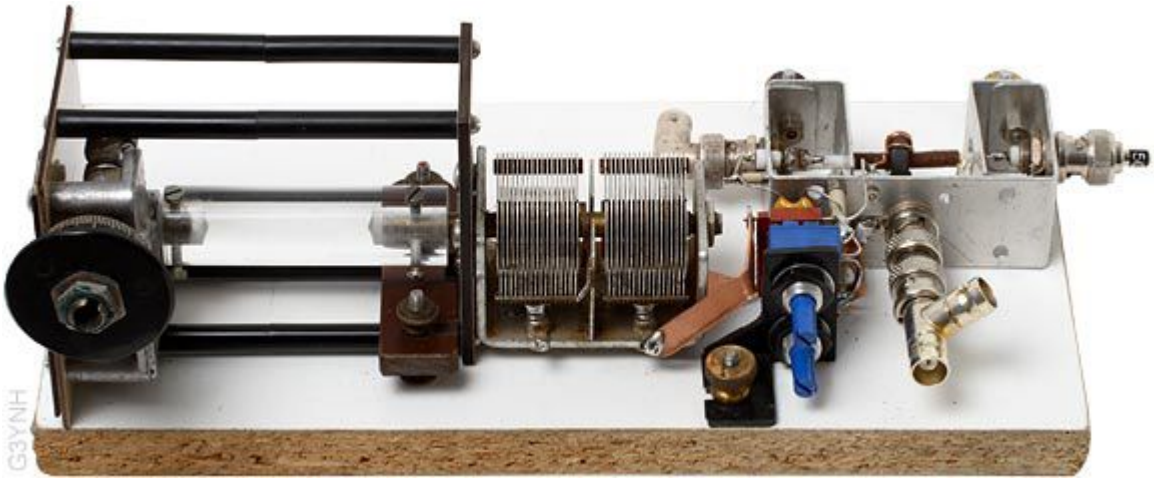

Bridge on baseboard with 500 pF variable capacitor fitted.

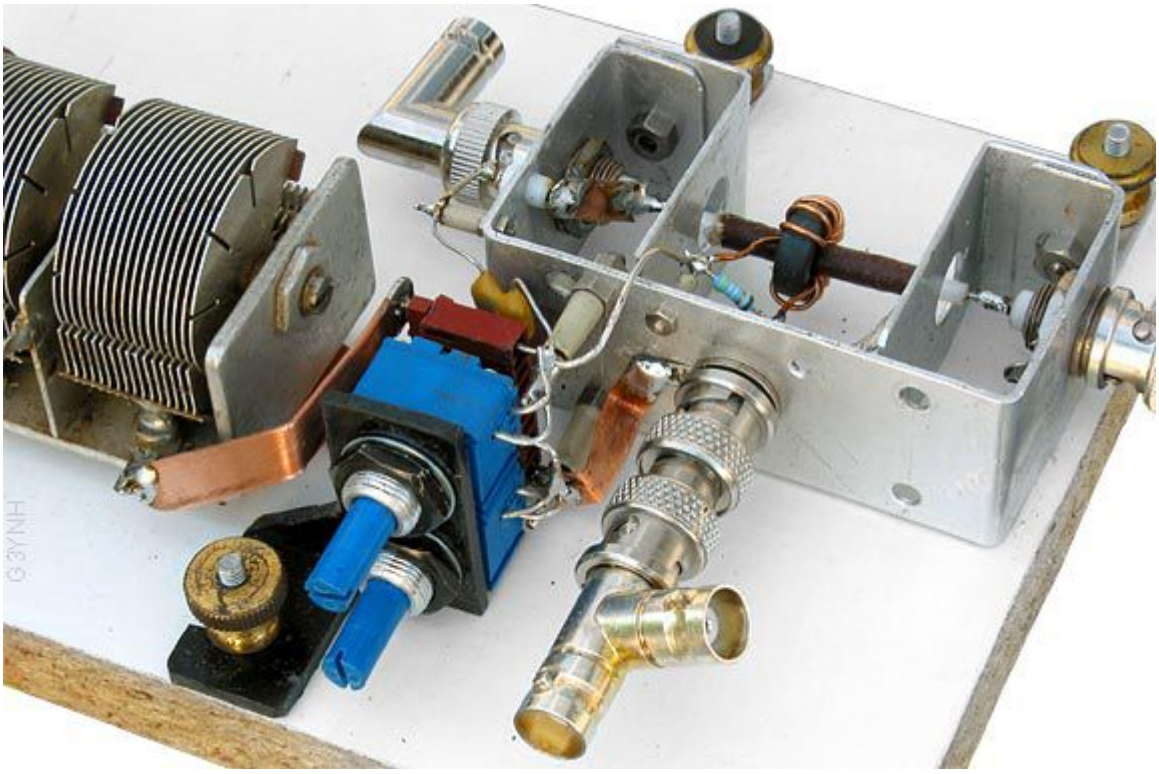

Close-up view of the voltage-sampling network. To minimise interaction between the in-phase and quadrature balance adjustments; the potentiometer mounting bracket is made from polypropylene and the network is earthed at the detector socket via a copper strap.

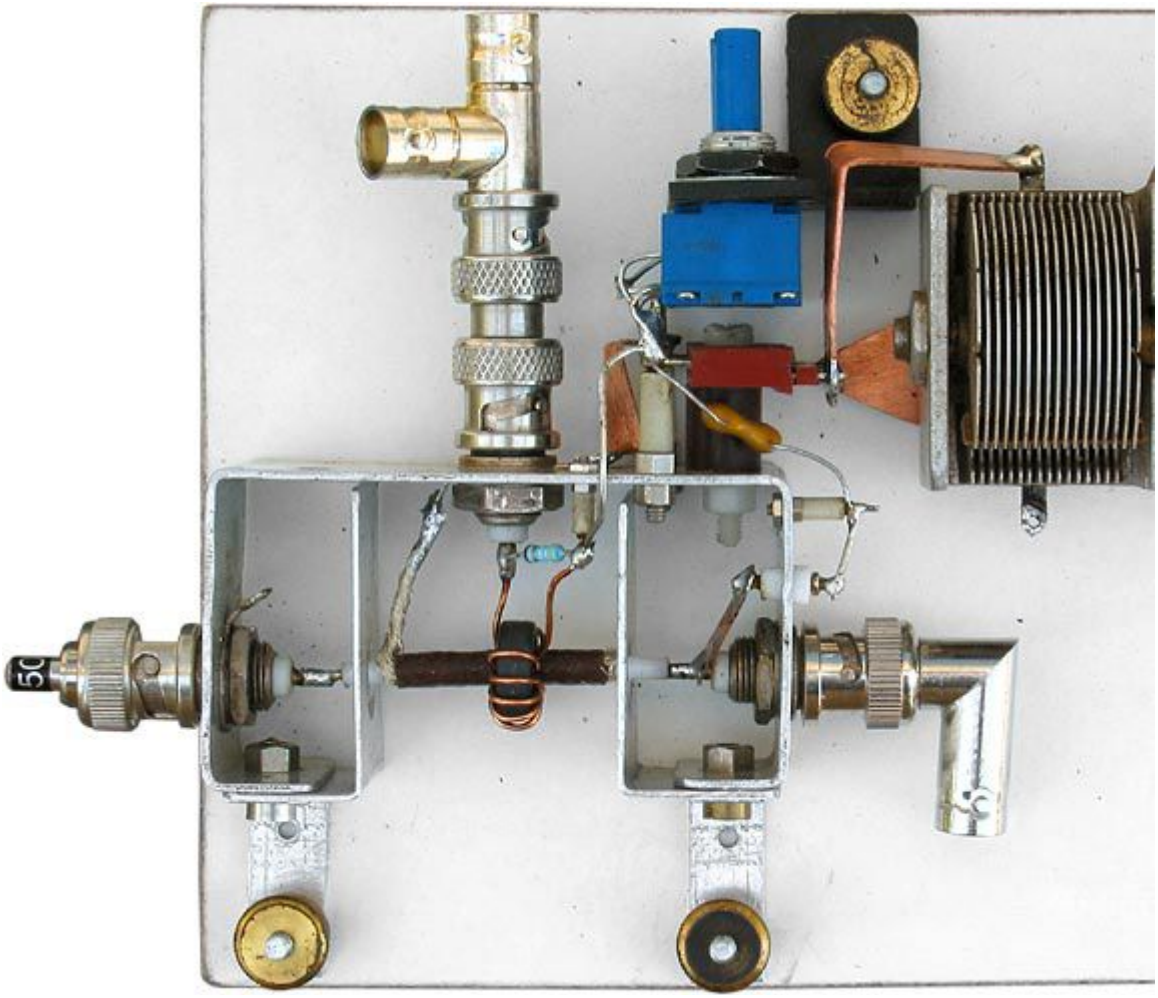

Plan view of bridge with 500 pF capacitor fitted. The bridge is quickly released by loosening three knurled nuts and pulling it away from the reference capacitor. An inductance balance coil is not fitted in the configuration shown (it is bypassed by a wire link, in series with C_2, adjacent to the RF input socket.)

8. Reciprocity error due to radiated signals

After elimination of the common-mode signal, and after changing the transformer secondary load resistor from two 100 Ω resistors in parallel (about 1 pF parallel capacitance) to a single 49.9 Ω resistor (about 0.4 pF), the apparent phase-crossover frequency for the 12-turn transformer went up from 14.1 MHz to 22 MHz. At 21 MHz, with R_v still in range of the two Cermet pots, it was found that there was still some residual reciprocity error. The error was tiny in phase terms, but sufficient to affect R_v by several kΩ in this critical region.

In the process of investigating this problem it was discovered that, having balanced the bridge to the point where the signal had disappeared into the receiver noise; a weak signal (not sufficient to move the S-meter) would reappear on unplugging the cable leading to the radio receiver. Hence the bridge balance point was being skewed slightly by a radiated signal picked up by the cable. The signal became stronger on moving the receiver cable close to the generator cable.

A major part of this spurious sensitivity was traced to a nickel-plated connector at the receiver antenna socket (several milli Ohms resistance at the shield connection). Replacing the offending connector with a silver-plated version reduced the signal by an order of magnitude. The very weak residual signal was then attributed to the imperfect shielding provided by the RG58 cable in use at the time. When the receiver cable was changed to triple-shielded Belden 9880 10Base5 Ethernet cable there was no detectable pickup from the generator with the cable unplugged from the bridge, regardless of proximity to the generator cable. The bridge showed perfect reciprocity within the measurement repeatability at all frequencies after that substitution.

Receiver input cable. Foil and double-braid shielded Belden 9880 (10Base-5 cable) with silver-plated connectors and adapters. The four Mn-Zn Ferrite beads at the receiver end give an additional 30 µH of choking inductance. Immunity from shield pickup requires that the PL259 connector and elbow at the receiver socket are done-up tightly.

9. Capacitance of the reference load resistor

A coaxial resistor, for all its pretensions, is just a resistor in a tube; and low value resistors (presuming that they are properly designed for RF applications) tend to be capacitive at high frequencies. As will be demonstrated in **Section 14**, a correction for the secondary parallel capacitance of the current transformer can be had by connecting a capacitor across the load port. Therefore, any parasitic capacitance across the reference load gives the impression that the 'self capacitance' of the transformer is less than it really is.

With the test bridge operating at a frequency just below the phase crossover point (21 MHz), a variety of load resistors of differing sizes and power-ratings were tried in order to see the effect on R_v. Observe here that load resistors with residual capacitance have the effect of shifting the apparent phase crossover to higher frequency; i.e., the load with the least capacitance (the best reference load) gives the lowest measured crossover frequency. R_v was found to vary over the range from about 7 kΩ to 16 kΩ depending on the load, but note that this only corresponds to about 0.1° change in phase angle. Perhaps not surprisingly, the best resistor (the one giving R_v=16 kΩ) was also physically the smallest.

In the absence of evidence to the contrary, the best selected reference load resistor has to be assumed to be a pure resistance. Any residual reactance adds uncertainty to to the derived secondary parallel capacitance C_i.

10. Post optimisation test data

After completion of the optimisation work, two new datasets for the 12-turn FT50-61 current transformer were obtained. The first experiment was conducted using the 500 pF variable reference capacitor, and the second with the 40 pF (8-48 pF) variable capacitor and a 68 pF padding capacitor to bring it into range. The data analyses were performed as described in previous sections, the only difference being that values for $C_1'_m$ were obtained from capacitor dial-readings by means of the appropriate fitting function (see sheet 4 of spreadsheets **testbrg61-12_2.ods** and **testbrg61-12_3.ods**). The value for C_2 was amended to 10.3 ±0.2 pF for both of these fits on the basis of an estimated 0.3 pF of strays across the upper voltage-sampling arm.

In both experiments, the data for C_1' were fitted perfectly on the assumption that the non-ideality of the reference capacitor can be modelled as a series inductance. In both cases, the graph of residuals (observed minus calculated) was chaotically scattered around zero, indicating that what is is left over after the fitting process is mainly statistical noise. The 500 pF reference capacitor turned out to have an effective series inductance of 62 nH and a precision of ±0.14 pF (obtained by adjusting the ESD of an observation to obtain a reduced χ^2 of about 1). The 8 pF to 48 pF variable capacitor with 68 pF in parallel turned out to have a effective inductance of 81 nH and a precision of 0.08 pF. As mentioned previously, the inductances obtained from the fits are slightly lower than the true values due to the neglect of the inductance associated with C_2.

The extracted voltage-sampling network parameters are summarised below. Note that the accuracy of the capacitance measurement (about ±1.1 pF) is a lot worse than the precision, the overall uncertainty being responsible for the differences between C_1' and C_{1s} for the two experiments; but for bridge evaluation purposes, it is the change in capacitance rather than the absolute capacitance that must be determined.

	500 pF ref. cap.	40 pF ref. cap.	
Data file	**testbrg61-12_2.ods**	**testbrg61-12_3.ods**	See sheets 2 and 3
Parameter	Value ±ESD	Value ±ESD	
C_1'	109.0 ±1.1 pF	107.3 ±1.1 pF	Corrected for L_1
L_1	62.3 ±0.5 nH	80.8 ±0.3 nH	Effective inductance of the ref. cap.
C_{1s}	10.8 ±3 pF	12.5 ±3 pF	Stray capacitance.

The data for R_v were not so well behaved and show a clear deviation from the model in the 14 MHz to 21 MHz region, as can be seen in the graph of $L_i'=N R_0 C_2 R_v$ vs. frequency reproduced below.

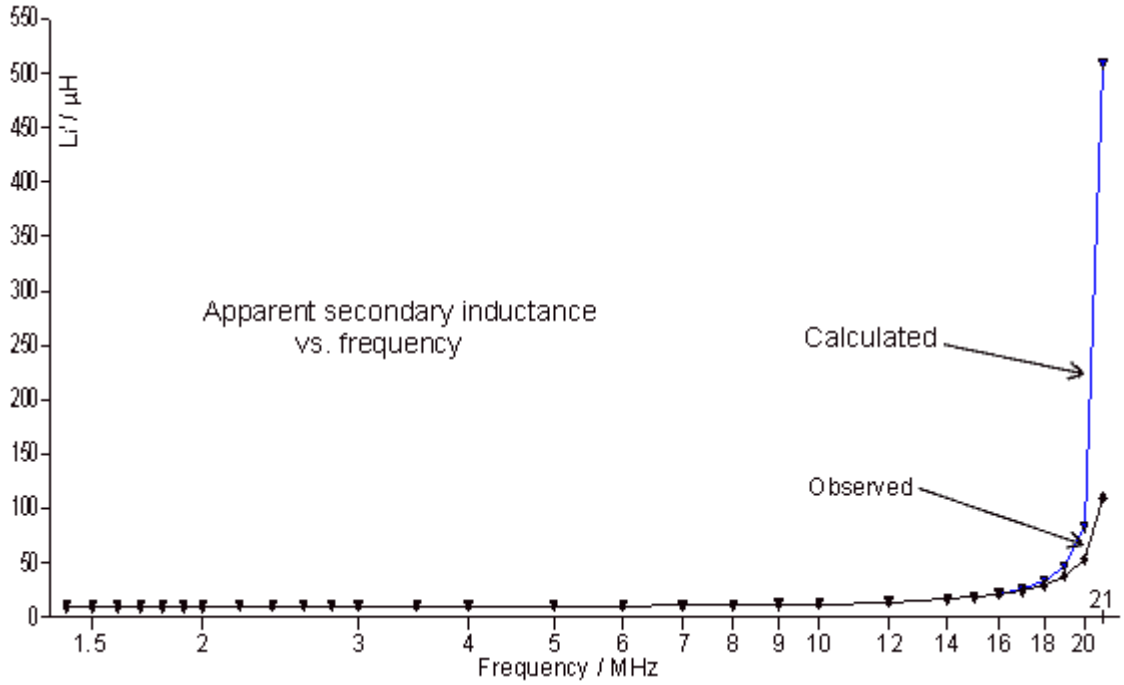

It was found for both experiments, that if the uncertainty of an R_v measurement was taken to be 0.25%, then the datasets could be fitted up to 14 MHz with a reduced χ^2 (i.e., χ^2/ν) of just less than 1. Trying to fit all of the data however, pushed the χ^2/ν to about 60, indicating a failure of the model (or perhaps, given the faith often placed in naive circuit simulations, a failure of reality). Interestingly, if the data were only fitted up to 5 MHz, the χ^2/ν went to 1 for an ESD of observation of about 0.06%, which happens to be the same as the stated accuracy of the Fluke 8060A used for the resistance measurements. This would seem to indicate that the balance-point determinations were very nearly exact, and that something not described by the model is happening above 5 MHz.

There are several possible sources for the anomaly, all of which might be active to some extent:

● High-order effects due to circuit parasitic reactances.

● Failure to include transformer leakage inductance and winding resistance in the model.

● Breakdown of the lumped-component approximation (transmission-line effect).

● Dispersion in the permittivity associated with the transformer 'self-capacitance' (variation of velocity factor with frequency).

● Dispersion in the permeability, and hence A_L, of the transformer core, causing L_i to vary with frequency.

In looking for evidence of dispersive effects, we can observe that every measurement of R_v can be regarded as an indirect measurement of C_i if L_i is a constant, or as an indirect measurement of L_i if C_i is a constant. Hence, if L_i is set to an estimated value, we can use the observed value of R_v at a particular frequency to compute a corresponding value for C_i. Similarly, if C_i is set to an estimated value, we can use the observed value of R_v to compute a corresponding value for L_i. The required relationship for such computations was given earlier as equation **(3.3)**:

$1 / (N R_0 C_2 R_v) = (1 / L_i) - (2\pi f)^2 C_i$

Rearranging this in favour of C_i gives:

$C_i = [(1 / L_i) - 1 / (N R_0 C_2 R_v)] / (2\pi f)^2$ . . . . . **(10.1)**

The result of computing C_i in this way is shown in the graph below. The upper curve uses L_i=8.970 µH, which is the inductance obtained by fitting all of the data up to 14 MHz. The lower curve uses L_i=8.982 µH, which is the inductance obtained by fitting all the data up to 5 MHz.

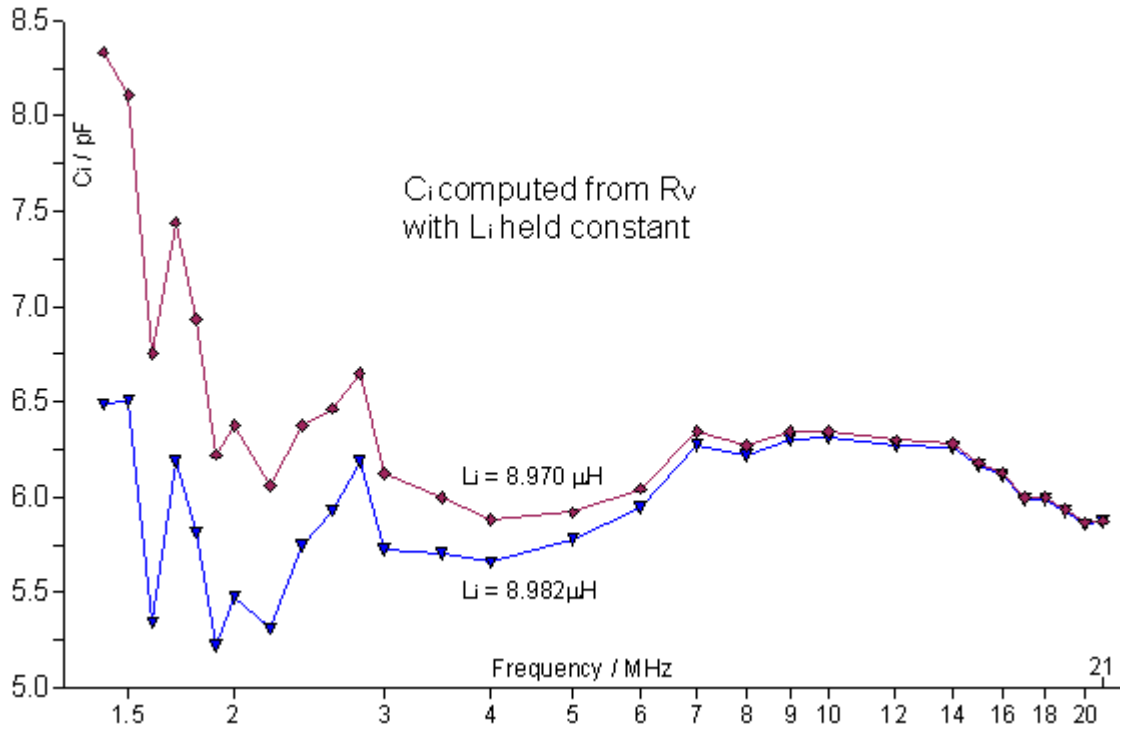

The capacitance graphs are chaotic below 3 MHz because the small amount of information in each observation amplifies the measurement uncertainty. C_i begins to assert itself above 3 MHz however, and soon becomes well defined. What we see then is a hump in the apparent capacitance between about 6 MHz and 20 MHz, and this is indeed characteristic of a dispersive effect. It is not necessarily indicative of a dispersion in permittivity however, as we may observe by differentiating equation **(10.1)** with respect to L_i.

$\partial C_i / \partial L_i = -1 / (2\pi f L_i)^2$

C_i is negatively correlated with L_i; and we could flatten the line for C_i by allowing L_i to rise in the 6 MHz to 20 MHz region. There is very good reason for wanting to do so, as can be seen by examining the manufacturer's graph of complex permeability for type 61 ferrite material.

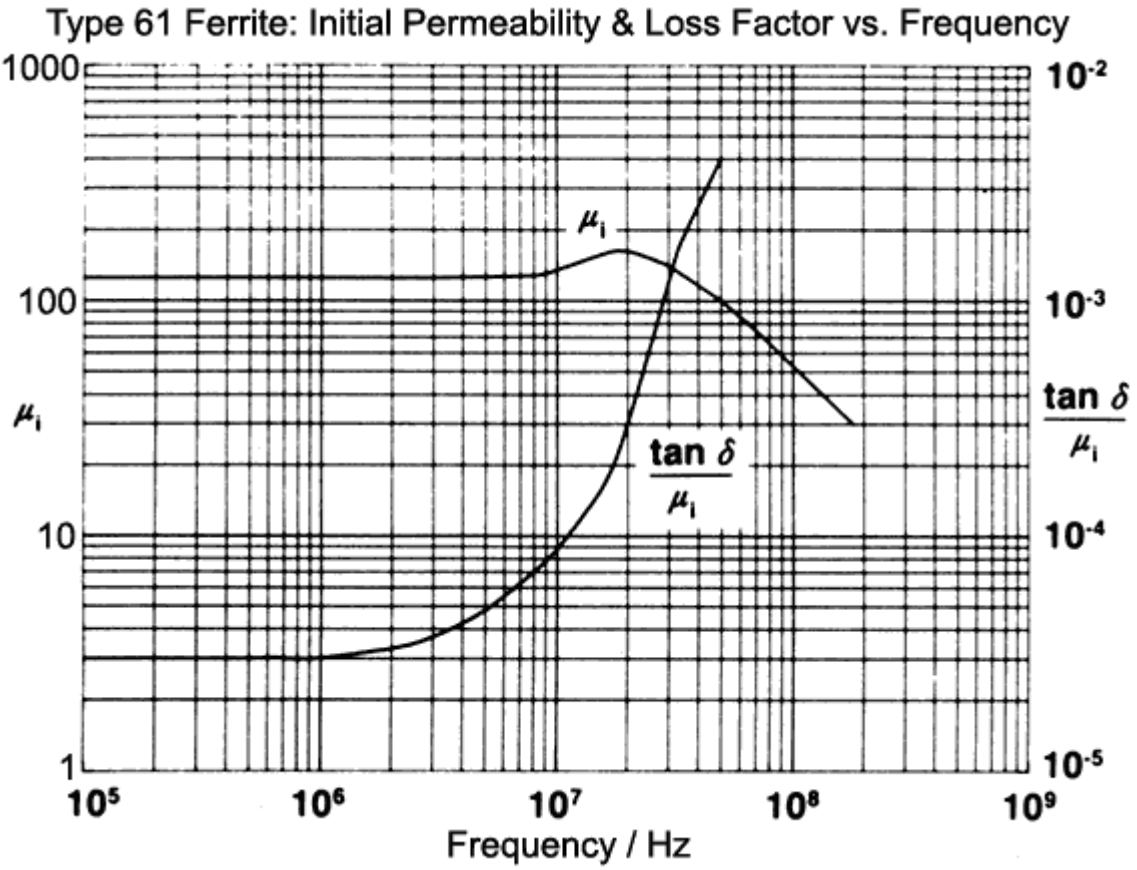

The manufacturer's data show classic dispersive behaviour, with the onset becoming evident in the real part of the permeability at about 8 MHz. Note that the inductance of a coil is directly proportional to the permeability of the core material. Hence, viewing the graph, we would expect to see a rise in L_i on moving above 8 MHz, followed by a fall commencing somewhere around 18 MHz.

Rearranging equation **(3.3)** in favour of L_i gives:

$$L_i = 1 / [(2\pi f)^2 C_i + 1 / (N R_0 C_2 R_v)] \quad \ldots\ldots \textbf{(10.2)}$$

Shown below are two graphs of L_i computed from R_v via equation **(10.2)**. The upper curve uses $C_i = 5.74$ pF, which is the value obtained by fitting the data up to 5 MHz, and the lower curve uses $C_i = 6.29$ pF, which is the value obtained by fitting the data up to 14 MHz.

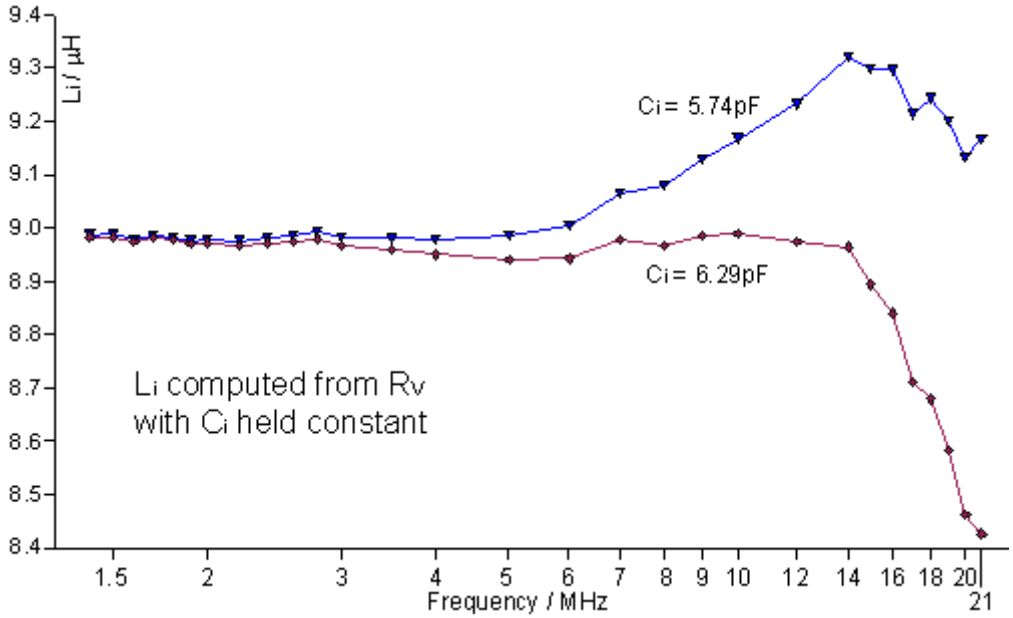

The upper curve bears a striking similarity to the dispersion shown in the permeability data and must leave us in little doubt that one cause of deviation from the model has been identified. There is a little more to it than that however. Estimation from the manufacturer's graph shows that the permeability of the ferrite rises from 125 at low frequencies to about 160 at 18 MHz. Hence we would expect the inductance to rise in proportion from 9 µH at low frequencies to 11.5 µH at 18 MHz. Computed on the basis that C_i is constant however, the inductance starts to drop away at about 15 MHz after a rise to only 9.4 µH. This could be indicative of other unknown effects, but it could also merely indicate the increasing dominance of the capacitance, and inapplicability of the manufacturer's permeability graph. By modelling the complex permeability on the basis of a single relaxation process it was possible to produce curves consistent with the data, but this matter is too conjectural to be worth pursuing.

Note, incidentally, that these investigations of model breakdown do not imply that the experiment has in some way failed. It is rather the fact that the data are somewhat better than expected. Had the R_v measurements been made with a meter having an accuracy of 2% instead of 0.06% , then all of the data could have been fitted with a χ^2/ν of 1 , and we would have remained blissfully unaware of the additional information lurking in the noise.

Shown below is the spread of results obtained by fitting the quadrature-balance data in different ways. Given that we know that the A_L value for the core varies with frequency above 5 MHz, it seems sensible to take the low-frequency inductance value from the average of the R_v readings up to 5 MHz.

	500 pF ref. cap.	40 pF ref. cap.	
Data file	**testbrg61-12_2.ods**	**testbrg61-12_3.ods**	See sheet 1*
Parameter	Value ±ESD	Value ±ESD	ESD in grey is precision from the fit.
L_i	**8.98 ±0.18** µH	**9.01 ±0.18** µH	Fitting data up to 5 MHz
	8.97 ±0.18 µH	8.98 ±0.18 µH	Fitting data up to 14 MHz
	9.08 ±0.18 µH	9.09±0.18 µH	Fitting all data
C_i (apparent)	**5.74** ±0.07 pF	**5.74** ±0.08 pF	Fitting data up to 5 MHz
	6.29 ±0.13 pF	6.55 ±0.02 pF	Fitting data up to 14 MHz
	5.81 ±0.03 pF	6.11 ±0.03 pF	Fitting all data

* L_2 fitting flag (Sheet 1, cell B7) must be set to zero to reproduce these results.

The uncertainties for the capacitance determinations represent precision from the fit, not accuracy. As we shall soon see moreover, there is no point in considering any of these results to represent a good value for C_i because there are a number of systematic error contributions that need to be taken into account first. With a view to understanding how large the residual systematic errors are however, it is interesting to compare the results obtained so far with the hypothesis that 'self capacitance' is a lumped-component alias for time delay. If the effective velocity for an electromagnetic wave travelling along the winding wire is taken to be exactly c (the speed of light), then the equivalent capacitance is given by:

$$C_i' = \ell_w / (2\, R_i\, c)$$

Where ℓ_w is the length of the secondary winding[13]. The wire length for the test transformer was 228 mm, which predicts C_i' =7.6 pF. Naively adding about 0.4 pF to this, to allow for the capacitance of the secondary load resistor, we thus predict C_i = 8 pF. From this we might conclude; either, that the effective velocity is greater than c ; or, that the data are skewed. A velocity-factor of greater than 1 is by no means impossible, but for a transmission line system in proximity to a high-permeability medium it is only likely to occur on the high-frequency side of a major dispersion such as the half-wave line resonance (which for 0.228 m of wire occurs at 657 MHz). Hence we are looking for errors of at least 2 pF to 2.5 pF.

As mentioned previously, we are to some extent cursed by the quality of the data; and there has to be a cut-off point in the matter of how far we go in accounting for minor discrepancies. Engaging in a search for a missing 2 pF might therefore seem unreasonable; but any effect that makes the coil self-capacitance seem smaller than it really is can provide the basis for a high-frequency phase-compensation scheme.

13 **Current transformers**, D W Knight, www.g3ynh.info/zdocs/bridges/Xformers/part_2.html, section 13

11. Faraday shield displacement current

In the test bridge used during the previous experiments (shown below), the Faraday shield earth connection was made on the load-port side. The unconnected end of the coaxial-cable braid protruded from the transformer core to a distance of about 13.5 mm when measured from the middle of the core. 50 Ω coax. has a capacitance per unit length (C_0) of about 100 ±5 pF/m (a 34.5 mm length of the URM108 used here measured 33 pF, i.e., 96 pF/m), and so the capacitance between the protruding part of the braid and the central conductor, allowing a little extra for the fringing fields at the end, is about 1.6 ±0.1 pF. The displacement current for this capacitance passes through the transformer core on its way to ground and will therefore add a quadrature component to the transformer output.

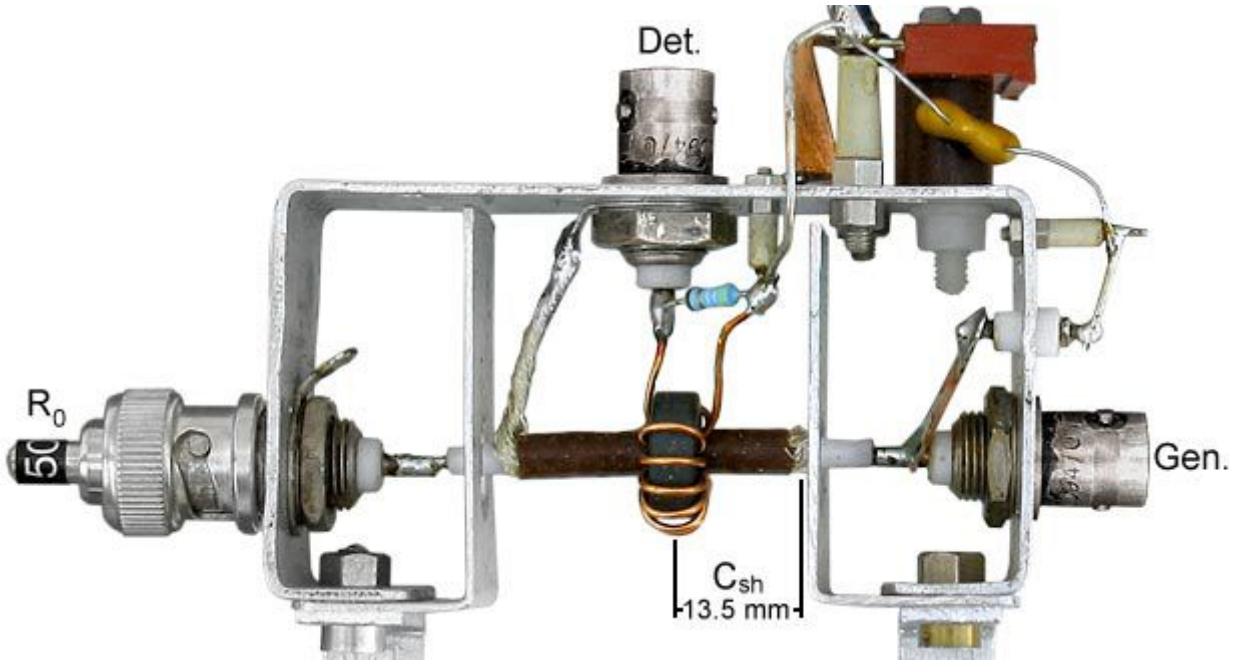

The situation is represented in the equivalent circuit shown below. Subject to the approximation that no voltage is developed across the shield (the consequences of which will be discussed in **section 18b**) the primary current is $\mathbf{I} + \mathbf{I}_{sh}$, where:

$\mathbf{I} = \mathbf{V} / R_0$

and

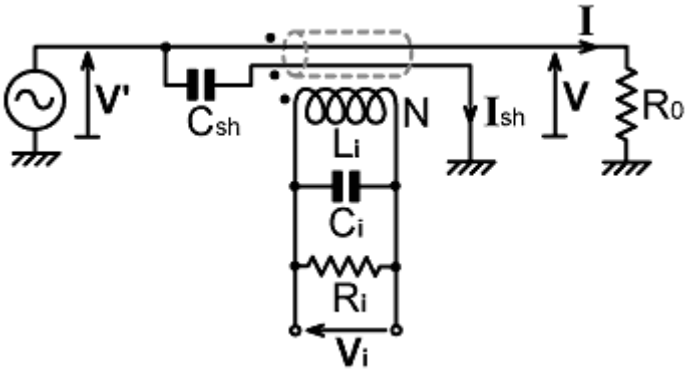

$\mathbf{I}_{sh} = \mathbf{V}' / (\mathbf{j}X_{Csh})$

or, using the approximation that $\mathbf{V}' = \mathbf{V}$

$\mathbf{I}_{sh} = \mathbf{V} / (\mathbf{j}X_{Csh})$

Now, if we use the definition:

$\mathbf{Z}_i = (R_i // \mathbf{j}X_{Li} // \mathbf{j}X_{Ci})$

Then, by the ampere-turns rule:

$\mathbf{V_i} = (\mathbf{I} + \mathbf{I_{sh}})\,\mathbf{Z_i} / N$

i.e.:

$$\mathbf{V_i} = \frac{\mathbf{V}\,\mathbf{Z_i}}{N}\left[\frac{1}{R_0} + \frac{1}{\mathbf{j}X_{Csh}}\right]$$

Now notice that

$(1/R_0) + (1/\mathbf{j}X_{Csh}) = 1 / (R_0 \,//\, \mathbf{j}X_{Csh})$

Hence, in terms of its effect on the current-transformer output, the Faraday shield protrusion can be considered to act (to a fair approximation) as an extra capacitance in parallel with the primary load.

Note incidentally, that it is only the unconnected portion of the Faraday shield protruding beyond the exact centre of the transformer core that concerns us here. The shield on the load side also has capacitance, but if the cable used has a characteristic resistance equal to the load resistance R_0, then the inductance per unit length (L_0) balances the capacitance per unit length such that $\sqrt{(L_0/C_0)} = R_0$ and there is no net effect. It is the fact that the capacitive current from the unterminated end of the shield must pass through the transformer core (and only that) that gives rise to the additional quadrature component in the transformer output.

What we need to do now is to write an expression for the current transfer function and compare it with the transfer function for a model with no Faraday shield protrusion capacitance. The difference in the imaginary part between the new model and the old model will tell us the apparent or 'effective' secondary parallel capacitance (C_{ieff} say) in the event that the Faraday shield protrusion displacement-current exists.

For a transformer with no shield displacement-current, the transfer function is:

$\mathbf{V_i} / \mathbf{V} = \mathbf{Z_i} / (N\,R_0)$

The apparent secondary capacitance is of course hidden within $\mathbf{Z_i}$, and since it is easier to expand this in reciprocal form, we will work with reciprocal transfer functions. Hence:

$$\frac{\mathbf{V}}{\mathbf{V_i}} = N\,R_0\left[\frac{1}{R_{ieff}} + \frac{1}{\mathbf{j}X_{Li}} + \frac{1}{\mathbf{j}X_{Cieff}}\right] \qquad (11.1)$$

Notice here that R_i has also been changed to an effective value to allow for the fact that if the shield protrusion capacitance (C_{sh}) changes the phase of the transformer output, then it will also affect the magnitude (and hence the apparent transfer efficiency).

Now, to include the effect of C_{sh}, we simply replace R_0 with $(R_0 \,//\, \mathbf{j}X_{Csh})$, and C_i and R_i change from their effective values to their 'true' (i.e., less-seriously skewed) values. Thus:

$$\frac{\mathbf{V}}{\mathbf{V_i}} = N\,(R_0 \,//\, \mathbf{j}X_{Csh}) \left[\frac{1}{R_i} + \frac{1}{\mathbf{j}X_{Li}} + \frac{1}{\mathbf{j}X_{Ci}} \right]$$

Expanding the parallel product gives:

$$\frac{\mathbf{V}}{\mathbf{V_i}} = N \frac{R_0\,\mathbf{j}X_{Csh}}{(R_0 + \mathbf{j}X_{Csh})} \left[\frac{1}{R_i} + \frac{1}{\mathbf{j}X_{Li}} + \frac{1}{\mathbf{j}X_{Ci}} \right]$$

and multiplying numerator and denominator by the complex conjugate of the denominator gives:

$$\frac{\mathbf{V}}{\mathbf{V_i}} = N \frac{R_0\,\mathbf{j}X_{Csh}\,(R_0 - \mathbf{j}X_{Csh})}{(R_0^2 + X_{Csh}^2)} \left[\frac{1}{R_i} + \frac{1}{\mathbf{j}X_{Li}} + \frac{1}{\mathbf{j}X_{Ci}} \right]$$

This is not a particularly tractable expression as it stands, but we can make the observation here that C_{sh} is a small capacitance in HF radio engineering terms and therefore $X_{Csh}^2 >> R_0^2$. Hence we can delete R_0^2 from the denominator without making a significant difference. Thus:

$$\frac{\mathbf{V}}{\mathbf{V_i}} = N R_0 \frac{\mathbf{j}X_{Csh}\,(R_0 - \mathbf{j}X_{Csh})}{X_{Csh}^2} \left[\frac{1}{R_i} + \frac{1}{\mathbf{j}X_{Li}} + \frac{1}{\mathbf{j}X_{Ci}} \right]$$

Multiplying out the left-most bracket (and noting that $\mathbf{j}^2 = -1$) gives:

$$\frac{\mathbf{V}}{\mathbf{V_i}} = N R_0 (1 + \mathbf{j}R_0 / X_{Csh}) \left[\frac{1}{R_i} + \frac{1}{\mathbf{j}X_{Li}} + \frac{1}{\mathbf{j}X_{Ci}} \right]$$

and multiplying out completely gives:

$$\frac{\mathbf{V}}{\mathbf{V_i}} = N R_0 \left[\frac{1}{R_i} + \frac{1}{\mathbf{j}X_{Li}} + \frac{1}{\mathbf{j}X_{Ci}} + \frac{\mathbf{j}R_0}{X_{Csh}\,R_i} + \frac{\mathbf{j}R_0}{\mathbf{j}X_{Csh}\,X_{Li}} + \frac{\mathbf{j}R_0}{\mathbf{j}X_{Csh}\,X_{Ci}} \right]$$

Now, noting that $\mathbf{j} = -1/\mathbf{j}$, the admittances in brackets can be regrouped thus :

$$\frac{\mathbf{V}}{\mathbf{V_i}} = N R_0 \left[\frac{1}{R_i} + \frac{R_0}{X_{Csh}\,X_{Li}} + \frac{R_0}{X_{Csh}\,X_{Ci}} + \frac{1}{\mathbf{j}X_{Li}} + \frac{1}{\mathbf{j}X_{Ci}} - \frac{R_0}{\mathbf{j}X_{Csh}\,R_i} \right]$$

Comparing this with equation **(11.1)**, we get:

$$\frac{1}{R_{ieff}} = \frac{1}{R_i} + \frac{R_0}{X_{Csh}\,X_{Li}} + \frac{R_0}{X_{Csh}\,X_{Ci}}$$

which is the same as:

$R_{ieff} = R_i \,//\, [\, -L_i / (C_{sh} R_0) \,] \,//\, (X_{Csh} X_{Ci} / R_0)$	**11.2**

Thus the shield displacement-current does affect the in-phase output, but since the magnitudes of the additional parallel components will be much larger than R_i, we can expect the difference identified here to be lost in the uncertainty of the transformer efficiency.

The capacitive susceptances tell a different story however:

$$\frac{1}{X_{Cieff}} = \frac{1}{X_{Ci}} - \frac{R_0}{X_{Csh}\,R_i}$$

i.e.:

$-2\pi f\, C_{ieff} = -2\pi f\, C_i + 2\pi f\, C_{sh}\, R_0 / R_i$

Hence:

$C_{ieff} = C_i - C_{sh}\, R_0 / R_i$	**11.3**

This expression tells us that if the earth connection to the Faraday shield is made on the load side of the transformer core, then the capacitance of the braid protruding from the other side reduces the apparent secondary parallel capacitance. In the preceding experiments, with $R_0 = R_i$, we measured an effective secondary capacitance of about 6 pF, expected at least 8 pF on the basis of time delay, and the shield protrusion capacitance was about 1.6 pF. So far, so good, but the true test of a hypothesis lies not in what it explains but in what it predicts.

Consider what happens when the earth connection to the Faraday shield is made on the generator side. The currents flowing through the transformer core are shown on the circuit diagram on the right. Now we have:

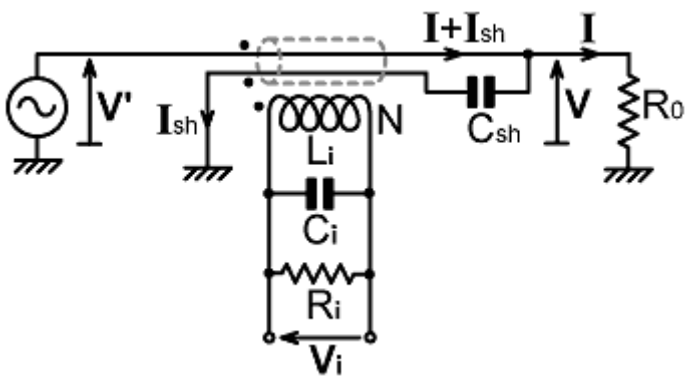

$\mathbf{V}i = (\mathbf{I} + \mathbf{I}_{sh} - \mathbf{I}_{sh})\, \mathbf{Z}_i / N$

i.e.:

$\mathbf{V}_i = \mathbf{I}\, \mathbf{Z}_i / N$

The shield protrusion displacement-current makes a hairpin loop through the core and cancels itself

out. Hence we predict the following:

● When the shield earth is on the generator side, the apparent secondary capacitance will be higher than for the converse configuration.

● When $R_0 = R_i$, the difference will be approximately equal to the capacitance of the shield protrusion for the case when the shield is earthed on the load side.

We can also note that the value of C_i obtained from bridge-parameter measurements when the shield is earthed on the generator side is the best starting point for estimating the true secondary capacitance.

In order to test the theory outlined above, the bridge used in the previous experiments was rebuilt with the Faraday shield earth connection on the generator side. The arrangement is shown below.

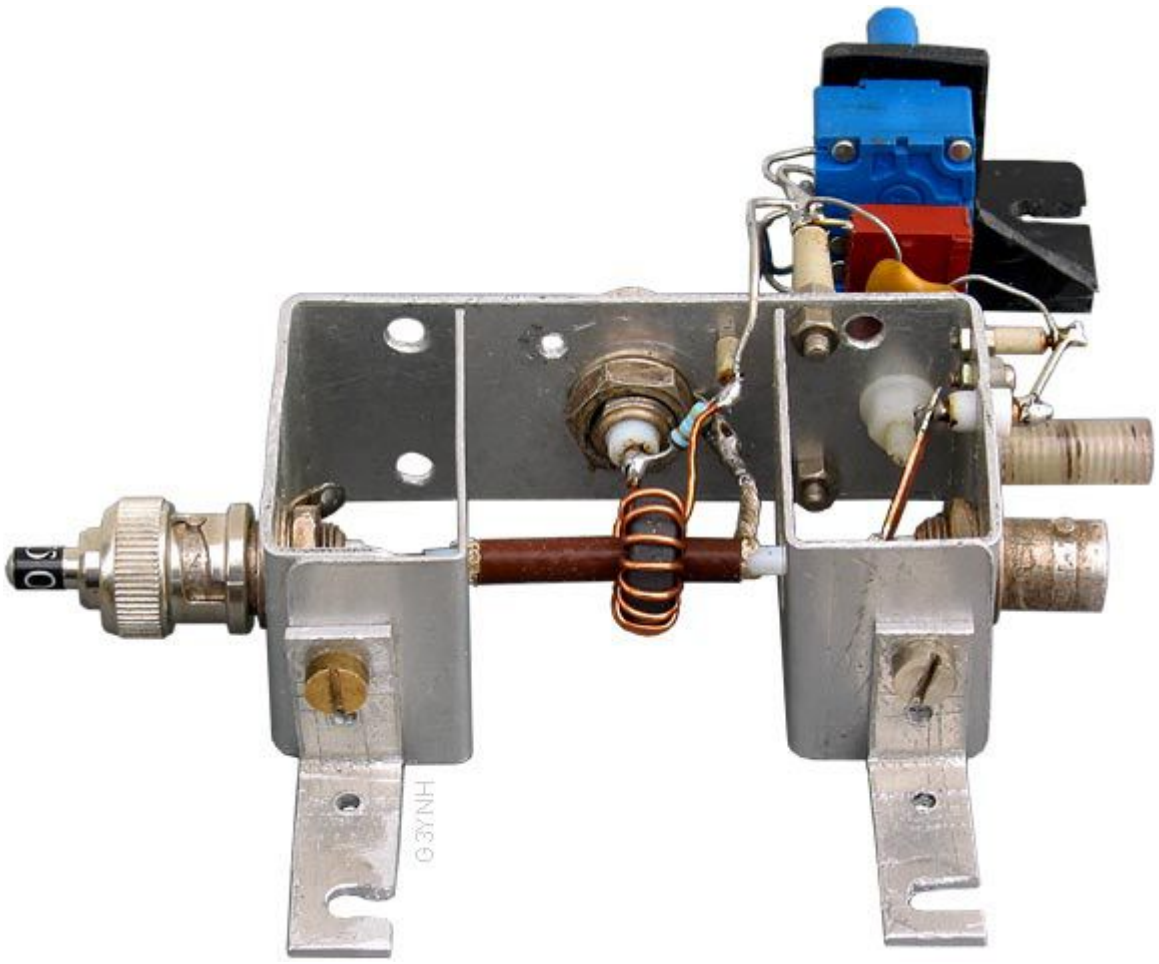

Care was taken to minimise disturbance to the circuit layout, but inevitably the various stray capacitances could not be exactly the same as before. The shield protruding beyond the transformer towards the load port measured 18.5 mm from the middle of the core (about 2.1 pF) but in this case we do not expect it to contribute to the apparent secondary capacitance. It was found that the phase crossover frequency had dropped from about 21 MHz to just over 18 MHz as a result of the shield reversal. Bridge balance datasets were acquired using both of the available reference capacitors and the results are summarised and compared with the previous experiments in the tables below. More detail can be had by downloading and studying the spreadsheets.

	Shield earthed on load side	Shield earthed on generator side	500 pF ref. cap.
Spreadsheet	**testbrg61-12_2.ods**	**testbrg61-12_4.ods**	See sheets 1 - 3.
Parameter	Value ±ESD	Value ±ESD	ESD in grey is precision from fit.
C_1'	109.0 ±1.1 pF	109.3 ±1.1 pF	
L_1	62.3 ±0.5 nH	61.6 ±0.4 nH	
C_{1s}	10.8 ±3 pF	10.4 ±3 pF	
L_i	8.98 ±0.18 µH	8.95 ±0.18 µH	Fitting data up to 5 MHz*
C_i	5.74 ±0.07 pF	7.94 ±0.07 pF	

	Shield earthed on load side	Shield earthed on generator side	40 pF ref. cap.
Spreadsheet	**testbrg61-12_3.ods**	**testbrg61-12_5.ods**	See sheets 1 - 3.
Parameter	Value ±ESD	Value ±ESD	ESD in grey is precision from fit.
C_1'	107.3 ±1.1 pF	107.4 ±1.1 pF	
L_1	80.8 ±0.3 nH	79.4 ±0.3 nH	
C_{1s}	12.5 ±3 pF	12.4 ±3 pF	
L_i	9.01 ±0.18 µH	8.94 ±0.18 µH	Fitting data up to 5 MHz*
C_i	5.74 ±0.08 pF	8.14 ±0.06 pF	

* L_2 fitting flag (Sheet 1, cell B7) must be set to zero to reproduce these results.

Shield reversal increased the apparent secondary capacitance by 2.2 pF, as against a prediction of about 1.6 pF based on the length of the shield protrusion when the earth was on the load side. Note here that the precision from the fit is not a fair estimate of the standard deviation of the secondary capacitance. Given the difficulty of maintaining exactly constant experimental conditions apart from the shield reversal, the true ESD is of the order of ±1 pF. Hence the experiment does confirm the shield displacement-current hypothesis to within the experimental accuracy.

For those who remain sceptical of shield displacement-current, the following experiment should settle any residual doubts. The bridge was re-jigged with the Faraday-shield earth on the load side and a trimmer capacitor was connected from the generator terminal to the unconnected end of the shield. The arrangement is shown below.

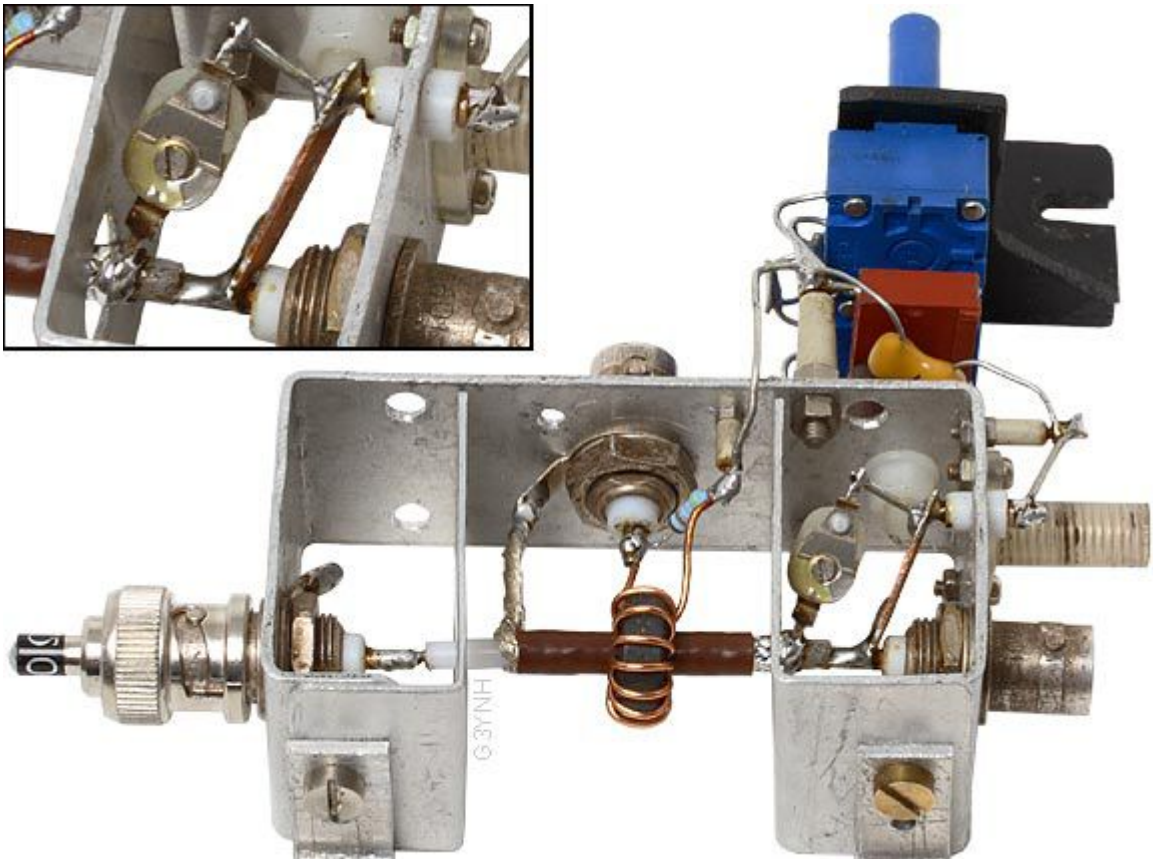

The bridge was balanced at 2 MHz by adjustment of R_V. Then the generator was tuned to 30 MHz, and without adjusting R_V, the bridge was balanced by adjusting the trimmer. Adjustments of R_V at 2 MHz and the trimmer at 30 MHz were repeated until no further improvement could be obtained (only two rounds of iteration were required in practice). The result was a bridge that balanced with the same value of R_V at both 2 MHz and 30 MHz. Only bridges with no effective secondary capacitance can do this.

Thus we must observe that, although the Faraday shield is at approximately earth-potential, it does not perform the simple screening function that is generally assumed. If the shield is grounded on the load side, the capacitance of the protrusion on the generator side partially neutralises the transformer secondary capacitance. Injecting an additional capacitive current into the free end of the shield can give complete neutralisation, thus confirming the displacement-current effect. It follows, that if the shield protrusion is too long, the transformer can appear to have a negative self-capacitance.

For the neutralisation experiment described above, the shield protrusion measured 16.5 mm from the middle of the transformer core (about 1.9 pF). The trimmer was carefully removed after adjustment and its capacitance was measured to be 5.6 pF. Strays across the trimmer body when mounted in the test jig were probably about 0.1 pF. Hence, by this crude method, we would expect the effective value of C_i to be about 7.6 pF with the shield earth on the generator side.

12. Inductance of the upper voltage-sampling arm

The quadrature balance condition for Douma's bridge was given in section **3** as:

$$\frac{1}{N R_0 R_v C_2} = \frac{1}{L_i} - (2\pi f)^2 C_i \qquad (3.3)$$

As has been mentioned previously however, this expression contains the assumption that C_2 does not vary with frequency, i.e., it assumes that there is no inductance in the upper voltage-sampling arm. More realistically, the wiring between the take-off point and the summing point has considerable inductance, as does the capacitor itself, and the total must amount to several tens of nano-Henries. This parasitic inductance is represented as a lumped component L_2 in the diagram below.

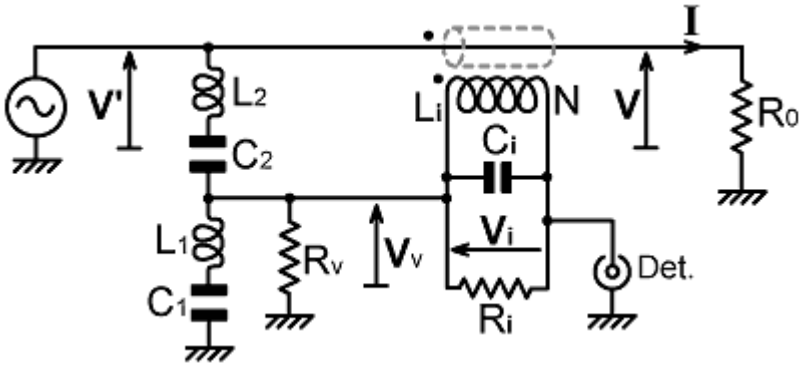

We can account for the existence of L_2 by replacing C_2, in equation (**3.3**) with a new quantity C_2' . A definition for C_2' is obtained by working backwards from the total reactance of the arm, i.e.:

$$X_{C2}' = X_{C2} + X_{L2}$$

Hence:

$$-1 / (2\pi f C_2') = [-1/(2\pi f C_2)] + 2\pi f L_2$$

which, upon multiplying both sides by $-2\pi f$ gives:

$$1 / C_2' = (1 / C_2) - (2\pi f)^2 L_2$$

We will leave the expression in its reciprocal form, because that is how we will need to use it.

Equation **(3.3)**, with the modified definition for C_2 becomes:

$$\frac{1}{N R_0 R_v} \left[\frac{1}{C_2} - (2\pi f)^2 L_2 \right] = \frac{1}{L_i} - (2\pi f)^2 C_i \qquad (12.1)$$

This can be re-grouped:

$$\frac{1}{N R_0 R_v C_2} = \frac{1}{L_i} - (2\pi f)^2 \left[C_i - \frac{L_2}{N R_v R_0} \right] \qquad (12.2)$$

Hence, comparing this with equation (**3.3**) reproduced above, we can see that L_2 reduces the apparent or 'effective' value of the secondary parallel capacitance. The adjustment caused by L_2 can be written:

$C_{ieff} = C_i - L_2 / (N R_v R_0)$	**12.3**

Now note that, if C_i represents a time delay in the transformer, we would expect L_2 to decrease its apparent value because a series inductance in the path through the voltage sampling network will have the effect of delaying the voltage sample. It is not so much that L_2 stores energy, but that it increases the distance that EM radiation has to travel before reaching the summing point.

Expression **(12.3)** above is perfectly valid for a working bridge, which has a fixed value for R_v. For the test bridge however, which is operated by adjusting R_v to track the changing balance point, it causes C_{ieff} to become frequency dependent. The result will be a slight deviation from the model used for the data analysis technique developed in section **3**. The solution is to correct the y-values used in the least-squares fit by subtracting the quantity $(2\pi f)^2 L_2 / (N R_0 R_v)$; i.e., the linear regression formula now becomes:

$$\frac{1}{N R_0 R_v}\left[\frac{1}{C_2} - (2\pi f)^2 L_2\right] = \frac{1}{L_i} - (2\pi f)^2 C_i$$

$$y = a + x\, b$$

In this way, a value for C_i that is already corrected for L_2 is obtained from the fit. The correction has in fact been included in the spreadsheets used for the post-optimisation data analysis (version 1.00 and above) and a flag is provided so that it can be turned on and off. For the test bridges studied so far, putting in 50 nH as a plausible value for L_2 causes a slight decrease in the reduced χ^2 for the fit and increases C_i by about 0.06 pF. Hence the small parasitic inductance of the upper voltage-sampling arm does not make much difference to the apparent value of C_i, but a more substantial difference will be obtained when we later insert an inductor in series with C_2 to correct the in-phase balance condition for the inductance of the lower potential-divider capacitor (see section **17**).

13. Inductance of the secondary load resistor

In section **11**, we wrote down an expression for the reciprocal transfer function of the 'ideal current transformer with parallel reactance' model:

$$\frac{\mathbf{V}}{\mathbf{V_i}} = N R_0 \left[\frac{1}{R_{ieff}} + \frac{1}{\mathbf{j}X_{Li}} + \frac{1}{\mathbf{j}X_{Cieff}} \right] \qquad (11.1)$$

This can be used as the basis for working-out all of the parasitic reactance corrections associated with the current transformer network; the trick being to include the component and drop the "eff(ective)" from the subscripts on R_i and C_i. Rearranging the new equation into the same form as **(11.1)** allows us to find the correction by comparing terms.

In the circuit on the right, the secondary load resistor has been allowed to have a finite inductance L_h. Thus the impedance of the secondary load resistor ($\mathbf{Z}_{Ri}$ say) becomes:

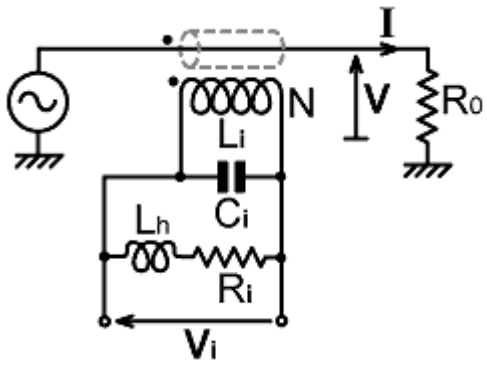

$$\mathbf{Z}_{Rieff} = R_i + \mathbf{j}X_{Lh}$$

Substituting this into equation **(11.1)** (and changing X_{Cieff} to X_{Ci}) gives:

$$\frac{\mathbf{V}}{\mathbf{V_i}} = N R_0 \left[\frac{1}{R_i + \mathbf{j}X_{Lh}} + \frac{1}{\mathbf{j}X_{Li}} + \frac{1}{\mathbf{j}X_{Ci}} \right]$$

Multiplying numerator and denominator of the first term in square brackets by the complex conjugate of its denominator then gives:

$$\frac{\mathbf{V}}{\mathbf{V_i}} = N R_0 \left[\frac{R_i - \mathbf{j}X_{Lh}}{R_i^2 + X_{Lh^2}} + \frac{1}{\mathbf{j}X_{Li}} + \frac{1}{\mathbf{j}X_{Ci}} \right]$$

But L_h is a very small inductance in HF radio engineering terns (<20 nH if the resistor wires are kept short) and so we may reasonably apply the approximation $R_i^2 >> X_{Lh}^2$. This allows us to delete X_{Lh}^2 from the denominator of the first term. Hence:

$$\frac{\mathbf{V}}{\mathbf{Vi}} = N R_0 \left[\frac{1}{R_i} + \frac{1}{\mathbf{j}X_{Li}} + \frac{1}{\mathbf{j}X_{Ci}} - \frac{\mathbf{j}X_{Lh}}{R_i^2} \right]$$

The term containing X_{Lh} has been grouped with the capacitive admittances because an inductance divided by a resistance-squared has dimensions of capacitance. Comparing this with equation **(11.1)** reproduced above, and noting that $\mathbf{j}=-1/\mathbf{j}$, we get:

$-2\pi f\, C_{ieff} = -2\pi f\, C_i + 2\pi f\, L_h / R_i^2$

i.e.:

$C_{ieff} = C_i - L_h / R_i^2$	**13.1**

In the optimised test bridge, the secondary was terminated by a single 49.9 Ω 0.6 W metal-film resistor. It was thought initially that the use of such a component would help to minimise parasitic reactance, but suspicions began to arise in the process of reconciling the data from different experiments. Finally, the paint was scraped from one of the units to see what lay beneath, and the sorry outcome is shown below.

Low Q current-sheet inductor described in the sales literature as a "resistor".
N = 4.5 , ℓ = 4.2 mm , d = 1.7 mm ,
giving L_{body} =11.6 nH .
R = 49.9 Ω.
For C = 0.4 pF , SRF = 2.3 GHz .

We might guess that cutting a helix is cheaper than depositing a thinner film or making a number of offset slits. Whatever the reason for the abomination however, the result is not optimal for RF applications. A current-sheet formula gives the partial inductance of the body as 11.6 nH which, with an allowance for the end-caps and the short connecting wires (the distance between the terminals was 10.5 mm), makes the total partial inductance contribution up to about 15 ±2 nH. A properly designed resistor of the same body and lead dimensions would have had an inductance of 6 nH.

Using equation **(13.1)**, it can be determined that a 49.9 Ω resistor with an inductance of 15 ±2 nH reduces the apparent secondary capacitance by 6 ±0.8 pF. Hence, the inductance of the secondary load resistor has a large effect on the apparent value of C_i .

Equation **(13.1)** also tells us that the secondary capacitance can be neutralised by adjusting the series inductance of the secondary load resistor. This is the basis of an empirical high-frequency bridge compensation scheme patented by Will Herzog, K2LB, in 1988 [**US Pat. No. 4739515**]. Hence L_h is 'Herzog's inductance', and the subscript h is used here for that reason. For bridges with relatively few turns in the transformer secondary, such as the ones so-far studied, the additional inductance required is extremely small; and indeed, it is possible to over-compensate merely by leaving long wires on the resistor.

The secondary parallel capacitance can be split into two components:

$C_i = C_i' + C_{is}$

Where C_i' is the 'self-capacitance' of the coil and C_{is} is the stray capacitance across the winding. Hence we can rewrite equation **(13.1)**:

$C_{ieff} = C_i' + C_{is} - L_h / R_i^2$	**13.2**

C_{is} is mainly attributable to the load resistor, and for a typical ½ W metal-film resistor amounts to about 0.4 pF. Hence, in this application, the inductance of the resistor reduces the apparent self-capacitance to a greater extent than the capacitance of the resistor increases it.

Notice here that if two resistors in parallel are used for the secondary load, the inductance will be halved and the capacitance doubled. The total contribution from the resistor in the example above is:

-6 + 0.4 = -5.6 pF

but for two ½ W resistors of similar inductance in parallel it would be

-3 + 0.8 = -2.2 pF

Observe also that the resistor provides a neutral termination when:

$C_{is} - L_h / R_i^2 = 0$

i.e., when

$R_i = \sqrt{(L_h / C_{is})}$

This is a transmission-line formula that defines the properties of a perfectly matched terminating resistor. The smaller the values of inductance and capacitance used to match the resistance, the higher the self-resonance frequency (SRF) of the resistor.

14. Mismatch of the main transmission line

The main transmission line or 'through-line'; passing from the generator port, through the transformer core, to the load port; is not correctly terminated. In particular, the short sections of unshielded central conductor before and after the Faraday shield will raise the average characteristic resistance to be somewhat greater than that of the shield cable.

The impedance transformation due to a lossless transmission line is given by:

$$\mathbf{Z}_{in} = \frac{R_{line} [\mathbf{Z}_L + \mathbf{j} R_{line} \operatorname{Tan}(2\pi \ell' / \lambda_0)]}{[R_{line} + \mathbf{j} \mathbf{Z}_L \operatorname{Tan}(2\pi \ell' / \lambda_0)]}$$

where: R_{line} is the characteristic resistance (here we use R_{line} instead of R_0 to avoid confusion with the reference load resistor), $\mathbf{Z}_L$ is the load impedance, ℓ' is the electrical length of the line, $\mathbf{Z}_{in}$ is the impedance looking into the line, λ_0 is the free-space wavelength, and $2\pi \ell' / \lambda_0$ is in radians.

In the test bridge, the distance from the centre of the transformer core to the load terminal is about 3 cm. About 2 cm of that distance lies inside a coaxial cable with PTFE insulation. PTFE has a dielectric constant (ε_r') of about 2.05 , and hence a velocity factor of $1 / \sqrt{\varepsilon_r'} = 0.7$. Thus the total electrical distance ℓ' is about 1 + 2 / 0.7 = 3.9 cm . At the high end of the HF spectrum, the wavelength is 10 m. Hence $\operatorname{Tan}(2\pi \ell' / \lambda_0) = 0.0082$. If $\mathbf{Z}_L = 50 + \mathbf{j}0\ \Omega$, and we guess that the average characteristic resistance is about 60 Ω , then the transmission line equation gives $\mathbf{Z}_{in} = 49.994 + j0.151\ \Omega$, which has a phase angle of 0.17°. This is a very small phase error of course; but as we will see, it is actually at least twenty times greater than the resolution of the experimental method, and a better understanding of the bridge phase response can be had by taking it into account.

The characteristic resistance (or 'surge resistance') of a lossless transmission line is given by:

$$R_{line} = \sqrt{(L_0 / C_0)}$$

where L_0 is the inductance *per unit length* and C_0 is the capacitance *per unit length*. For a short length of line, we can treat the distributed inductance and capacitance as lumped components L_0 and C_0 . Hence:

$$R_{line} = \sqrt{(L_0 / C_0)}$$

A characteristic resistance higher than the target load resistance implies that the inductance will dominate slightly over the capacitance; and as we will now show, the result will be a shift in the apparent self-capacitance of the secondary winding.

The capacitance of the transmission line on the load side of the transformer core is represented in the diagram on the right. We can account for it by replacing R_0 with $R_0 // \mathbf{j}X_{C0}$ in equation **(11.1)**. There is no need to bother with the rest of the working however, because the situation is exactly analogous to the effect of the Faraday shield protrusion capacitance as discussed in section **11**. Hence, taking the solution from equation **(11.3)**:

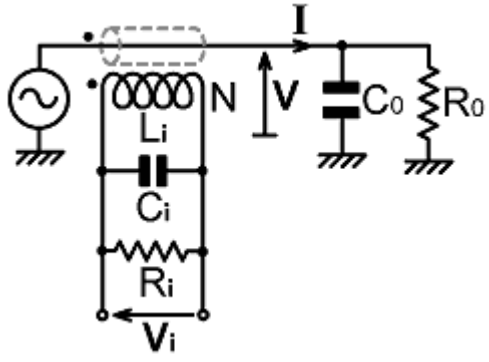

$C_{ieff} = C_i - C_0 R_0 / R_i$	**14.1**

From the sign of the contribution, it is evident that the transformer secondary capacitance can be neutralised by placing a capacitor across the load port.

C_0 will also have a small effect on the in-phase response of the transformer. Taking the solution from equation(**11.2**) we get:

$R_{ieff} = R_i // [-L_i / (C_0 R_0)] // (X_{C0} X_{Ci} / R_0)$	**14.2**

In order to account for the transmission-line inductance, we can replace R_0 in equation **(11.1)** with $R_0 + \mathbf{j}X_{L0}$. This gives:

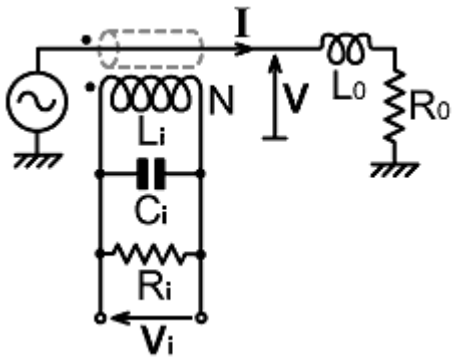

$$\frac{\mathbf{V}}{\mathbf{V_i}} = N\,(R_0 + \mathbf{j}X_{L0})\left[\frac{1}{R_i} + \frac{1}{\mathbf{j}X_{Li}} + \frac{1}{\mathbf{j}X_{Ci}}\right]$$

Since we need to put this into a form comparable to equation **(11.1)**, we will start by factoring out R_0. Thus:

$$\frac{\mathbf{V}}{\mathbf{V_i}} = N\,R_0\left[1 + \frac{\mathbf{j}X_{L0}}{R_0}\right]\left[\frac{1}{R_i} + \frac{1}{\mathbf{j}X_{Li}} + \frac{1}{\mathbf{j}X_{Ci}}\right]$$

Multiplying-out the brackets gives:

$$\frac{\mathbf{V}}{\mathbf{V_i}} = N\,R_0\left[\frac{1}{R_i} + \frac{1}{\mathbf{j}X_{Li}} + \frac{1}{\mathbf{j}X_{Ci}} + \frac{\mathbf{j}X_{L0}}{R_0 R_i} + \frac{\mathbf{j}X_{L0}}{\mathbf{j}R_0 X_{Li}} + \frac{\mathbf{j}X_{L0}}{\mathbf{j}R_0 X_{Ci}}\right]$$

and the terms can be regrouped into conductive, inductive and capacitive admittances:

$$\frac{\mathbf{V}}{\mathbf{V_i}} = N\,R_0\left[\frac{1}{R_i} + \frac{L_0}{R_0 L_i} + \frac{X_{L0}}{R_0 X_{Ci}} + \frac{1}{\mathbf{j}X_{Li}} + \frac{1}{\mathbf{j}X_{Ci}} - \frac{X_{L0}}{\mathbf{j}R_0 R_i}\right]$$

This allows us to make the identifications:

$C_{ieff} = C_i + L_0 / (R_0 R_i)$	**14.3**

and

$R_{ieff} = R_i // (R_0 L_i / L_0) // (R_0 X_{Ci} / X_{L0})$	**14.4**

Now, to obtain the combined effect of the through-line inductance and capacitance on the apparent secondary capacitance, we combine equations **(14.1)** and **(14.3)**:

$C_{ieff} = C_i + [\ L_0 / (R_0\ R_i\ )] - C_0\ R_0 / R_i$

i.e.:

$C_{ieff} = C_i + (1/R_i)\ [\ (L_0 / R_0) - C_0\ R_0\ ]$	**14.5**

but recall that $R_{line} = \sqrt{(L_0/C_0)}$, i.e.,

$L_0 = C_0\ R_{line}^2$

Hence:

$C_{ieff} = C_i + (C_0 / R_i)\ [\ (R_{line}^2 / R_0) - R_0\ ]$

or alternatively

$C_{ieff} = C_i + [\ C_0 / (\ R_0\ R_i\ )\ ]\ (\ R_{line}^2 - R_0^2\ )$	**14.6**

which tells us that the through-line mismatch adds a fixed component to the apparent secondary capacitance, unless $R_{line} = R_0$, in which case the contribution is zero. If $R_{line} > R_0$, as is usually the case, the contribution is positive.

One conclusion that we can draw here is that the stub of coaxial cable used for the Faraday-shielded primary should normally have a characteristic resistance that is the same as R_0. It is also advisable to keep the stripped sections before and after the transformer as short as possible, since these will raise the average surge-resistance of the through-line and so lower the phase-crossover frequency of the transformer output.

The effect of through-line mismatch on the in-phase transformer response is obtained by combining equations **(14.2)** and **(14.4)**.

$R_{ieff} = R_i\ //\ (\ R_0\ L_i\ /\ L_0\ )\ //\ [\ -L_i\ /\ (\ C_0\ R_0\ )\ ]\ //\ (R_0\ X_{Ci}\ /\ X_{L0}\ )\ //\ (\ X_{C0}\ X_{Ci}\ /\ R_0\ )$

This is easier to parse when expressed as a series of conductances:

$$\frac{1}{R_{ieff}} = \frac{1}{R_i} + \frac{L_0}{R_0\ L_i} - \frac{C_0\ R_0}{L_i} + \frac{X_{L0}}{R_0\ X_{Ci}} + \frac{R_0}{X_{C0}\ X_{Ci}}$$

Which can be rearranged thus:

$$\frac{1}{R_{ieff}} = \frac{1}{R_i} + \frac{1}{L_i}\left[\ \frac{L_0}{R_0} - C_0\ R_0\ \right] - (2\pi f)^2\ C_i\left[\ \frac{L_0}{R_0} - C_0\ R_0\ \right]$$

and then factorised:

$$\frac{1}{R_{ieff}} = \frac{1}{R_i} + \left[\frac{1}{L_i} - (2\pi f)^2 C_i \right] \left[\frac{L_0}{R_0} - C_0 R_0 \right]$$

Once again we can use the substitution $L_0 = C_0 R_{line}^2$, hence:

$$\frac{1}{R_{ieff}} = \frac{1}{R_i} + \left[\frac{1}{L_i} - (2\pi f)^2 C_i \right] \frac{C_0}{R_0} (R_{line}^2 - R_0^2)$$

As before, the contribution is zero when $R_{line} = R_0$, but a frequency dependence is introduced when there is a mismatch. The change in the apparent efficiency of the transformer is however very weak for realistic parameters (<0.2%), as can be seen by examining the simulation in the spreadsheet **mismatch_sim.ods**. It is also similar in form to the effect of the inductance of the lower voltage sampling network capacitor, and so its effect on the in-phase balance condition will be absorbed into any inductance-balance correction.

Notice incidentally that the factor $(1/L_i) - (2\pi f)^2 C_i$ is $1 / L_i'$, which is the reciprocal of the apparent secondary inductance as used in the least-squares fitting procedure described in section **3**.

One way to show the effect of the transmission-line mismatch is to measure (or attempt to measure) the apparent secondary capacitance with two different values of load resistor. This is done in the spreadsheets listed below:

testbrg61-12_6.ods	75.5 Ω reference load. Generator-side shield earth.
testbrg61-12_7.ods	50 Ω reference load. Generator-side shield earth.

The dominance of the line capacitance for the bridge with the 75.5 Ω load is so great that the apparent secondary capacitance is negative.

15. Correction series for effective transformer-secondary capacitance

The full menagerie of parasitic inductances and capacitances, or at least the ones that make a significant contribution, are shown on the diagram below.

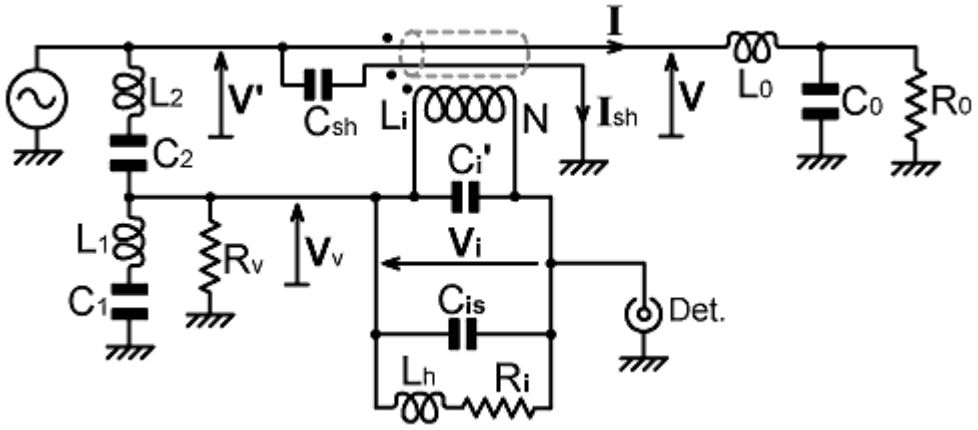

Combining equations **(13.1)**, **(12.3)**, **(14.1)**, **(14.3)** and **(11.3)** gives an arithmetic series for the apparent secondary capacitance of the current transformer; i.e., the capacitance that, in combination with the secondary coupled inductance L_i , determines the phase crossover frequency and the bridge phase-error at high frequencies.

$$C_{ieff} = C_i' + C_{is} - \frac{L_h}{R_i^2} - \frac{L_2}{N R_v R_0} + \frac{L_0}{R_i R_0} - \frac{C_0 R_0}{R_i} - \frac{C_{sh} R_0}{R_i} \qquad (15.1)$$

Sec. Load | VS network | Through-line

It is now possible to see why there has never been a consistent view regarding the importance of transformer self-capacitance in determining bridge performance. If the apparent secondary capacitance included in the basic model (section **2**) is attributed to self-capacitance alone; then bridge designers (should they have a method for measuring it) will find that self-capacitance can be either positive, negative, or accidentally zero. It all depends on the physical layout, the parasitic reactances of the components, and the lengths and diameters of the various wires and cables. While such issues remain uncontrolled, it will be impossible for one constructor to reproduce the results obtained by another.

It is perhaps relevant at this point to ask whether equation **(15.1)** is complete (at least with regard to effects that make a difference of more than about 0.1 pF), and the answer is "not quite". There is nothing in the theory developed so-far that accounts for the fact that the effective velocity for a wave travelling in the line from the voltage sampling point to the current-transformer is less than c . The PTFE dielectric used in the test bridge has a velocity factor of 0.7 . The small additional delay will increase C_{ieff} slightly, but in terms of the model, it will merely decrease the effective inductance of the upper voltage sampling arm (i.e, a small delay in the current sampling path is equivalent to a small advance in the voltage sampling path).

In equation **(15.1)**, all of the terms with a (-) sign represent possible methods for neutralising the transformer self-capacitance, and there are others. Neutralisation techniques are explored in section **18**.

16. Bridge performance evaluation

In normal design practice, component tolerances and uncertainty in the known value of the transformer secondary coupled inductance dictate that the LF compensation resistance R_v should be made adjustable. Likewise, a lack of knowledge of the transformer losses and coupling factor and the amount of stray capacitance dictates that the voltage sampling network ratio should be made adjustable. As has been demonstrated by the previous experiments however, these two adjustments are only sufficient to allow the bridge to be calibrated at a single frequency, and there will be some error everywhere else. A question that needs to be answered therefore is: "If a bridge is calibrated at some specified frequency, how accurate will it be at other frequencies?"

As was mentioned in the introduction, a direct answer to this question can only be had by using a dummy antenna and some kind of impedance analyser; but we can turn the problem on its head by choosing notional 'set' values for the adjustable components and then measuring how far the actual components need to differ from the set values in order to balance the bridge. These parameter shifts are 'perturbations', which can be applied to the circuit model in order to determine the extent to which the load impedance must differ from the target load impedance if the bridge is to balance using the set values.

The situation that needs to be analysed here is that of a bridge that is calibrated at some frequency by adjustment of C_1 and R_V as shown in the diagram below. At the calibration frequency, the bridge balances when connected to a reference impedance R_0; but in normal service C_1 and R_V cannot be changed, and so at frequencies other than the calibration frequency, the load impedance required to balance the bridge ($\mathbf{Z}_{bal}$) will differ from R_0. Our objective is to determine $\mathbf{Z}_{bal}$ at some arbitrary frequency by balancing the bridge with R_0 connected, measuring C_1 and R_V, and comparing these values with the values (C_{1set} and R_{Vset} say) that were required at the calibration frequency.

The overall balance condition for a Douma bridge was given earlier as:

$$[\,(\mathbf{j}X_{C1} \,//\, \mathbf{j}X_{C2} \,//\, R_V) / \mathbf{j}X_{C2}\,]\,[\,1 + \mathbf{Z}_i / (R_0\,N^2)\,] = \mathbf{Z}_i / (N\,R_0) \qquad \ldots\ldots\ldots \textbf{(16.1)}$$

Where:

$\mathbf{Z}_i = R_i \,//\, \mathbf{j}X_i$

and in this case

$X_i = 2\pi f\, L_i'$

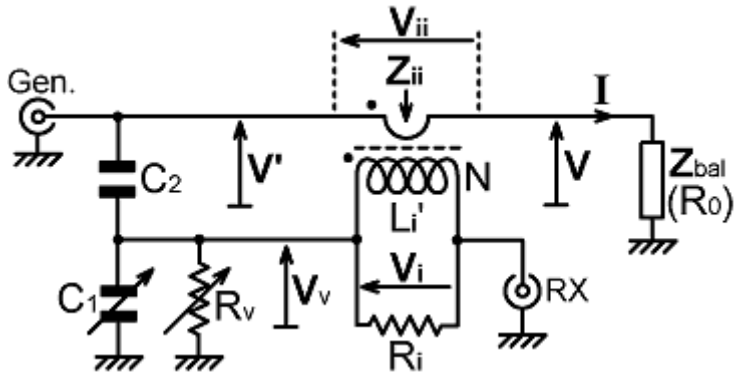

If the bridge is out of balance at the test frequency because C_{1set} and R_{Vset} are used instead of the optimal values, then equation **(16.1)** becomes:

$$[\,(\mathbf{j}X_{C1set} \,//\, \mathbf{j}X_{C2} \,//\, R_{Vset}) / \mathbf{j}X_{C2}\,]\,[\,1 + \mathbf{Z}_i / (\mathbf{Z}_{bal}\,N^2)\,] = \mathbf{Z}_i / (N\,\mathbf{Z}_{bal}) \qquad \ldots\ldots \textbf{(16.2)}$$

Hence, the relationship between $\mathbf{Z}_{bal}$ and R_0 can be determined by dividing equation **(16.1)** by equation **(16.2)**:

$$\frac{\mathbf{Z}_{bal}}{R_0} = \frac{[\,(\mathbf{j}X_{C1} \,//\, \mathbf{j}X_{C2} \,//\, R_V) / \mathbf{j}X_{C2}\,]\,[\,1 + \mathbf{Z}_i / (R_0\,N^2)\,]}{[\,(\mathbf{j}X_{C1set} \,//\, \mathbf{j}X_{C2} \,//\, R_{Vset}) / \mathbf{j}X_{C2}\,]\,[\,1 + \mathbf{Z}_i / (\mathbf{Z}_{bal}\,N^2)\,]}$$

Now, to make the problem mathematically tractable, we may note that the factors $1 + \mathbf{Z_i} / (R_0 N^2)$ and $1 + \mathbf{Z_i} / (\mathbf{Z_{bal}} N^2)$ are present only to account for the small difference between **V** and **V'** . Since these factors are already close to unity, and we do not expect $\mathbf{Z_{bal}}$ to differ greatly from R_0, we may reasonably use the approximation:

$$1 + \mathbf{Z_i} / (R_0 N^2) = 1 + \mathbf{Z_i} / (\mathbf{Z_{bal}} N^2)$$

This gives the simplification:

$$\frac{\mathbf{Z_{bal}}}{R_0} = \frac{\mathbf{j}X_{C1} // \mathbf{j}X_{C2} // R_V}{\mathbf{j}X_{C1set} // \mathbf{j}X_{C2} // R_{Vset}}$$

If we also define a new variable:

$$C_V = C_1 + C_2$$

and a new parameter

$$C_{Vset} = C_{1set} + C_2$$

then

$$X_{C1} // X_{C2} = X_{CV}$$

etc.. Hence:

$$\frac{\mathbf{Z_{bal}}}{R_0} = \frac{R_V // \mathbf{j}X_{CV}}{R_{Vset} // \mathbf{j}X_{CVset}}$$

Expanding the parallel products gives:

$$\frac{\mathbf{Z_{bal}}}{R_0} = \frac{\mathbf{j}\, R_V X_{CV} (R_{Vset} + \mathbf{j}X_{CVset})}{(R_V + \mathbf{j}X_{CV})\, \mathbf{j}\, R_{Vset} X_{CVset}}$$

and recalling that $X_C = -1 / (2\pi f C)$

$$\frac{\mathbf{Z_{bal}}}{R_0} = \frac{R_V C_{Vset} (R_{Vset} + \mathbf{j}XC_{Vset})}{R_{Vset} C_V (R_V + \mathbf{j}X_{CV})}$$

Now we can multiply the numerator and denominator by the complex conjugate of the denominator with a view to putting the equation into a+**j**b form:

$$\frac{\mathbf{Z_{bal}}}{R_0} = \frac{R_V C_{Vset} (R_{Vset} + \mathbf{j}X_{CVset})(R_V - \mathbf{j}X_{CV})}{R_{Vset} C_V (R_V^2 + X_{CV}^2)}$$

Multiplying out:

$$\frac{\mathbf{Z}_{bal}}{R_0} = \frac{R_V C_{Vset} [R_V R_{Vset} + X_{CV} X_{CVset} + \mathbf{j}(R_V X_{CVset} - R_{Vset} X_{CV})]}{R_{Vset} C_V (R_V^2 + X_{CV}^2)}$$

Thus we obtain the formula for bridge evaluation by perturbation analysis:

Let $U = R_V C_{Vset} / [R_{Vset} C_V (R_V^2 + X_{CV}^2)]$ where $C_V = C_1'_0 + C_{1s} + C_2$ $C_{Vset} = C_{1set} + C_2$ and let $\mathbf{Z}_{bal} = R_{bal} + \mathbf{j}X_{bal}$ Then $R_{bal} = R_0 U (R_V R_{Vset} + X_{CV} X_{CVset})$ $X_{bal} = R_0 U (R_V X_{CVset} - R_{Vset} X_{CV})$ $\|\mathbf{Z}_{bal}\| = \sqrt{(R_{bal}^2 + X_{bal}^2)}$ $\varphi_{bal} = \text{Arctan}(X_{bal} / R_{bal})$	**16.3**

Note that the C_1' required here is the true value (corrected for inductance), i.e., $C_1'_0$; the point being that the frequency at which the reference capacitor was calibrated should not have any bearing on the outcome of the test. A definition for $C_1'_0$ is given by rearrangement of equation **(4.2)**:

$$C_1'_0 = 1 / [(1 / C_1'_m) + (2\pi f_m)^2 \ L_1]$$

$C_1'_m$ being the raw measured value and f_m the measuring frequency. When the capacitance meter operates at 10^7 radians/sec this becomes:

$$C_1'_0 = 1 / [(1 / C_1'_m) + 10^{14} L_1]$$

In practice, this correction is small, but since it can be computed easily it might as well be included.

The value of C_{1s} does not need to be known accurately. In the evaluation spreadsheet discussed below, C_{1s} is calculated from the transformer constant, which is defined as:

$$K_T = C_1 / C_2 = (N R_0 / k R_i) + (1 / N) - 1$$

where

$C_1 = C_1'_0 + C_{1s}$

but it can be put in directly if so desired. If the value used is accurate, then the value of C_{1set} that gives optimal performance will be accurate; otherwise, the determined value for C_{1set} will be nominal only. It is a good idea to ensure that C_{1s} is plausible, but the chosen value makes little difference to the outcome of the analysis.

Notice also that the formula **(16.3)** contains no current-transformer network parameters. The details of the current transformer are irrelevant as far as the evaluation procedure is concerned; the test merely determines how well the bridge stays in balance as the frequency is changed.

16a. Performance of uncorrected bridges

In sections **10** and **11** we extracted the lumped-component circuit parameters from four datasets, the raw data and mathematical analysis being given in the spreadsheets listed below:

Faraday shield earth ↓	500 pF ref. cap.	40 pF ref. cap.
Load side	**testbrg61-12_2.ods**	**testbrg61-12_3.ods**
Generator side	**testbrg61-12_4.ods**	**testbrg61-12_5.ods**

In each case, the data were also subjected to the perturbation analysis developed above, the details appearing on sheet 5 of the spreadsheet.

The most striking outcome in every case is that the graph of phase error in degrees vs. frequency is always a straight line; so straight in fact that an additional least-squares routine was written to extract the gradient. The result for the bridge with the Faraday shield earthed on the generator side (taken from **testbrg61-12_4.ods**) is shown below:

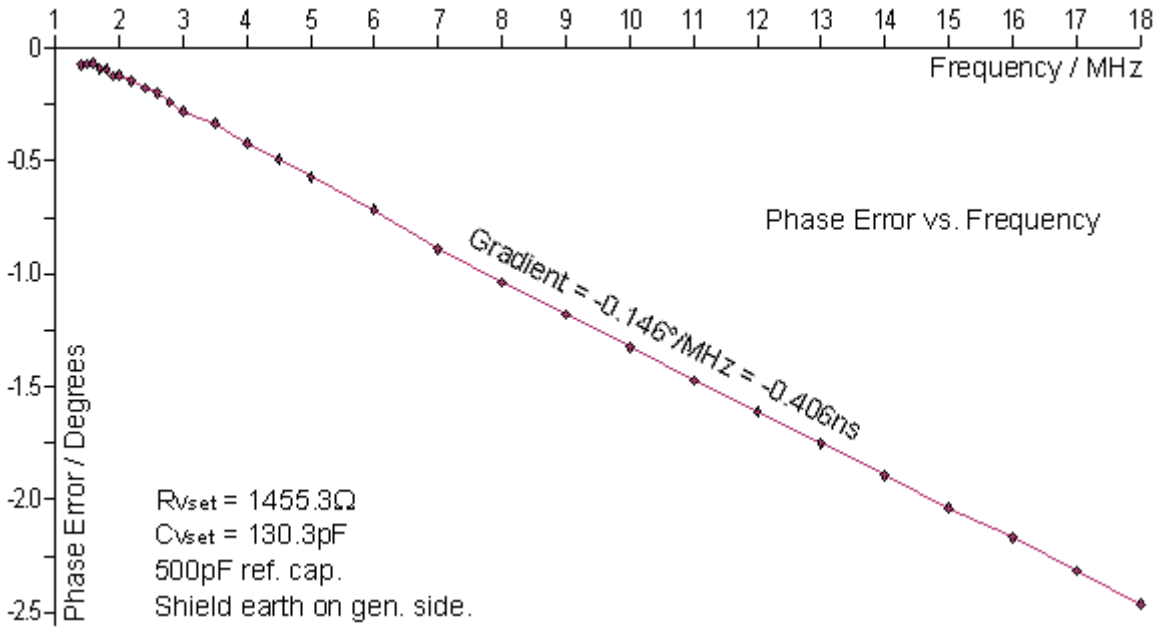

A measurement in degrees per MHz is a ***time***. Specifically it is only necessary to divide the gradient by 360 to get a time in microseconds. The fit to the phase error returned a gradient of -0.1461°/MHz , which corresponds to a time of -0.4059 ns (negative because it is a delay).

The linearity of the graph is a clear indication that the phase error of the bridge is merely an error of time-coincidence. This can best be understood by considering the bridge as an optical interferometer. An EM wave enters the bridge and is split into two components. The two components make separate journeys over electrical distances that do not have to be identical, one is inverted, and then the waves are combined. Any difference in the electrical paths results in incomplete cancellation. Much of the error can be accounted for merely by considering the distances involved, but the various inductances and capacitances encountered along the way alter the apparent propagation velocity in the regions in which they reside. A series inductance largely serves to convolute the path, and the delay can be deduced approximately by unravelling the wire and measuring it. A parallel reactance however acts as a scattering element, by storing energy and returning it to the system with a shift of phase. It is the combination of the incident and the

scattered wave that appears to have a velocity that differs from c.

What is remarkable is not that the bridge can be understood in terms of time and distance, but that the lumped component theory accounts for its behaviour so well. The only component that seems to come from nowhere is the 'self-capacitance' of the transformer C_i', and although it is difficult to control the experiment well enough to prove it exactly, a plausible value, definitely close to the true one, is obtained by taking the average distance that must be travelled by a wave propagating through the transformer. That distance is half the electrical length of the secondary winding wire, plus the electrical distance from the voltage sampling point to the transformer core.

For the test bridge with the Faraday shield earthed on the generator side, the distance from the input port to the middle of the transformer was 28 mm, 12 mm of that being inside a cable with PTFE dielectric. The length of the secondary winding wire was 228 mm. Assuming an effective propagation velocity of c within the transformer, this gives:

$$C_i' = [\ (228 / 2) + 1.6 + 1.2 / 0.7\ ]\times 10^{-3} / (R_i\ c) = 0.1173 / (49.9\ c) = 7.8\ \text{pF}$$

The corresponding time delay is:

$$0.1173 / c = 0.3913\ \text{ns}.$$

This is remarkably close to the gradient of the graph above, but from the discussion in sections **12** to **15**, the agreement is obviously accidental. In practice, the effective velocity within the transformer will be somewhat less than c , and C_i' will be correspondingly increased.

So, hopefully having laid to rest the idea that the self-capacitance of a coil is due to the proximity of adjacent turns, we can now admit that the graph of phase error vs. frequency is not perfectly linear. The deviation is however very small, as can be seen by noting the scale of the y-axis in the graph below.

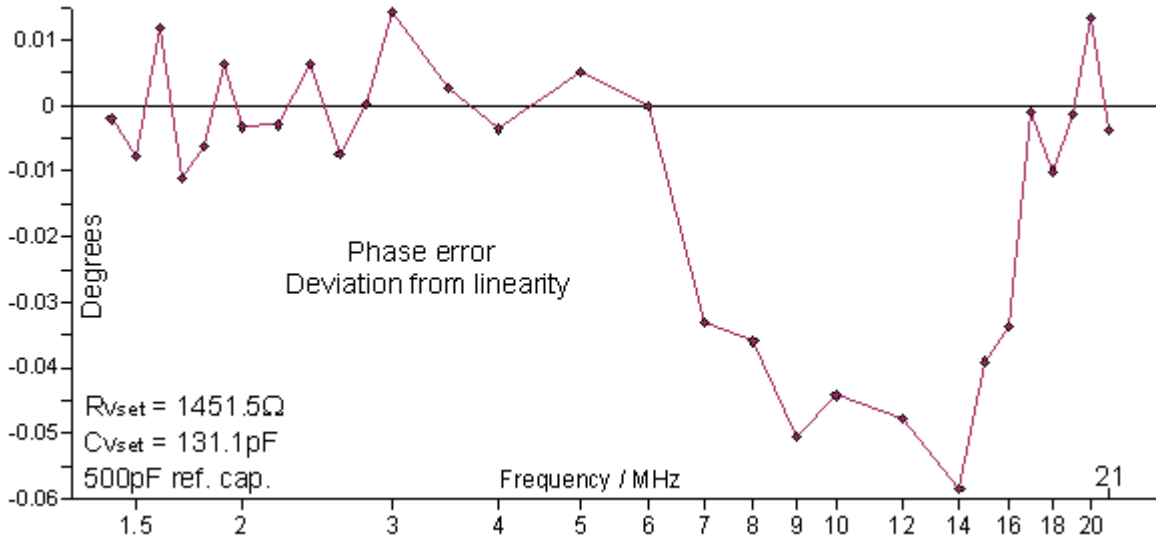

There is a slight increase in the phase lag between about 6 MHz and 17 MHz. This, of course, corresponds to the increase in permeability at the onset of a dispersion region in type 61 ferrite material, as was discussed in Section **10**. The reason why the peak is inverted in the graph above is that an increase in the inductance of a parallel LCR system (i.e., the transformer secondary) gives greater dominance to the capacitive arm. The deviation amounts to about 60 milli degrees, and so, if the system is adjusted to absorb it, it limits the ultimate phase performance of transformers using

type 61 material to about ±0.03° (and other ferrites are similar). When the dispersion peak is excluded from the fit, the rest of the data (for any of the experiments) can be fitted with an RMS deviation of about ±0.0075°, i.e., 7.5 thousandths of a degree. This is the phase-resolution of the experimental method.

The perturbation method also produces magnitude information. Shown below are graphs of magnitude error, the two curves giving a comparison between the results obtained with the 40 pF reference capacitor, which has an effective series inductance of about 80 nH (neglecting L2) ; and the 500 pF capacitor, which has an effective inductance of about 62 nH.

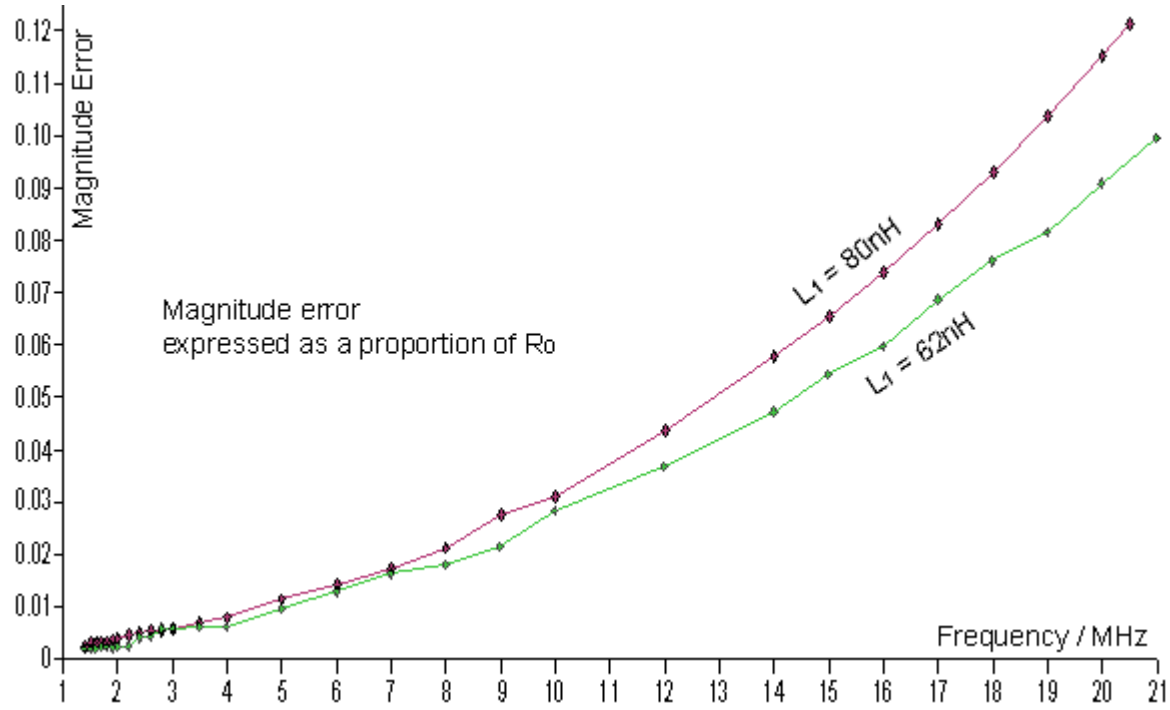

The inductance of the 500 pF reference capacitor gives rise to a magnitude error of about 10% at 21 MHz, i.e., a bridge that should balance with a load of 50 Ω will actually balance when the load is 55 Ω . In a working bridge, of course, we might minimise this error by keeping the wires short and using very small components for C_1 ; but the test bridge had a divider ratio of only about 11.6:1 in the voltage sampling network. For a bridge with a larger transformer turns-ratio, or a lower value of R_i (i.e., a larger transformer constant), the asymmetry of the voltage network will be greater and so too will be the effect of the parasitic inductance. The uncorrected test bridge is barely good enough for crude SWR measurements using a diode detector. Many bridges described in the literature are a lot worse than this; but on the subject of accuracy, most writers have so far shown a tendency to avoid comment.

17. Voltage sampling network inductance balance

In order to obtain a flat frequency response from a capacitive potential divider; it is not necessary that the arms should be composed of pure capacitance, but only that the two capacitive reactances should remain in constant proportion as the frequency is varied. Consequently, insofar as the non-ideality of the dominant (i.e., lowest impedance) arm can be represented as a series inductance, a flat frequency response can be obtained by placing a balancing inductance in the other arm.

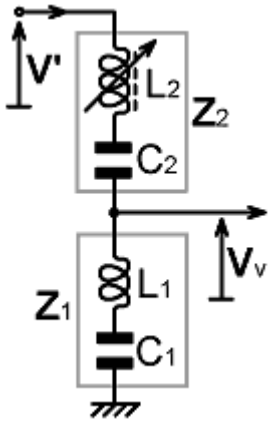

In the potential divider circuit shown right, the impedance marked $\mathbf{Z_1}$ is dominant and is provided by a capacitor with a series parasitic inductance L_1. L_2 is an adjustable inductance that includes the parasitic inductance of the capacitor C_2. The output of the network is given by:

$$\mathbf{V_V} = \mathbf{V'}\,\mathbf{Z}_1 / (\mathbf{Z}_1 + \mathbf{Z}_2)$$

Hence, working with the reciprocal transfer function:

$$\mathbf{V'} / \mathbf{V_V} = 1 + \mathbf{Z}_2 / \mathbf{Z}_1$$

i.e.

$$\frac{\mathbf{V'}}{\mathbf{V_V}} = 1 + \frac{\mathbf{j}(X_{C2} + X_{L2})}{\mathbf{j}(X_{C1} + X_{L1})}$$

Writing the reactances explicitly gives:

$$\frac{\mathbf{V'}}{\mathbf{V_V}} = 1 + \frac{[-1 / (2\pi f C_2)] + 2\pi f L_2}{[-1 / (2\pi f C_1)] + 2\pi f L_1}$$

and multiplying top and bottom of the right-most term by $-2\pi f$ gives:

$$\frac{\mathbf{V'}}{\mathbf{V_V}} = 1 + \frac{(1 / C_2) - (2\pi f)^2 L_2}{(1 / C_1) - (2\pi f)^2 L_1}$$

This rearranges to:

$$[(\mathbf{V'} / \mathbf{V_V}) - 1] [(1 / C_1) - (2\pi f)^2 L_1] = (1 / C_2) - (2\pi f)^2 L_2$$

Now grouping capacitance on one side and inductance on the other gives:

$$[(\mathbf{V'} / \mathbf{V_V}) - 1] (1 / C_1) - (1 / C_2) = [(\mathbf{V'} / \mathbf{V_V}) - 1] (2\pi f)^2 L_1 - (2\pi f)^2 L_2$$

The frequency dependence of this expression is removed when both sides are made equal to zero, i.e. when:

$$[(\mathbf{V'} / \mathbf{V_V}) - 1] L_1 = L_2$$

in which case also:

$$[(\mathbf{V'} / \mathbf{V_V}) - 1] (1 / C_1) = 1 / C_2$$

i.e.:

$$[(\mathbf{V'} / \mathbf{V_V}) - 1] = C_1 / C_2$$

Hence:

$L_2 = L_1 C_1 / C_2$	**17.1**

The relationship between C_1 and C_2 for a Douma bridge was given in equation **(2.1)**. Modified to allow for transformer efficiency it gives the transformer constant:

$$K_T = C_1 / C_2 = (N R_0 / k' R_i) + (1/N) - 1$$

For a bridge with $R_0 = R_i$, $N = 12$ and $k' = 0.96$, $C_1 / C_2 = 11.58$. If the bridge is constructed so that the capacitor C_1 has very short wires, the parasitic inductance might be kept down to about 20 nH. In that case, the required balancing inductance will be 232 nH. For the test bridge, due to the need to use large variable capacitors, the parasitic inductance is in the 60 nH to 80 nH range, and the required compensating inductance is 695 nH to 926 nH.

Note that there will be a frequency at which the balancing inductance L_2 resonates with C_2. This, in fact, is the same as the frequency at which C_1 resonates with L_1, because $L_1 C_1 = L_2 C_2$; but whereas resonance of the lower voltage sampling arm will merely result in inaccurate readings, resonance of the upper arm will present the generator with a short circuit. The frequency at which this short circuit occurs is:

$f_{s/c} = 1 / [2\pi \sqrt{(L_2 C_2)}]$	

If C_2 is 10 pF and L_2 is 232 nH , $f_{s/c} = 104$ MHz , safely away from the HF region. If C_2 is 10 pF and L_2 is 695 nH, $f_{s/c} = 60$ MHz , certainly too close for comfort if the bridge is to operate in the 6 m band, but acceptable for operation up to 30 MHz. Hence, for working bridges (as opposed to test bridges) it is desirable that the parasitic inductance in the lower voltage sampling arm be kept as small as possible. Observe also, that the bridge used in the example has only 12 turns on the transformer. For less sensitive (high-power) bridges, with more turns or a lower value of secondary load resistance, the asymmetry in the two arms of the voltage sampling network will be much greater, and so will the balancing inductance. It has to be said that a low-sensitivity bridge with a Douma-type voltage sampling network cannot give an acceptably flat amplitude response without balance compensation, but might have an unacceptably low $f_{s/c}$ with it. Hence, despite the ubiquity of Douma bridges with large N (30 or more turns) and no balance compensation, the amplitude performance of such bridges is bound to be poor.

The effect of the inductance balance coil on quadrature balance, being an adjunct to the parasitic inductance of the upper voltage sampling arm, is given by equation (**12.3**). As was mentioned before, L_2 partially neutralises the 'self-capacitance' of the transformer by increasing the length of the electrical path from the voltage sampling point to the summing point. The contribution is not great however, even for a relatively large inductance, as can be seen by differentiating equation **(15.1)**:

$\partial C_{ieff} / \partial L_2 = -1 / (N R_0 R_v)$

For the test bridge, with N = 12 , $R_0 = 50\ \Omega$ and $R_v = 1455\ \Omega$,

$\partial C_{ieff} / \partial L_2 = -1.15$ pF/μH

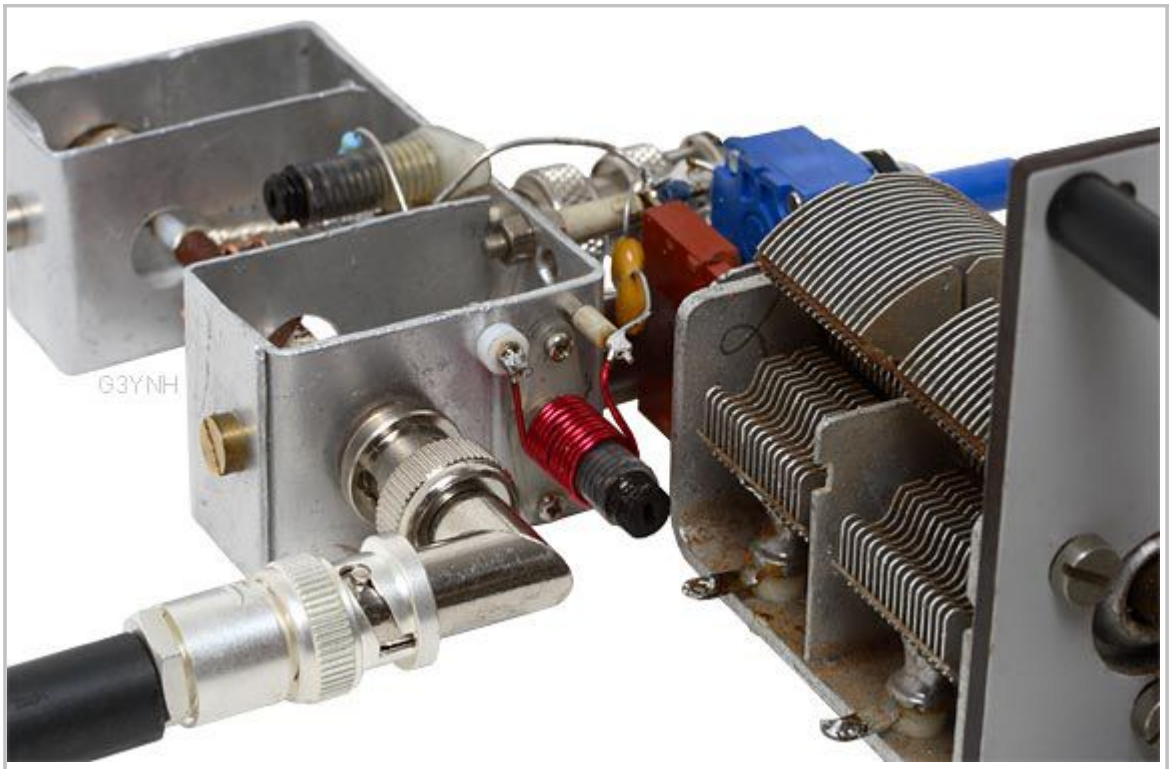

Voltage sampling network inductance balance coil (7 mm diameter PS former with M6-threaded dust-iron slug). In this case $C_1 / C_2 = 11.58$, and C_1 has a parasitic inductance L_1 of about 62 nH. Hence the balance coil must make the inductance of the upper voltage sampling arm (L_2) up to 721 nH, i.e., the coil shown has an inductance of around 700 nH .

Inductance balance compensation is simple and boringly effective. A small adjustable inductor, the number of turns easily determined by experiment, is all that is required. For tracking over the HF spectrum, the capacitor C_1 is adjusted at about 2 MHz, and the balance coil L_2 at a frequency a little below 30 MHz. The adjustments are repeated two or three times until no further improvement can be obtained. Amplitude flatness of better than ±0.4% (±0.034 dB) over the 1.6 MHz to 30 MHz range is easily achievable, even with the excessively inductive reference capacitors used with the test bridge. If the inductance of the lower voltage sampling arm is kept to a minimum, the flatness can be better than ±0.04% (see section **18c**).

There is no point in evaluating the technique separately. The performance figures given above will be corroborated by the experimental data to follow. An inductance balance coil should not be used during model-parameter determinations, because L_2 contributes to C_{ieff}, but one should always be included in a working Douma bridge.

18: Frequency tracking

In the next few sections we will look at techniques for neutralising bridge phase error. Several possibilities are obvious from the theoretical considerations of sections **11** to **14**, and it is now a matter of seeing how well they work in practice. There are further less-obvious neutralisation methods however, and these will be introduced.

With a balance coil to cancel the effect of the inductance of the lower voltage-sampling network capacitor, and some means for neutralising the apparent secondary capacitance, the bridge has 2-point frequency-tracking capability. Calibrating the bridge is then a matter of adjusting C_1 and R_v at some low frequency such as 2 MHz, and adjusting the inductance balance and phase neutralisation at some frequency approaching to the upper limit of the desired working range. Generally, the low and high-frequency settings interact slightly, and so the adjustments have to be repeated a few times until no further improvement can be obtained. Two or three cycles of adjustment is usually sufficient.

Achieving the maximum benefit from 2-point tracking is a matter of selecting the optimal upper calibration frequency. After calibration, the bridge is perfect at two frequencies but there will be some residual error elsewhere. Typically, the quadrature balance deviates slightly according to a curve that mimics the inverted real-part of the permeability dispersion in the core material. Apart from that, the phase error is proportional to frequency and eminently correctable; consistent with it being a timing error in a system that is free from any other significant dispersive effects. The residual error in the in-phase balance condition is a little more complicated however. It partially mimics the inverted imaginary part of the permeability dispersion, but there are other effects caused by the fact that the inductance of C_1 is not perfectly described as a single series component, and by the minor approximations inherent in ignoring the frequency-dependent effects of parasitic reactances on the apparent efficiency of the transformer.

Most of the experimental data given below was obtained using the 8 pF to 48pF reference capacitor described in section **6**. This capacitor has an equivalent series inductance of about 85 nH ; and since it has to be used with a parallel padding capacitor, lumping all of its inductance into a single series component does not provide a perfect description. Consequently, the in-phase performance of a bridge using this capacitor is limited to about ±0.2%. The reference capacitor was identified as the cause of this limitation by performing a control experiment using a 2.5 pF to 30 pF trimmer and padding capacitor with an equivalent series inductance of about 50 nH, i.e., by reverting to the method used with the prototype bridge described in section **3**. The business of unplugging a capacitor and measuring it on a separate bridge is too laborious for general adoption, and the data are not particularly precise (±0.25 pF). The results are nevertheless accurate, and show that the in-phase balance tracking is good to within ±0.03% if the inductance in the lower voltage-sampling arm is kept to a minimum.

Given that there are bound to be residual errors, the best upper calibration frequency is the one that gives approximately equal run-out above and below the target in-phase and quadrature balance points over the working range. For the bridges evaluated below, it lies somewhere in the 20 MHz to 28 MHz region and cannot always be determined prior to the first test-run. To avoid repeating experiments ad-nauseam without gaining any new information, most neutralisation methods are tested only once; which means that there may still be room for improvement. The ultimate performance obtainable from a particular neutralisation method is given by the least-squares fit to the phase error (see graph of obs-calc on sheet 5); and the optimal upper calibration frequency can usually be determined by adjusting the fitting weights for equal run-out above and below zero and noting the upper zero-crossing frequency for the error curve.

18a: Phase neutralisation by load port capacitance

The most straightforward and obvious method for neutralising the apparent secondary capacitance of the transformer is to add some capacitance across the load side of the through-line. The effect of such a capacitance is given by differentiating equation **(14.1)**:

$$\partial C_{ieff} / \partial C_0 = - R_0 / R_i$$

A bridge neutralised by this method is shown below.

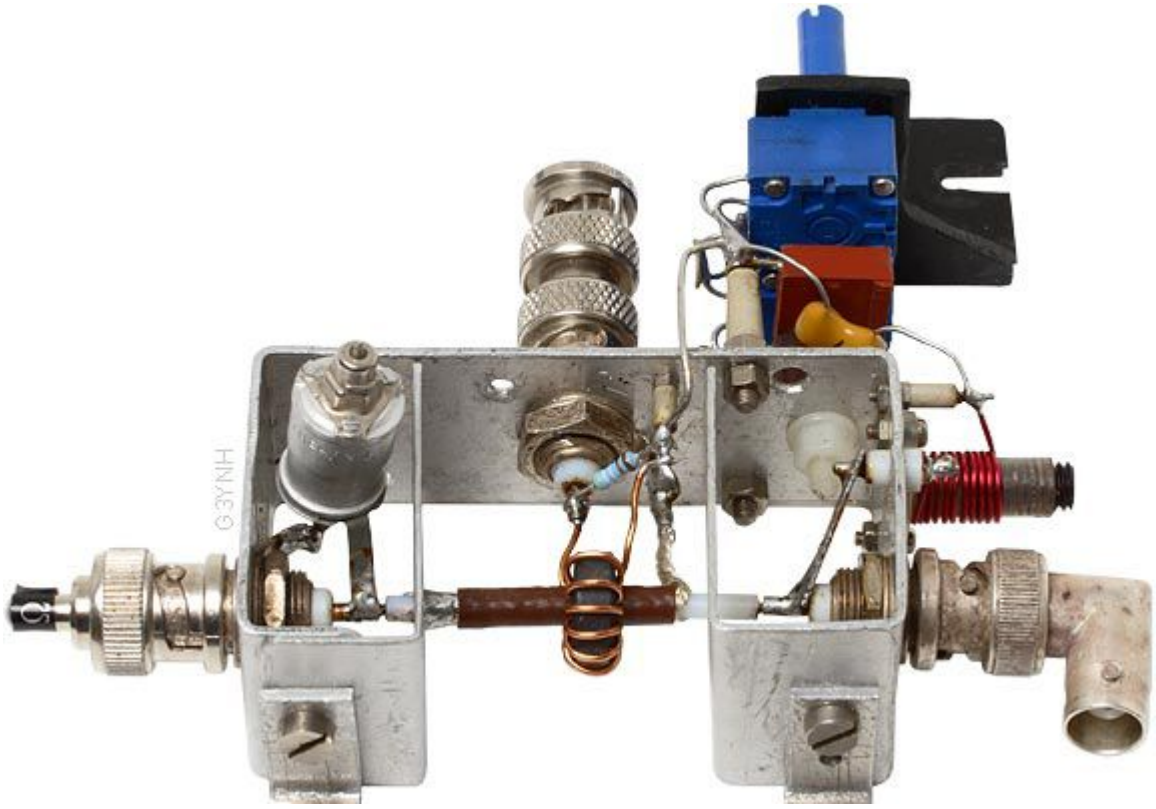

The bridge was calibrated at 2 MHz and 26 MHz and then evaluated according to the procedure outlined in section **16**. The spreadsheet reference and a summary of the outcome is as follows.

Gen. side shield earth. 1.6 MHz to 30 MHz	R_0 = 50 Ω , R_i = 50 Ω Inductance balance coil fitted.	Max. |Z| error.	Max. φ error ( ) → best possible
testbrg61-1212.ods	6.6 pF across load port	±0.25%	±0.12° (±0.09°)

The magnitude error is mainly attributable to the reference capacitor. The choice of 26 MHz as the upper calibration frequency was not optimal, and the regression line for the overall phase error indicates that the run-out can be reduced to ±0.09° by calibrating at 21 MHz.

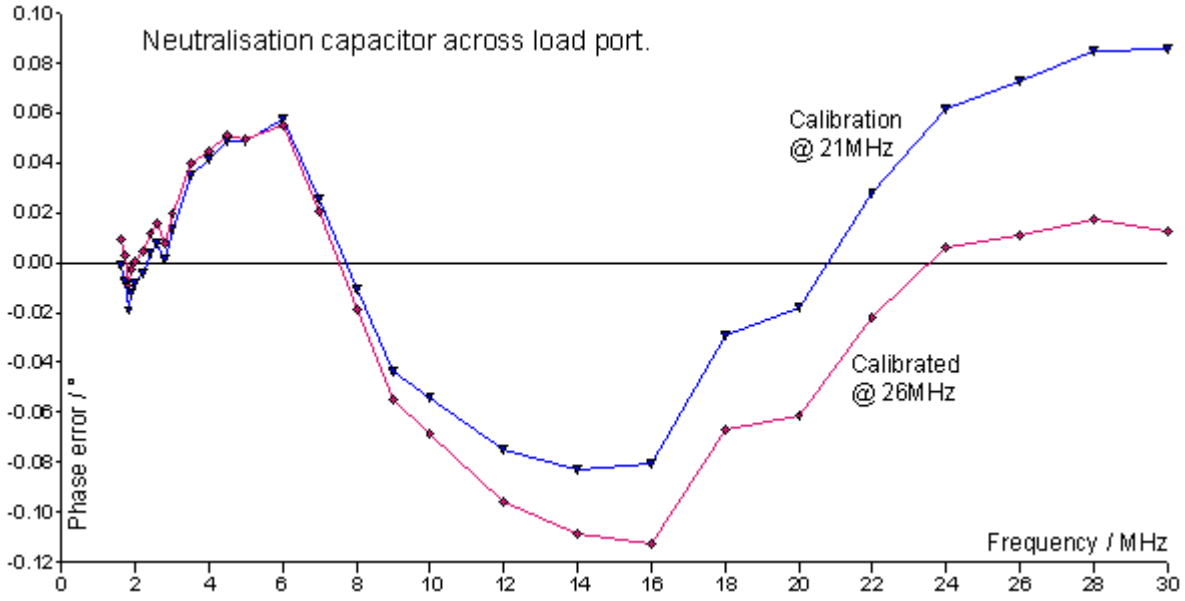

The result is, of course, at least an order of magnitude better than for any uncompensated bridge, but it is not the best that can be achieved. Placing capacitance across the through-line in addition to the voltage sampling network also adversely affects the generator power-factor; and although this problem is sometimes correctable, and does not matter if the bridge is to be taken out of circuit after use, loading the generator with extra capacitance is not generally desirable.

18b: Quadrature current compensation

The effect of the Faraday shield protrusion capacitance in a bridge with the shield earthed on the load side was investigated in section **11**. The theory developed there implies that the apparent secondary capacitance can be neutralised either by injecting a capacitive quadrature current into the shield itself, or into an additional compensation winding. Connecting the neutralising capacitor to the shield is the most economical method if the current is to be delivered from the generator terminal, and it is doubtful that the use of a separate winding will make any difference in that case. The initial test configuration is shown below; and the results and the filename of the analysis spreadsheet are given below that.

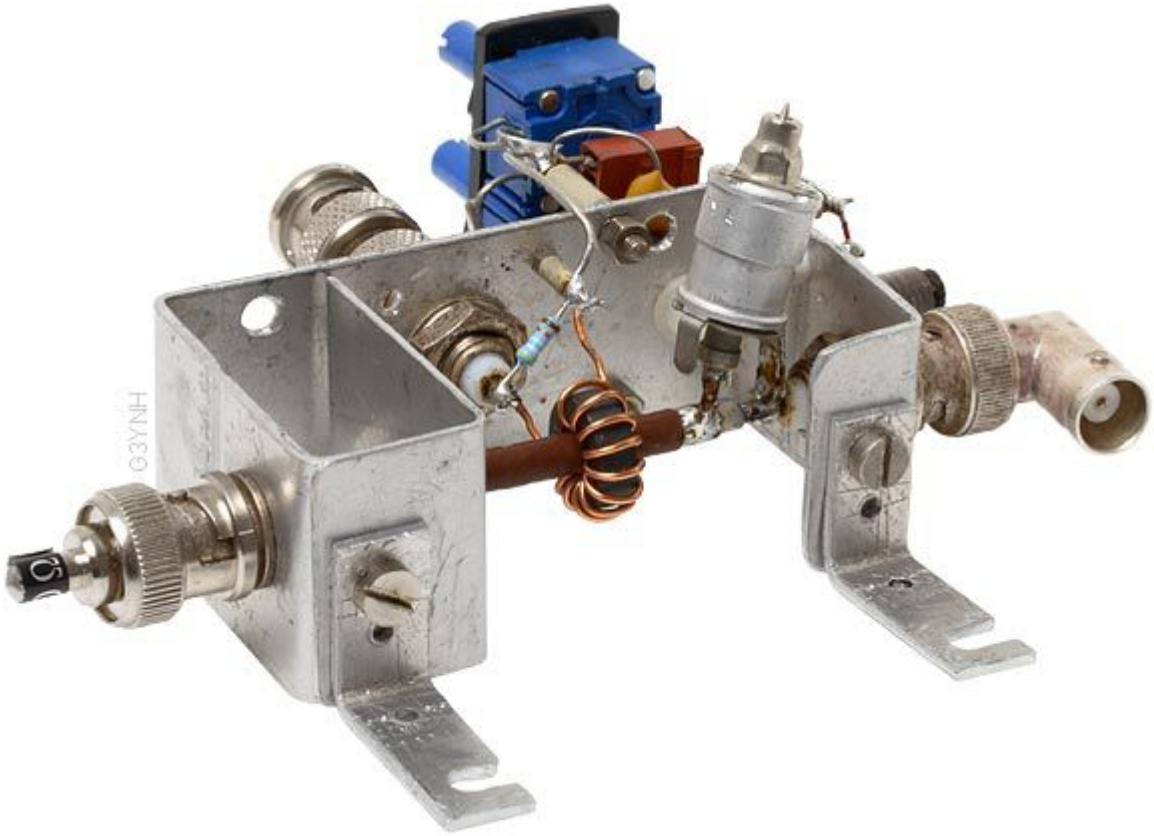

Load side shield earth. 1.6 MHz to 30 MHz	R_0 = 50 Ω , R_i = 50 Ω . Inductance balance coil fitted.	Max. |Z| error.	Max. φ error ( ) → best possible
testbrg61-1213.ods	6.7 pF, gen. to shield	±0.4%	±0.25° (±0.23°)

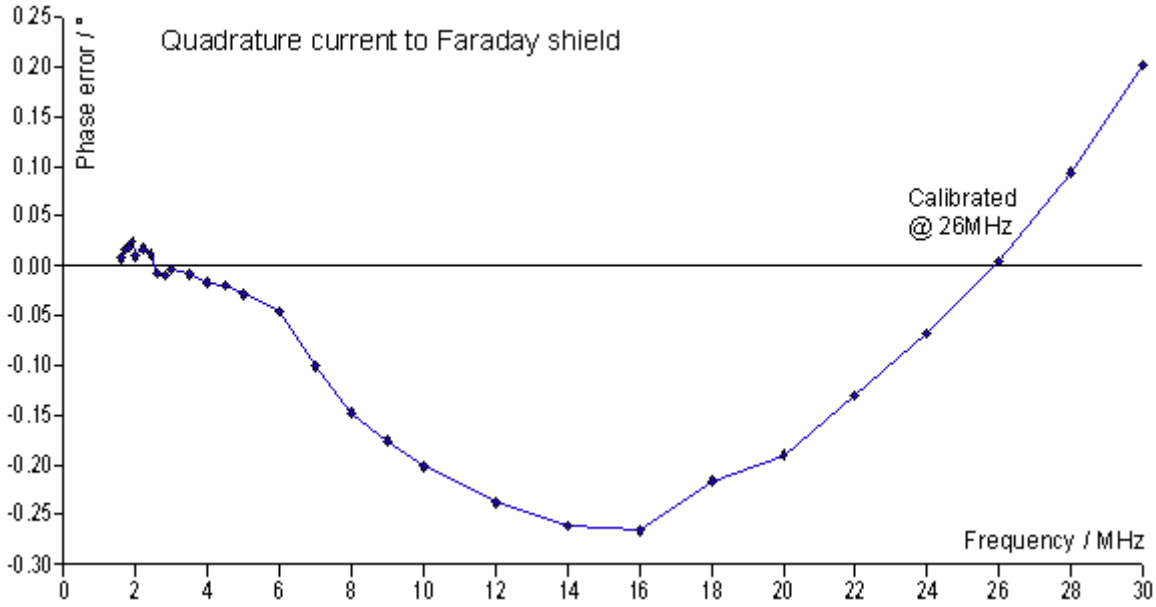

In the derivation given in section **11**, assumptions were made firstly: that no voltage is developed between the ends of the Faraday shield; and secondly: that the voltage drop across the transformer primary is negligible. With these simplifications, it was found that the shield capacitance has the same effect as placing a capacitance across the load port. Evidently the two neutralisation effects are not the same however, because placing a capacitor across the load port results in better overall performance than injecting a current into the shield.

In a current transformer, the flux-density in the core and hence the primary voltage $\mathbf{V}_{ii}$, is controlled by the main secondary load. Hence the shield, being effectively a secondary winding with the same number of turns as the primary, will develop a voltage that is of the same magnitude as $\mathbf{V}_{ii}$; but since the shield is loaded only by its own inductance, its voltage (V_a say) will be shifted +90° in phase relative to $\mathbf{V}_{ii}$. The voltage V_a must be subtracted from the voltage across the line-to-shield capacitance in order to establish the exact phase of the (not quite perfect) 'quadrature' current injected.

In the original derivation, the shield protrusion displacement current was given approximately as:

$$\mathbf{I}_{sh} = \mathbf{V} / (\mathbf{j}X_{Csh})$$

Now however, with the notation altered to suit the general context of neutralising currents injected into auxiliary windings, we have to admit that it is better described by the expression:

$$\mathbf{I}_{n} = (\mathbf{V} + \mathbf{V}_{ii} - \mathbf{V}_{a}) / (\mathbf{j}X_{Cn})$$

the reasoning being illustrated by the diagram below. Here the vector $\mathbf{I}_n$ (noting that **j** is on the bottom of the fraction and capacitive reactance is negative) lies at +90°, not to the voltage across the load, but to the vector $\mathbf{V}+\mathbf{V}_{ii}-\mathbf{V}_{a}$. This is the actual neutralisation reference voltage, to which we will assign the symbol $\mathbf{V}_{ref}$.

We can obtain a qualitative idea of how $\mathbf{V_{ref}}$ evolves with frequency by noting that $\mathbf{V_{ii}}$ is a scaled down version of $\mathbf{V_i}$; where $\mathbf{V_i}$ is the voltage across $\mathbf{Z_i}$, and the locus of $\mathbf{Z_i}$ in the Z-plane is a constant-conductance circle mainly determined by the relative magnitudes of R_i and X_{Li}. At low frequencies, $\mathbf{V_{ii}}$ leads $\mathbf{V}$, but moves into phase with it as X_{Li} increases with frequency. Hence we can draw the sum of the three vectors that make up $\mathbf{V_{ref}}$ and show that it is always slightly lagging; and that the lag increases with frequency. The result is that the neutralising current, (at +90° relative to $\mathbf{V_{ref}}$) is slightly out of true quadrature to $\mathbf{V}$, with a lag that gets worse as the frequency increases. The error is in the same direction as that caused by dispersion in the ferrite. The result is that the neutralising current does not cancel C_{ieff} to the limit permitted by the dispersion, but introduces an error in addition to the dispersive effect. This error moreover, permits the neutralising current to affect the in-phase balance condition, thereby also slightly degrading the bridge amplitude performance.

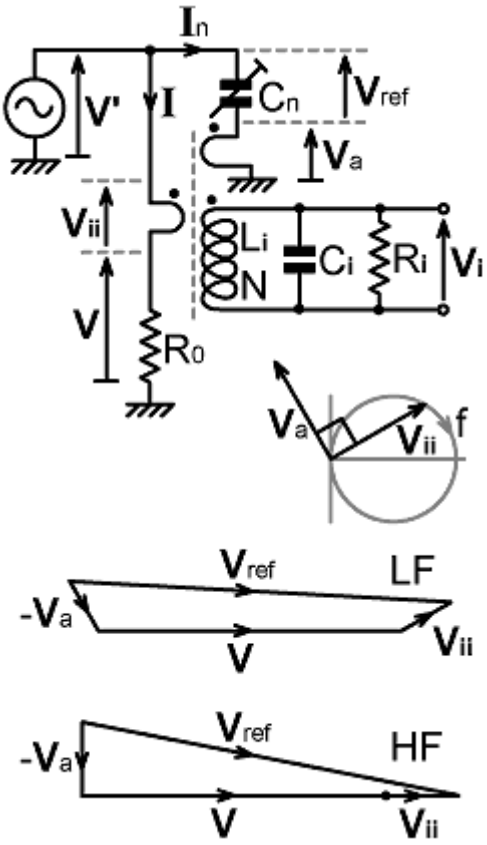

One point that arises from these considerations is that we do not want the partial neutralising effect that results from earthing the shield on the load side of the transformer core. Hence ***the shield should be earthed on the generator side*** (or perhaps omitted altogether - see section **19**). The subject of current-injection neutralisation is far from dead however; firstly because we can change the phase of $\mathbf{V_a}$ by loading the auxiliary winding; and secondly because, if we use an actual winding instead of the shield itself, we can connect the neutralisation capacitor to the load terminal instead of the generator terminal.

Consider what happens when a 1 turn auxiliary winding is resistively loaded with the same number of Ohms per turn as the main secondary. If the secondary has (say) 12 turns, and $R_i = 50\ \Omega$, then this involves placing a resistance of $50 / 12 = 4.2\ \Omega$ across the auxiliary winding. Now, in order to calculate $\mathbf{V_i}$, we can consider that the transformer has 13 turns loaded with 54.2 Ω, and that $\mathbf{V_i}$ is obtained by tapping in at the 12th turn. From that electrical equivalence, it should be obvious that $\mathbf{V_a}$ is now in phase with $\mathbf{V_i}$ and hence, to a very good approximation, identical in magnitude and phase to $\mathbf{V_{ii}}$. The result is that $\mathbf{V_{ref}}$ becomes equal in magnitude and phase to $\mathbf{V}$, as can be seen from the vector diagram on the right. Hence the neutralising current $\mathbf{I_n}$ will be in true quadrature to $\mathbf{V}$, and the neutralisation errors will be eliminated.

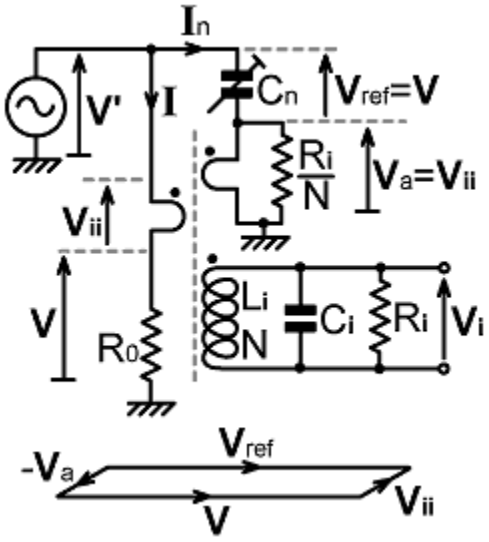

There is a problem with this improved neutralisation technique however, and it is this: If we make $\mathbf{V_{ref}}$ identical to $\mathbf{V}$, then we eliminate the approximations from the analysis given in section **11**. This means that the result, in phase performance terms, is identical to that of placing a capacitor across the load port. Hence the circuit is made more complicated for no benefit, and furthermore, the transfer efficiency of the transformer is reduced by a factor of N / (N+1). Consequently, it is difficult to see why anyone would want to

use this method, except perhaps that placing a resistance of R_i / N across the ends of a load-side earthed Faraday shield will eliminate the deleterious effects of the displacement current. This might be useful if the shield is earthed on the load side intentionally (e.g., to allow neutralisation by sliding the core along the shield - see notes at the end of this section).

Let us now turn our attention to what happens when the auxiliary winding is connected to the load terminal. The test bridge so configured is shown below, and a summary of the results is given below that.

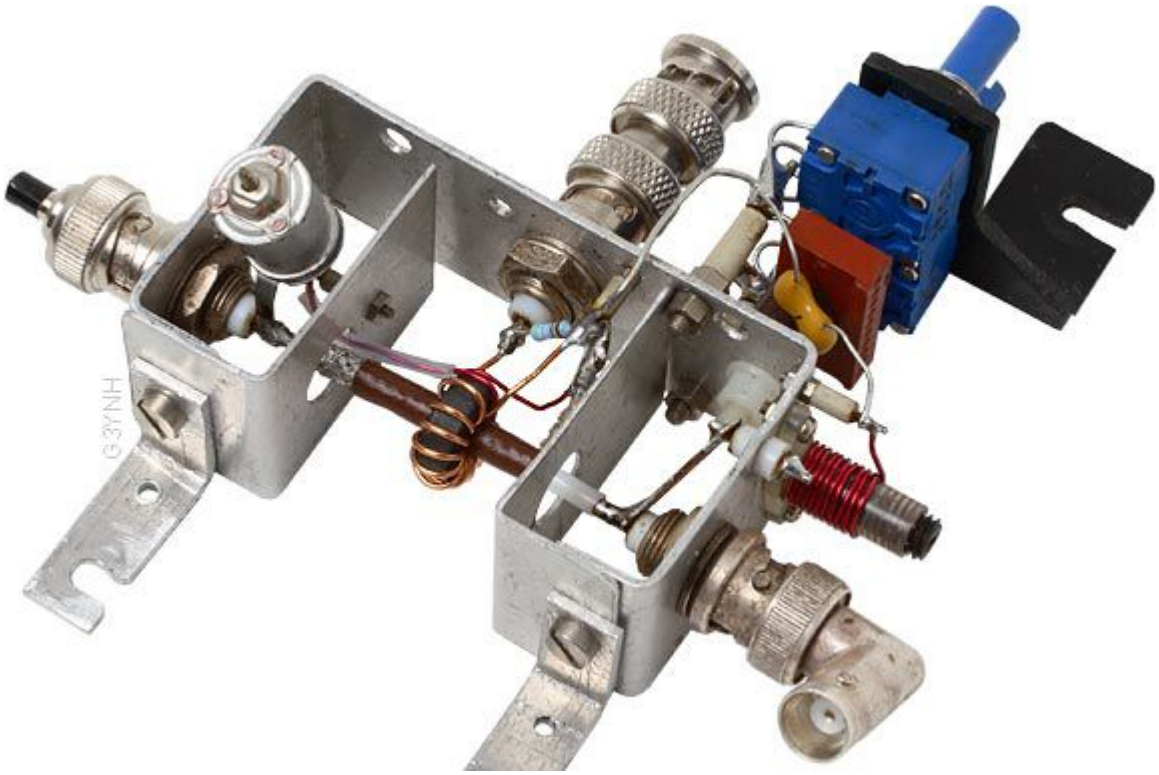

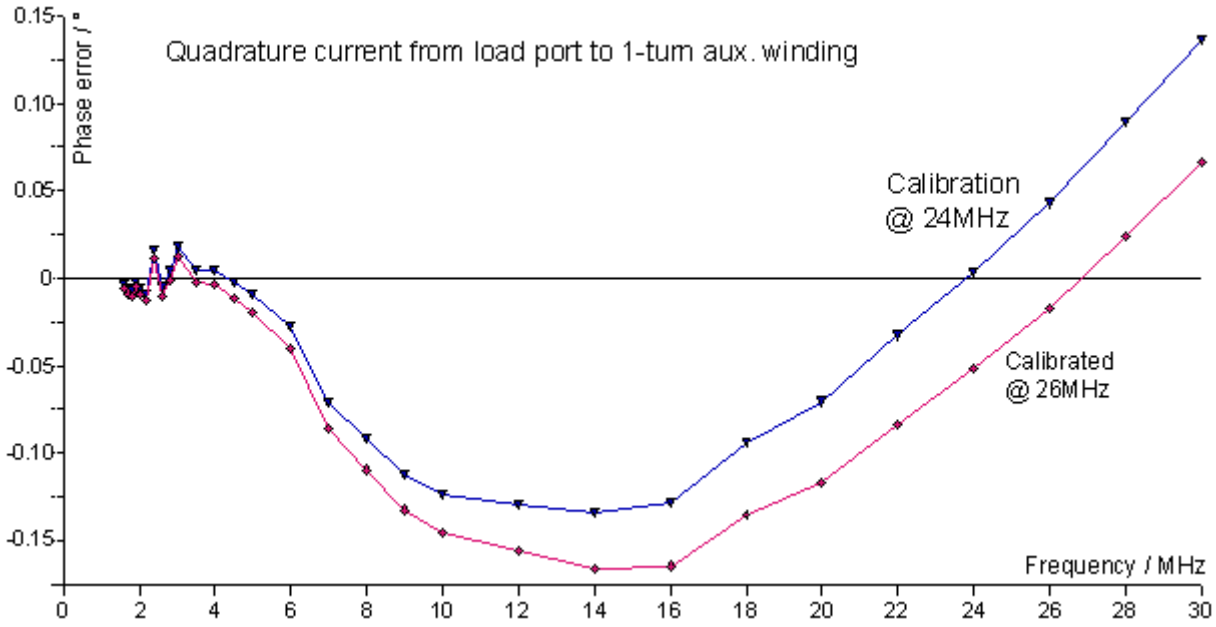

Gen. side shield earth. 1.6 MHz to 30MHz	R_0 = 50 Ω , R_i = 50 Ω . L-bal. coil. 1-turn I-compensation winding.	Max. |Z| error.	Max. φ error ( ) → best possible
testbrg61-13_2.ods	3.5 pF to load terminal.	±0.35%	±0.17° (±0.13°)

When the test bridge was neutralised by connecting a capacitor across the load port, or by injecting a quadrature current from the generator terminal, the neutralising capacitance required (measured after the test) was nearly 7 pF. When the neutralising current is taken from the load terminal however, the required capacitance is approximately halved. The reason for that can be understood by inspecting the diagram below, which shows that $\mathbf{I_n}$ flows through the transformer twice, once through the primary winding and once through the auxiliary winding. This gives the circuit a definite advantage over previous configurations, which is that neutralisation can be achieved with a reduced penalty in terms of generator power-factor. It is, of course, possible to reduce C_n still further by adding more turns to the auxiliary winding, but that is not a good idea because it will increase the quadrature error.

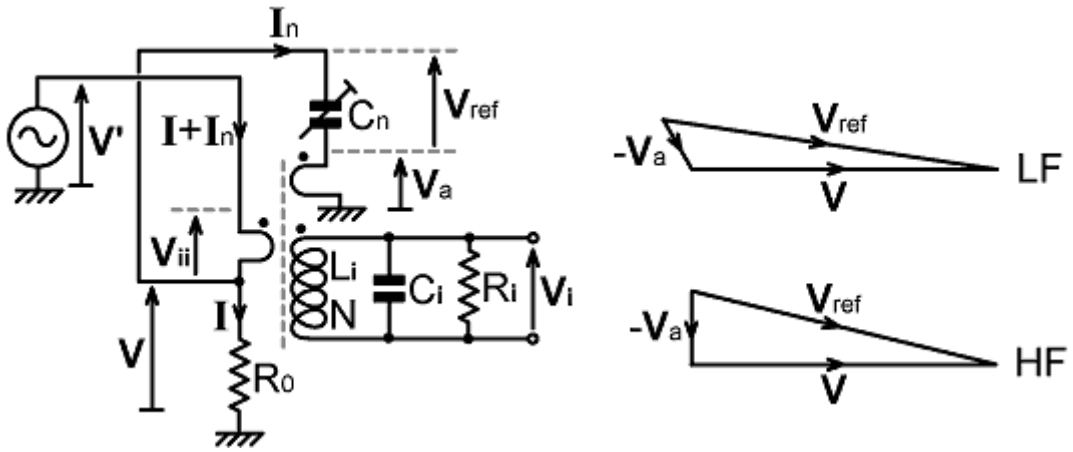

With regard to overall performance with the neutralisation current taken from the load terminal; it is better than when the current is taken from the generator terminal but not quite as good as when a capacitor is placed across the load port. The reason for that can be seen in the vector diagrams, which show a reference voltage with a residual phase lag that increases with frequency. This supplements the ferrite dispersion effect, as before, but less severely.

The obvious next experiment is to see what happens when the auxiliary winding is loaded with a resistance of about R_i / N to bring $\mathbf{V_a}$ into phase with $\mathbf{V_i}$. The test bridge with this addition is shown below and the test results are given below that.

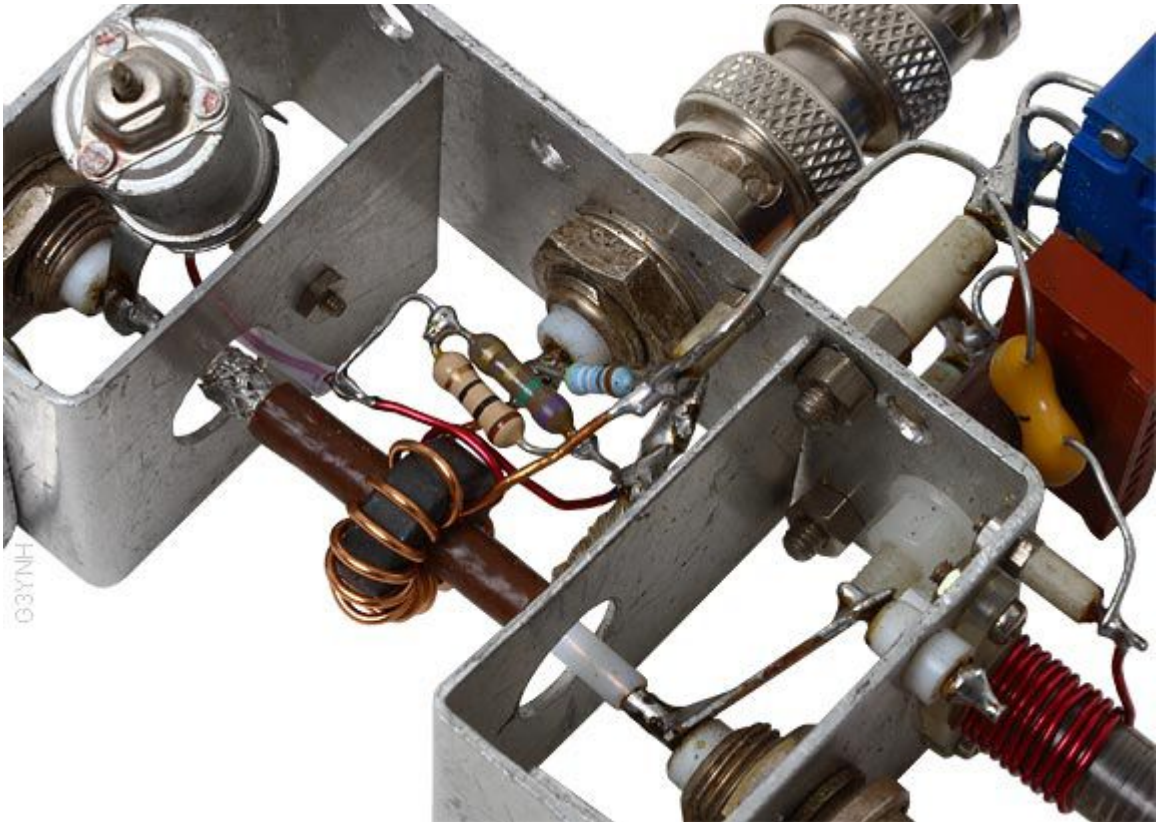

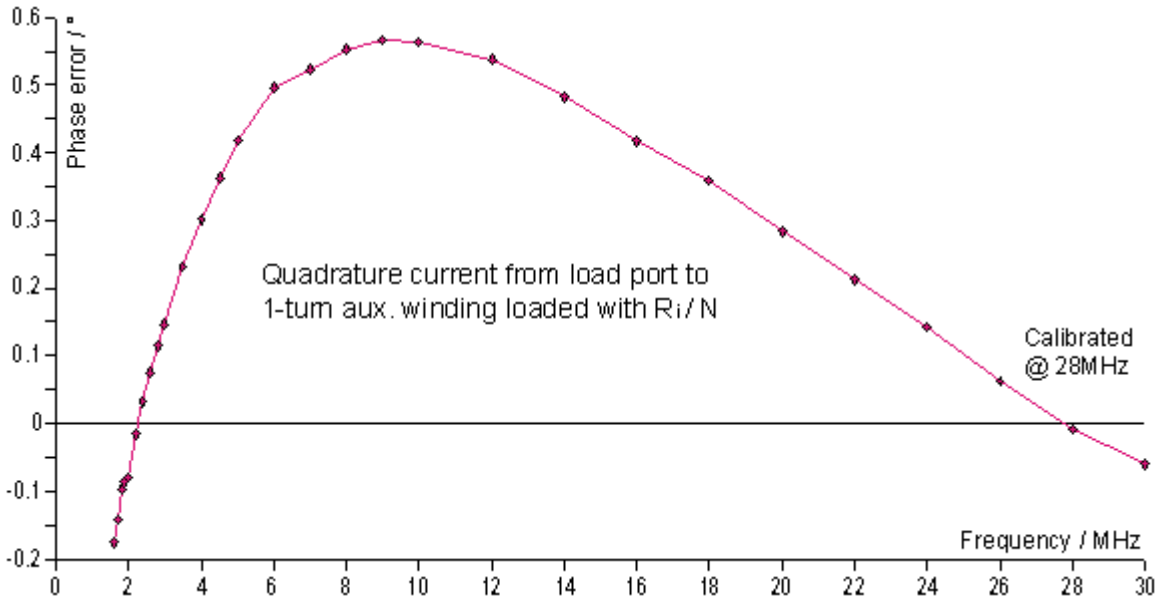

Gen. side shield earth. 1.6 MHz to 30 MHz	R_0 = 50 Ω, R_i = 50 Ω . L-bal. coil. 1-turn I-comp. winding // 4.26 Ω	Max. |Z| error.	Max. φ error ( ) → best possible
testbrg61-13_3.ods	3.4 pF to load terminal.	±0.69%	±0.57° (±0.36°)

The performance of this bridge is relatively poor, being barely an order of magnitude better than typical published designs; but it nevertheless has a very interesting property. The phase deviation curve has the opposite sense to that of the bridge with the unloaded auxiliary winding, and is also in the opposite sense to the deviation caused by the permeability dispersion. The reason can be understood by looking at the vector diagrams below, which show that the neutralisation reference voltage moves anti-clockwise with increasing frequency, whereas it moves clockwise when the auxiliary winding is unloaded.

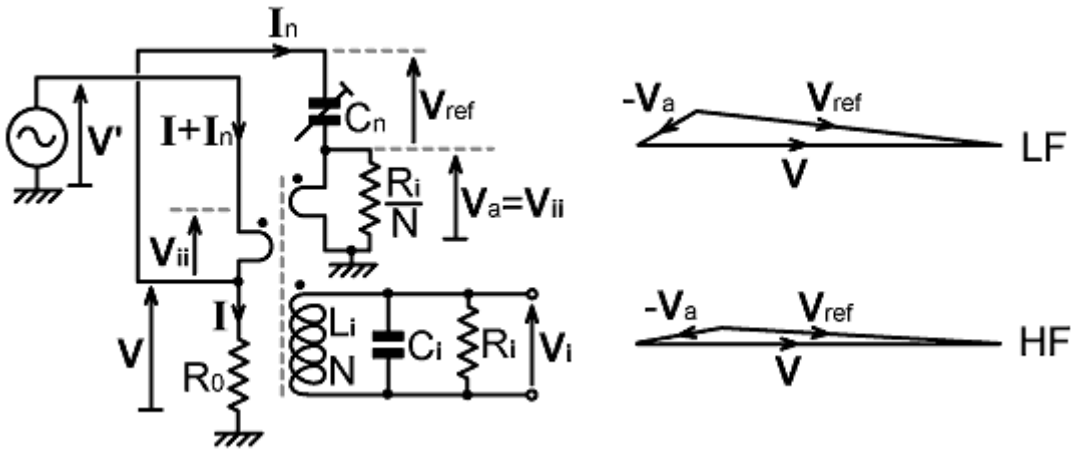

If the phase deviation is negative in the middle of the working frequency range when the neutralisation winding is unloaded, and positive when it is loaded with a resistance of R_i/N ; then logically, there must be an intermediate loading condition that brings the overall phase error to a minimum. To explore this possibility, the bridge was set up with a 100 Ω cermet variable resistor for the auxiliary load. With this modification, the bridge has 3-point frequency tracking for phase error and 2-point tracking for magnitude error.

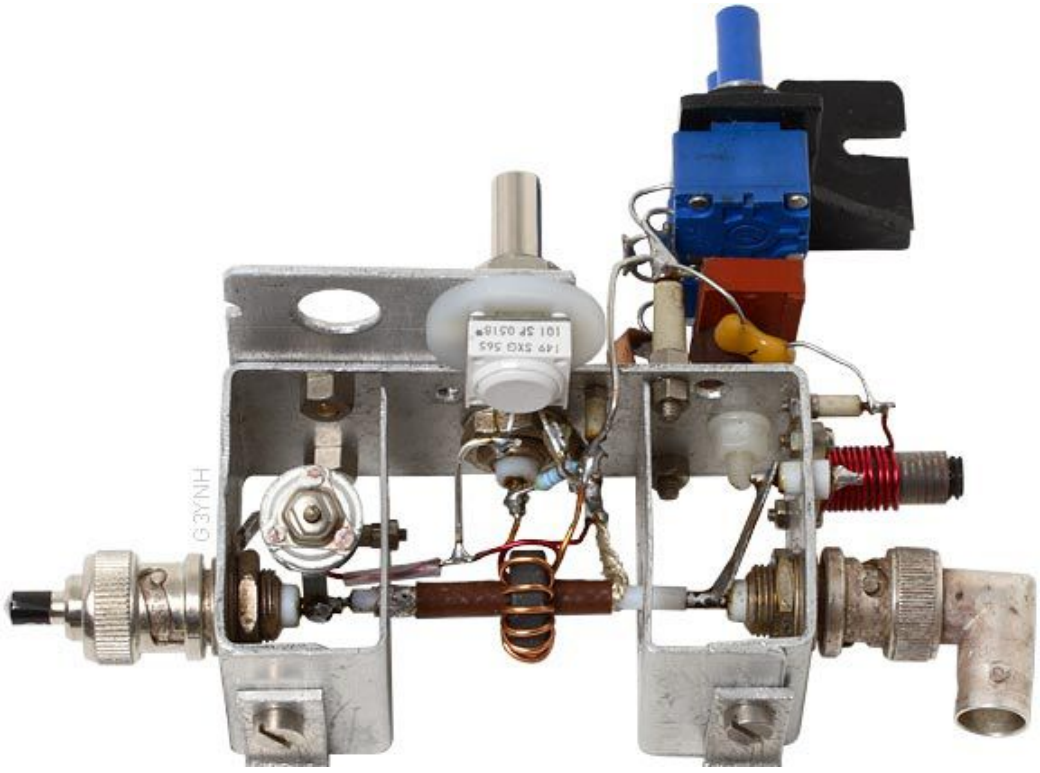

It was thought initially, that this new arrangement would be difficult to calibrate, but the task proved to be surprisingly straightforward. C_1 and R_V were adjusted at 2 MHz, C_n and L_2 at 26 MHz; and the loading resistance R_n was adjusted at 18 MHz, using C_1 for in-phase balance while the latter operation was being carried out. The adjustments were not strongly interactive, and only 3 rounds of iteration were required. It was also obvious that there was now considerable latitude in the choice of upper calibration frequency, since the bridge barely went out of balance during the search for maximum run-out.

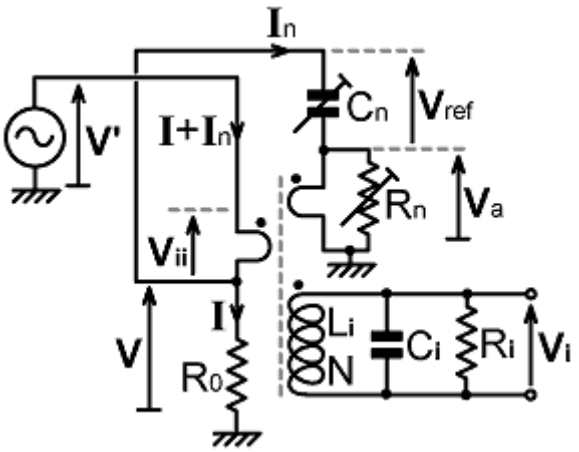

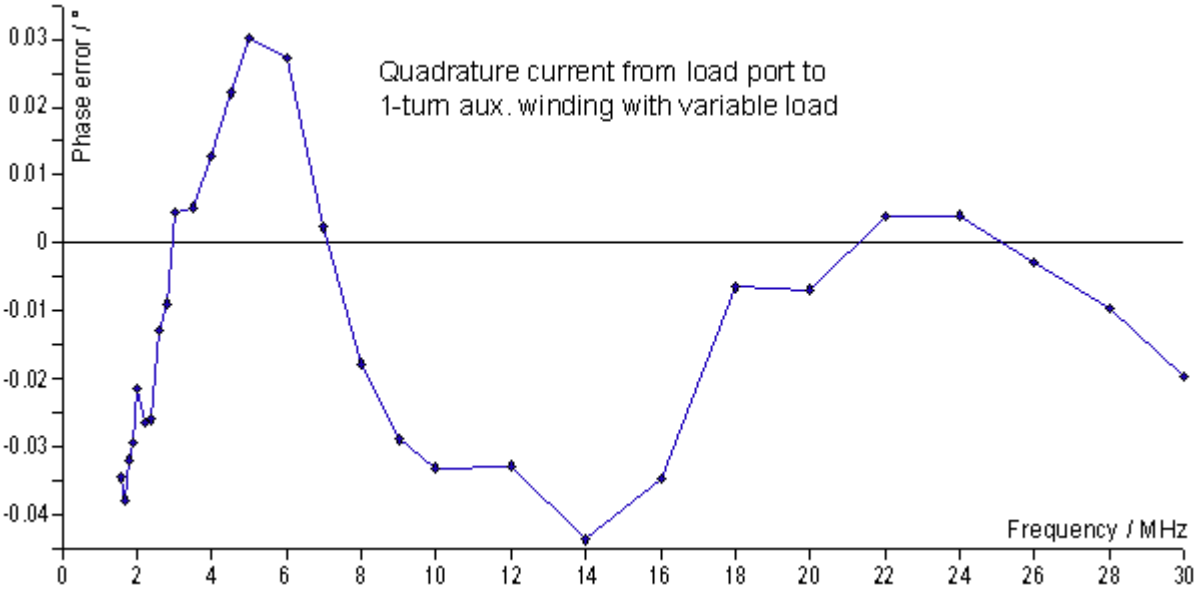

Gen. side shield gnd. 1.6 MHz to 30 MHz	R_0 = 50 Ω , R_i = 50 Ω . L-bal. coil. 1-turn I-comp. winding // 100 Ω pot.	Max. |Z| error.	Max. φ error ( ) → best possible
testbrg61-13_4.ods	Measured: C_n = 2.95 pF , R_n = 21.7 Ω	±0.12%	±0.044° (±0.038°)

There was certainly no need to use the coarse adjustment for R_V during the evaluation of this bridge. The reason is evident from the graph above. The chosen compromise between the negative mid-band run-out given by an unloaded neutralisation winding, and the positive run-out given by a heavily loaded winding has reduced the phase error to better than ±0.044°. Moving the mid-point adjustment from 18 MHz to about 17 MHz will reduce it further to about ±0.038° (i.e., it will drag the curve onto the zero line at 17 MHz).

This level of performance is easily two orders of magnitude better than that offered by typical current-transformer bridges; and led the author to the view that the quadrature-current neutralisation technique is a good candidate for the design of reference instruments. On that basis, a working bridge was constructed[14] and, by paying careful attention to layout, grounding, and minimisation of inductance in the lower arm of the voltage-sampling network, it was found possible to get the maximum phase error down to ±0.025° and the maximum magnitude error down to ±0.04%. It is

14 **A Self-evaluating precision reference bridge**. D W Knight. http://g3ynh.info/zdocs/bridges/ .

doubtful that such performance will hold for long periods without drift, but ±0.05° and ±0.1% is a perfectly reasonable expectation over a normal annual calibration interval.

Some additional comments on current-injection neutralisation:

● Impedance bridges are often used reversed (i.e., with the generator and load connections swapped) for forward power measurement, or to obtain a forward transmission reference for the measurement of SWR. It should be noted therefore, that current injection neutralisation is asymmetric; i.e., the condition required for obtaining perfect balance (minimum reverse power reading) is not the same as the condition required for perfect anti-balance (maximum forward power reading). In practice however, any neutralisation error in a forward-power bridge will make negligible difference to the reading. The purpose of neutralisation is to produce the rigorous conditions required for a null. Forward reading bridges do not null and so (assuming that the phase error is no more than a few degrees) do not need to be neutralised. Consequently, in an SWR bridge or directional power meter, neutralisation can be applied to ensure accurate reverse readings, and the very minor effect on the forward reading can generally be ignored.

● It was mentioned earlier that the Faraday shield should be earthed on the generator side in order to eliminate the uncontrolled neutralising effect of the shield protrusion capacitance. For practical purposes however, the extremes of accuracy demonstrated here are not usually needed. That being the case; there is a property of the load-side earthed shield configuration that might be used to eliminate an expensive trimmer capacitor in production bridges. In a private correspondence[15], David Stansfield, G0EVV, noted that it was possible to improve the frequency tracking of a bridge by sliding the transformer core along the shield. This action, of course, changes the shield protrusion capacitance; and so, with a little slack in the secondary connecting wires, sliding the core does the same job as adjusting a trimmer. There is a caveat however, which is that, once calibration has been accomplished, it must be ensured that the core will not move if the bridge is bumped or dropped.

● The current-injection neutralisation technique developed here is comparable to a method for cancelling the parasitic capacitance of power-supply filter inductors described by Neugebauer and Perreault[16]. In a current transformer, the cancellation can be considered to be referred either to the primary or to the secondary winding.

● There are other ways in which multiple frequency-tracking adjustments can be provided in bridges using load-port capacitance or current-injection neutralisation. For example: if a small adjustable inductor is placed in series with the neutralisation capacitor, the neutralisation capacitance will appear to increase with frequency. Such a combination can therefore compensate for a situation in which a bridge exhibits a lagging phase error at high frequencies but a leading phase error in mid band (such as can be arranged when the current-injection winding is loaded by a resistance).

---

15 David Stansfield, G0EVV, private e-mail communication, 16th Aug. 2007.
Part of e-mail exchange 2nd May 2007 - 22nd Aug. 2007.

16 **Parasitic Capacitance Cancellation in Filter Inductors**. T C Neugebauer and D J Perreault. 35th Annual IEEE Power Electronics Specialists Conference, 2004.
The parasitic capacitance of a power-supply filter inductor is cancelled by use of an auxiliary winding and a capacitor.

18c. Quadrature voltage compensation

The neutralisation techniques described in the previous two sections all carry a possible penalty in terms of generator power-factor; and although it will be difficult to improve on the performance of the 3-point tracking method described above, extreme accuracy is not always required. Indeed, a bridge that is accurate to within about ±0.5° and ±0.5% is almost certainly good enough for any circuit that uses a diode detector. Hence there is a place for neutralisation techniques that do not noticeably alter the characteristics of the through-line.

As was noted in the previous section, an unloaded auxiliary winding on a current transformer produces a voltage that lies at +90° relative to the main secondary voltage. Hence if a potentiometer of high-enough resistance not to constitute a significant load is placed across such a winding; it is possible to produce an adjustable quadrature voltage that can be added to the main output to cancel the high-frequency phase error. The principle of the technique is summarised in the diagrams below.

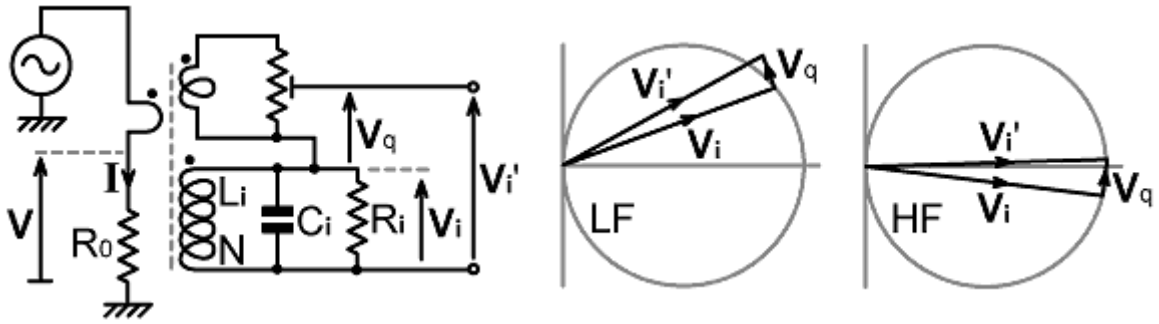

Ideally, the locus of the corrected output voltage should lie on a constant-conductance circle if the network is to give an accurate simulation of a transformer with no secondary capacitance. From the vector diagrams it can be seen that this does not happen in practice, but by adjusting R_V at the low end of the working frequency range and $|\mathbf{V_q}|$ at the high end, a reasonable compromise can be reached. The test bridge set up for quadrature voltage neutralisation is shown on the next page.

For the first attempt at testing the technique, a single turn compensation winding with a 250 Ω cermet potentiometer connected across it was used. This worked for a bridge with the Faraday shield earthed on the load side; but with the shield earthed on the generator side according to later-discovered best practice, C_{ieff} is greater and neutralisation could only just be achieved with the pot. set somewhere close to maximum. Since reaching the end-stop of a control interferes with the process of searching for nulls and makes calibration difficult to achieve, the compensation winding was changed to 2-turns and a 120 Ω resistor was placed in series with the pot.. The purpose of the additional resistor was to keep the loading light and bring the adjustment roughly to the middle of the available range.

One idiosyncrasy of quadrature voltage compensation is that it places additional DC resistance in series with the detector output. This resistance, which is the parallel combination of the two sides of the adjustment pot., will make practically no difference to the performance of a working bridge, but it lies in the way of measuring R_V via the detector port. Hence, designating the additional resistance R_q, the experimental quantity is $R_V + R_q$. For the evaluation experiments listed below, R_q was measured at the end of the test run by shorting R_V with a jumper lead. An extra column was then added to the analysis spreadsheet so that R_q could be subtracted from $R_V + R_q$ to obtain R_V.

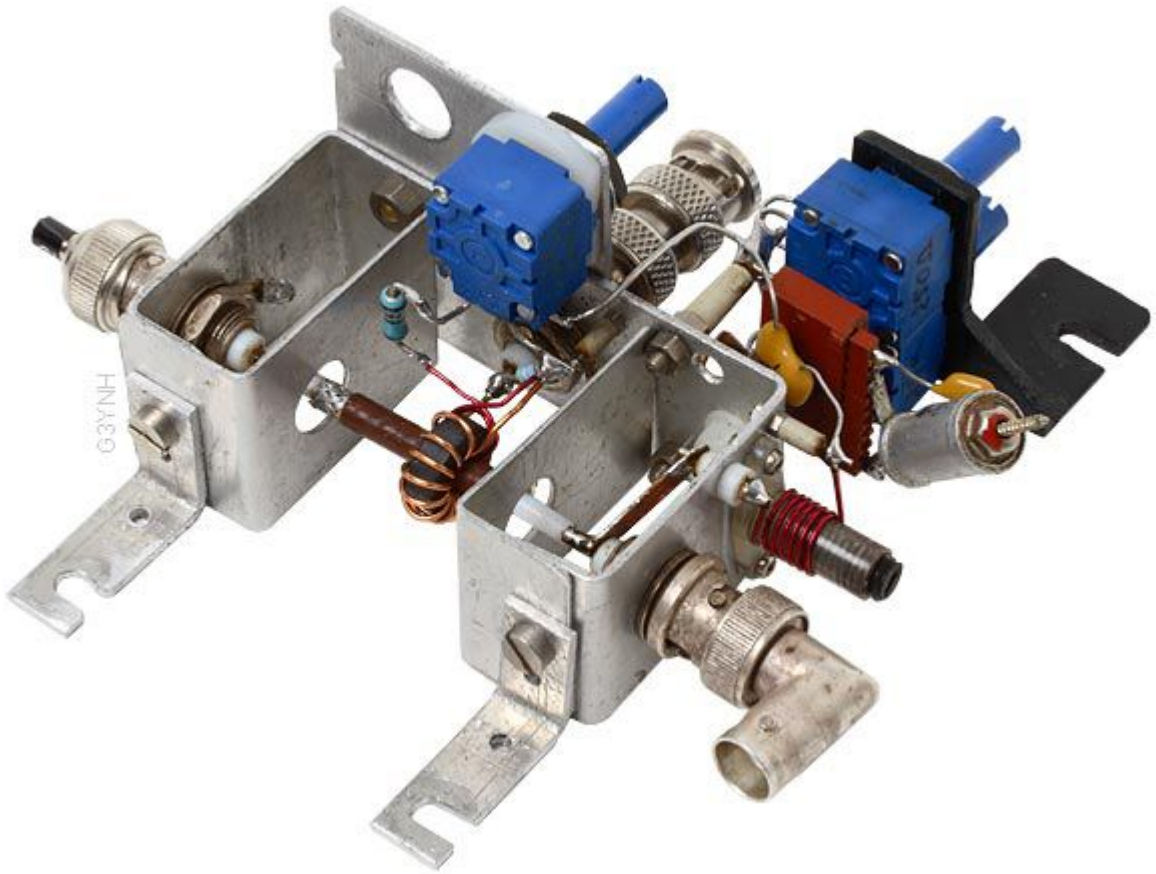

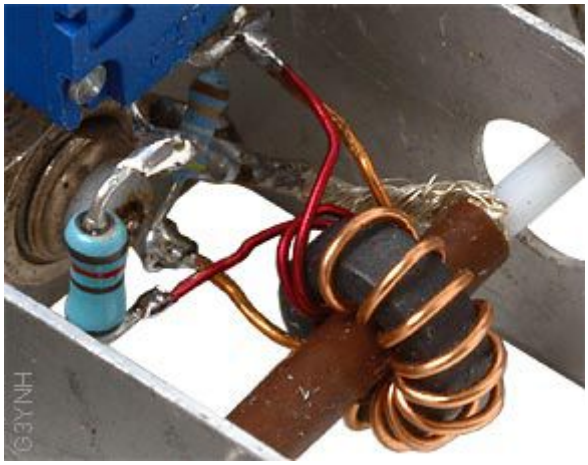

Bridge with 2-turn quadrature voltage compensation winding loaded with a 120 Ω resistor in series with a 250 Ω pot.. The adjustable leading quadrature voltage produced is placed in series with the current transformer output to cancel the high-frequency phase lag.

C_1' in this case is provided by a 2.5 pF - 30 pF trimmer in parallel with an 82 pF capacitor. The relatively low series inductance of this arm (ca. 50 nH) keeps the overall in-phase balance error to about ±0.03%.

Gen. side shield earth. 1.6 MHz to 30MHz	R_0 = 50 Ω , R_i = 50 Ω . L balance coil. 2-turn V-compensation winding with 250 Ω pot + 120 Ω .	Max. |Z| error	Max. φ error ( ) → best possible
testbrg61-14_2.ods	8 pF - 48 pF ref. cap. with 82 pF padding	±0.35%	±0.14° (±0.11°)
testbrg61-14_3.ods	3 pF - 30 pF trimmer with 82 pF padding.	±0.03%	±0.14° (±0.10°)

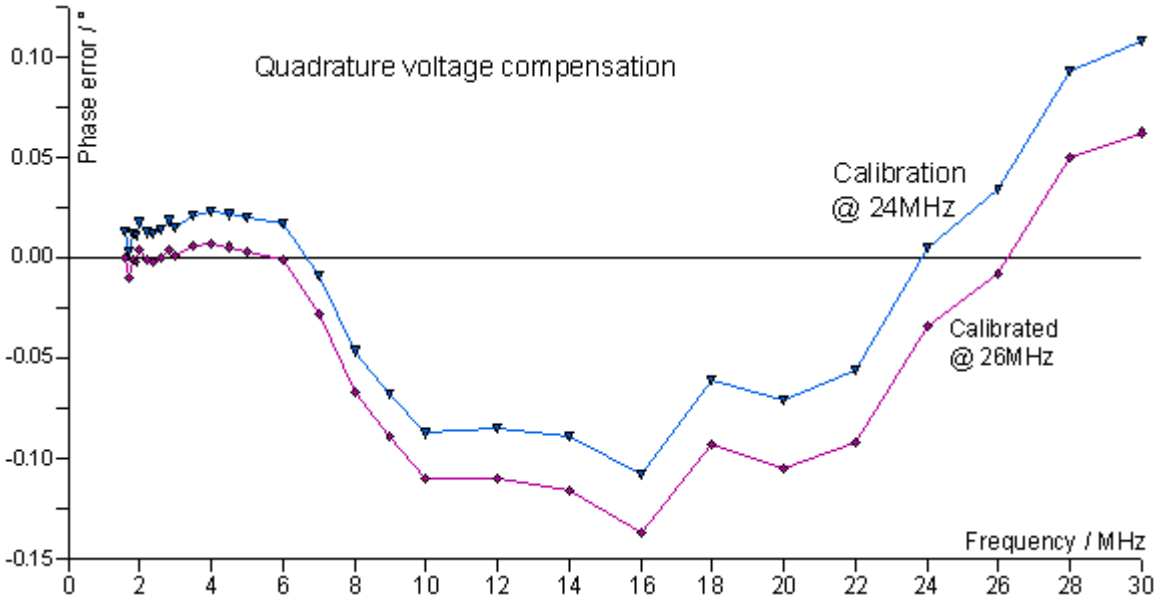

Two experimental runs were performed in this case, one using the 8 pF - 48 pF reference capacitor for C_1' and one using a 3 pF - 30 pF trimmer. Padding in both instances was 82 pF. The trimmer had to be removed and measured at each frequency point, considerably reducing the precision of the C_1' data, but the smaller assembly had an equivalent series inductance (L_1) of 50 nH, as opposed to 85 nH for the larger reference capacitor. The object of the exercise was to show that reducing L_1 (and also L_2) improves the magnitude performance without significantly affecting the phase performance.

The phase performance of the quadrature-voltage compensated bridge is very slightly inferior to that of the bridge compensated by means of a capacitance across the load port (section **18a**); but of course, quadrature-voltage compensation has no generator power-factor penalty.

18d. Phase-shift compensation

The quadrature voltage compensation method investigated in the previous section places an additional resistance in series with the detector port. This resistance is small in comparison to R_V, and so does not greatly affect the DC resistance of the network; but it increases the output impedance and it cannot be quantified exactly until calibration has been carried out. It may therefore be undesirable in some circumstances.

An alternative is to place a variable resistor directly across the auxiliary winding and connect the full output in series with the main secondary output. When the shunting resistance is set to a high value, the auxiliary output will be at +90° relative to V_i; and when the auxiliary winding is loaded with the same number of Ω/turn as the main secondary, the two outputs will be in phase. By choosing some intermediate setting, the phase error can be neutralised at the high-end of the working frequency range. The basic principle is illustrated in the diagrams below.

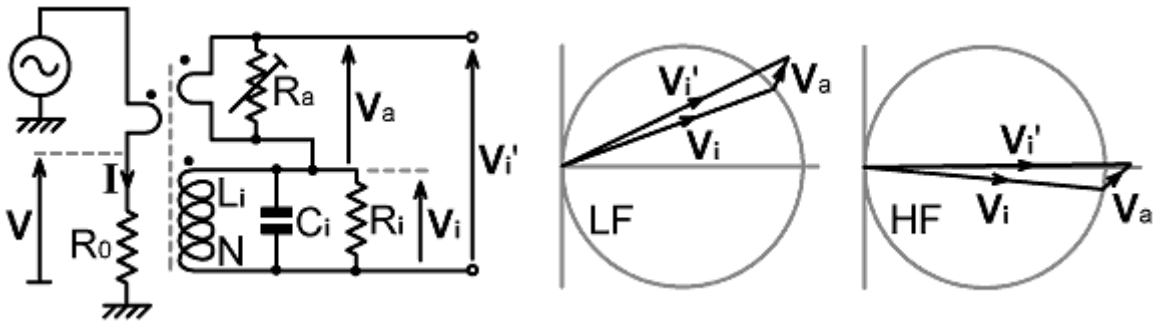

One drawback with this technique is that it makes a noticeable contribution to the magnitude of $\mathbf{V_i'}$ as well as to the phase. This means that the adjustments for in-phase and quadrature bridge balance interact more than they do with other methods. The problem is not particularly serious in practice however, and it was possible to set up the test bridge (shown right) with only three rounds of iteration.

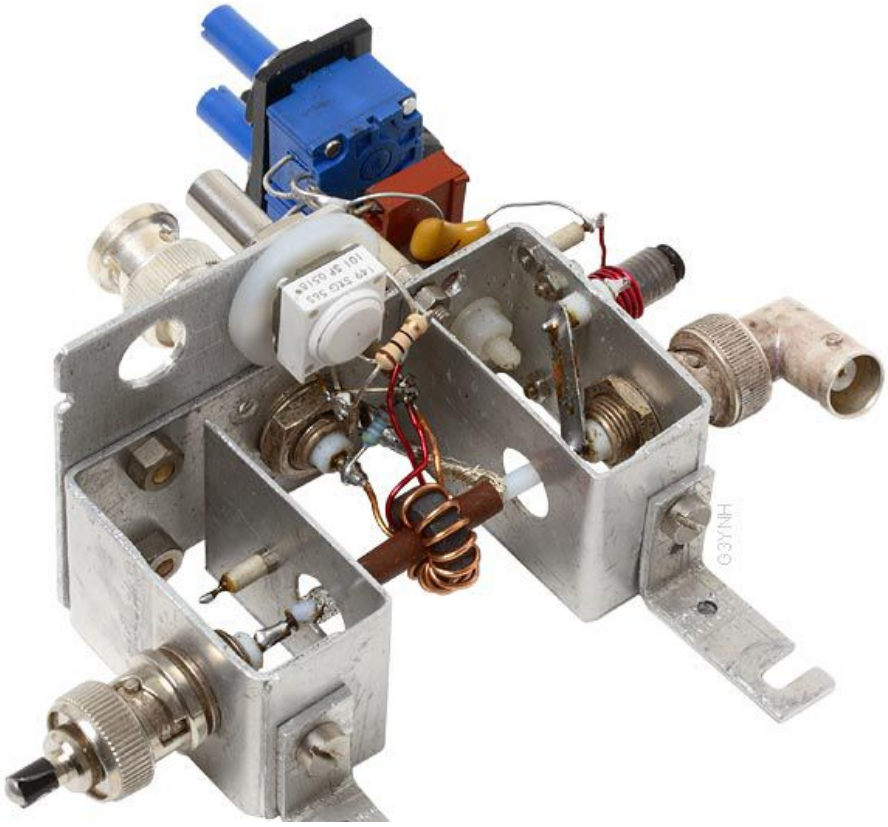

A single-turn compensation winding was sufficient to neutralise the test-bridge.

A 100 Ω cermet pot. was used for R_a because very low-value non-inductive variable resistors are difficult to obtain (lower value multi-turn cermet trimpots are available, but these have a limited operational life and the worm-drive is too slow for good null-seeking). This meant that the required resistance was very close to the minimum setting, making the adjustment rather fierce. The solution was to calibrate the bridge roughly and then place a fixed resistor across the pot. to bring the adjustment closer to the middle of the range. Final calibration was accomplished with a 10 Ω shunt resistor, as shown right, and the resistance of the parallel combination, measured after the test, was 7.49 Ω. This is 1.8 × the Ω/turn of the main secondary winding.

The test results, summarised below, are comparable to to the effect of placing a capacitor across the load port (but without the power-factor penalty), and slightly better than for quadrature-voltage compensation.

Gen. side shield gnd. 1.6 MHz to 30MHz	**Phase-shift neutralisation**. R_0 = 50 Ω , R_i = 50 Ω. L-bal. coil.	Max. |Z| error.	Max. φ error ( ) → best possible
testbrg61-13_5.ods	R_a = 7.49 Ω.	±0.32%	±0.12° (±0.10°)

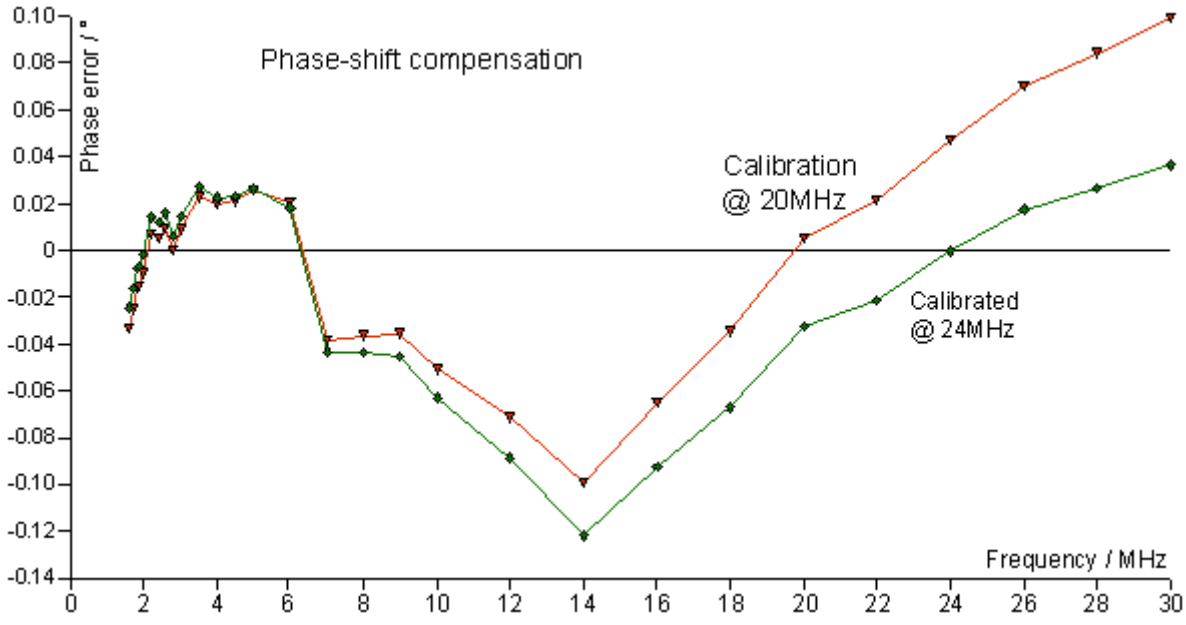

One peculiarity of the current transformer with phase-shift neutralisation is that it is not immediately obvious how to count the turns. In practice, it can be considered to behave either; like a transformer with N turns and an efficiency factor (k') of slightly greater than 1; or like a transformer with a non-integer number of turns between N and N-1. The reason that the effective number of turns is slightly *less than* N, rather than greater, is that the circuit gives more output than would be expected for a winding of N turns, whereas adding a turn to a normal current transformer makes the output level go down. The transformer constant is irrelevant to the perturbation analysis however (except it that can be adjusted to establish a realistic value for C_{1s}); and the network is intended for use in working bridges, not for circuit parameter determination.

18e. Herzog's HF compensation

The use of an inductance placed in series with R_i as a means for neutralising the phase error of a current-transformer bridge was patented by Will Herzog, K2LB, in 1988 [**US Pat. 4739515**]. Some additional qualitative discussion was given in a separate article[17].

In section **13**, it was indicated that the effective secondary capacitance has a large negative derivative with respect to the inductance of the secondary load resistor (here known as Herzog's inductance and given the symbol L_h). From equation **(13.1)**:

$$\partial C_{ieff} / \partial L_h = -1/R_i^2$$

Thus, for example, if R_i=50 Ω, then $\partial C_{ieff} / \partial L_h$ = -0.4 pF/nH. The effect is so great that, for the test bridge, the apparent secondary capacitance could be made negative merely by soldering the secondary load resistor in place without trimming its wires. Achieving the 7 pF or so of capacitance cancellation required for neutralisation was therefore not so much a matter of installing an inductor as of placing a slug of magnetic material in the vicinity of the resistor. To that end, and to provide a degree of adjustment, the resistor was bent into a U-shape over a 7 mm diameter coil former with an M6 dust-iron slug as shown below.

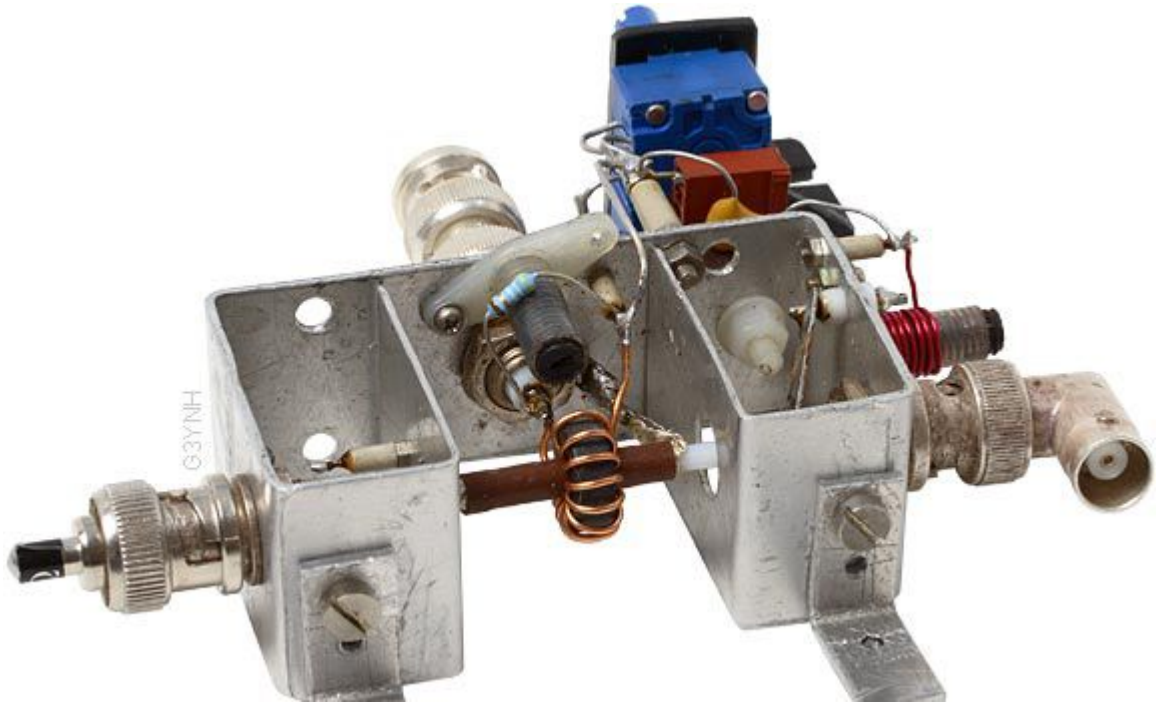

Gen. side shield gnd.. 1.6 MHz to 30MHz	**Herzog's neutralisation method**.	Max. |Z| error.	Max. φ error ( ) → best possible
testbrg61-1214.ods	R_0 = 50 Ω , R_i = 50 Ω. L-bal. coil.	±0.38%	±0.11° (±0.10°)

17 **VSWR Bridges**, Will Herzog K2LB, Ham Radio, March 1986, p37-40.
Brief review of the pitfalls of SWR bridge design, particularly the problem of phase error.

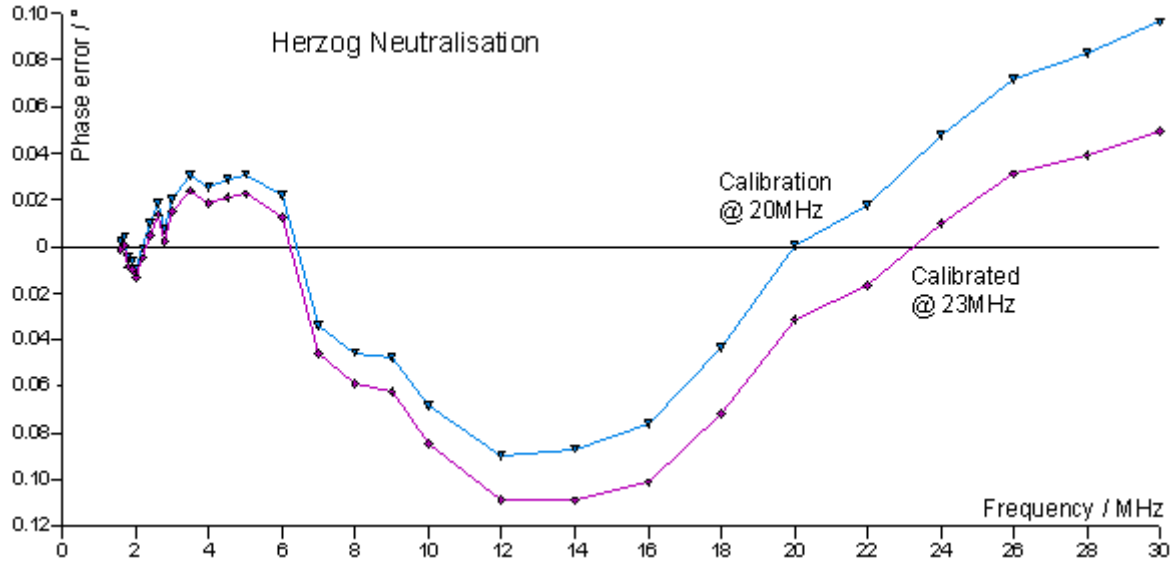

The phase performance obtained from the test bridge is fairly typical for a dispersion limited (2-point tracking) bridge.

One slight drawback of the method is the inherent unpredictability of the final physical construction. In an early experiment, with the Faraday shield earthed on the load side, it was found that a single 49.9 Ω helical-cut metal-film resistor, looped around a coil-former as shown above, provided too much inductance. The solution in that case was to use two 100 Ω resistors in parallel. An unshielded bridge discussed in section **19**, on the other hand, having a much larger C_{ieff} , required a whole turn around around the dust-iron core. The method works well, but some experimentation is required in order to get it to work.

In common with the other compensation methods tested, the amplitude error is largely attributable to the 8 pF - 48 pF reference capacitor. An early experiment, unfortunately invalidated by failure to control reciprocity error, gave a maximum amplitude error of ±0.28% when using the 500 pF reference capacitor.

18f. Load-side voltage sampling

The voltage sampling network of a Douma bridge constitutes a capacitive load across the generator. If the capacitance that would have to be placed across the load port in order to neutralise the bridge is within the acceptable limit for the generator (typically <14 pF for a 50 Ω system operating up to 30 MHz), then the voltage sampling network itself can be used as the neutralising capacitance.

The test bridge is shown below configured for load-side voltage sampling by the simple expedient of swapping the connections to the current-transformer secondary, reversing the Faraday shield, and swapping the generator and load plugs. The original fixed upper-voltage sampling capacitor C_2 has also been replaced by a 3 pF - 30 pF multi-turn (beehive) trimmer, the object of the exercise being to allow the input capacitance of the network to be adjusted to give the required degree of neutralisation.

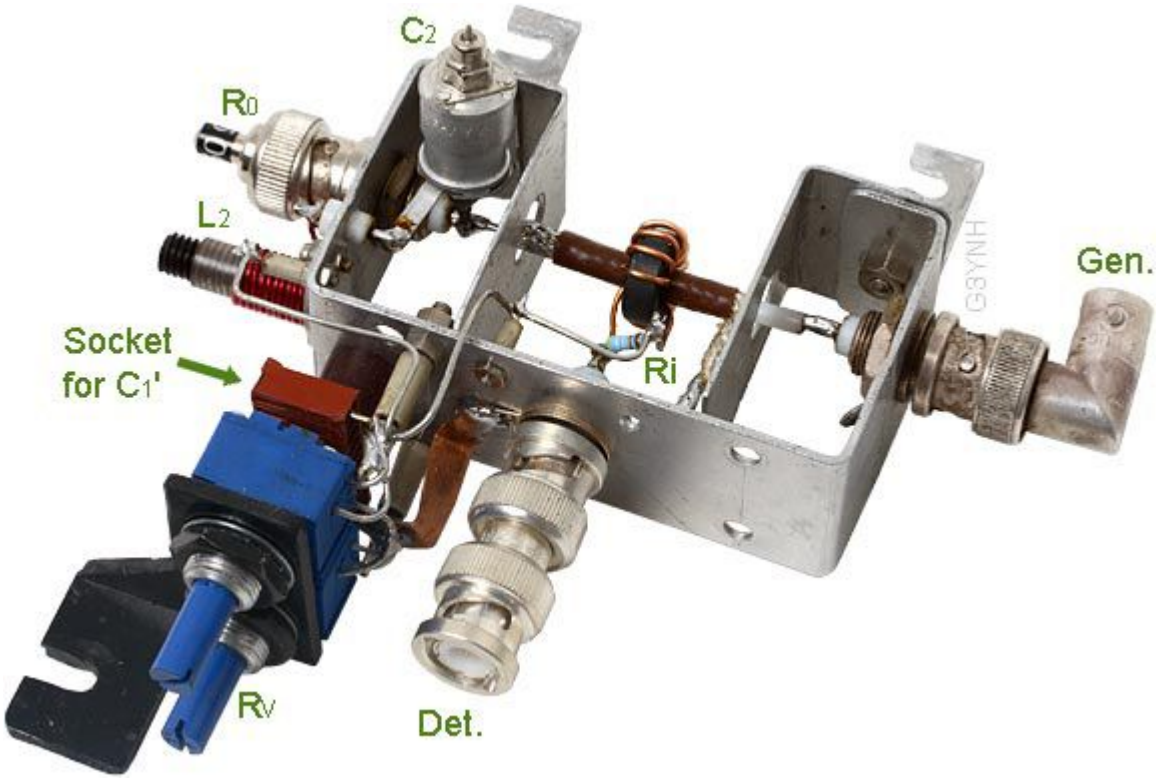

One problem with this configuration is that, in a calibration sequence that involves altering C_2, all of the adjustments become highly interactive. Indeed, it is not possible to distinguish between the effects of adjusting C_2 and L_2 at high frequencies, which means that calibration by observation only of bridge balance is effectively a non-convergent process. The solution used in the case of the test bridge was to measure R_V via the detector port in the same way as is done during evaluation, and to use this information as a guide for the setting of C_2. The procedure was as follows: The bridge was balanced at 2 MHz using C_1 and R_V, and at 26 MHz (which was found to be about the optimum upper calibration frequency) by adjusting L_2 and R_V. An increase in R_V on going to the upper frequency is indicative of a positive C_{ieff}, which means that C_2 needs to be increased. A decrease in R_V indicates a negative C_{ieff}, which means that C_2 needs to be decreased. The cycle was repeated until the change in R_V between the two calibration frequencies fell to less than 1%. Final adjustment required tiny changes to C_2, and calibration would have been extremely difficult using a half-turn trimmer capacitor (rather than a multi-turn type).

Gen. side shield gnd.. 1.6 MHz to 30MHz	**Load-side voltage sampling**. R_0 = 50 Ω , R_i = 50 Ω . L-bal. coil.	Max. |Z| error.	Max. φ error ( ) → best possible
testbrg61-1215.ods	C_2 = 8.7 pF*	±0.28%	±0.30° (±0.30°)

* The final value of C_2 was determined by adjusting it in the least-squares fit to the R_V data to reproduce the known value of L_i (8.98 µH).

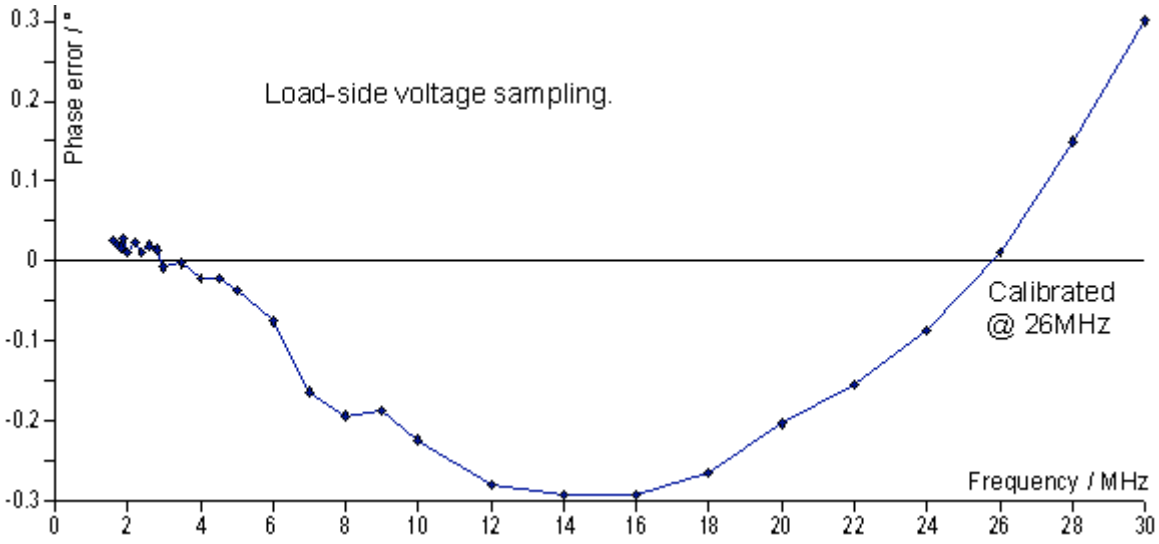

Notwithstanding the tedious process of calibrating it; in the final analysis, the self-neutralising bridge is slightly inferior to to the other configurations tested (although it is still very good). The reason is probably that the voltage sampling network is not a pure capacitance, having a resistive component due to R_V and an inductive component due to L_2. It is likely therefore that the performance can be improved by minimising L_1 (and hence L_2) and by increasing L_i to give an increase in the set value of R_V.

An alternative solution to the problem of how to use the VS network as a neutralising capacitance might be to over-neutralise slightly and then place a very small adjustable capacitance across the current transformer secondary winding. If this method is properly engineered, a conventional trimmer capacitor will be too large for the job; but a pair of short stiff wires that can be moved closer together or further apart (< 2 pF) will doubtless suffice.

18x. Collected results

The collected results for sections **18a** to **18f** are summarised below.

The common experimental conditions (unless stated otherwise) were:
- Generator side Faraday shield earth.
- Test frequency range: 1.6 MHz to 30 MHz
- Inductance balance coil in series with C_2, adjusted before test.
- C_2 = 10pF , R_0 = 50 Ω , R_i = 50 Ω . N = 12 , Core type = FT50-61 , L_{sec} = 9.25 µH .
- Reference capacitor: 8 pF - 48 pF with 82 pF in parallel. $L_1 \approx$ 85 nH .

Neutralisation method	**Data and analysis.**	Max. |Z| error.	Max. φ error ( ) → best possible?
Load-port capacitor.	**testbrg61-1212.ods**	±0.25%	±0.12° (±0.09°)
Quadrature current, 2-point tracking	**testbrg61-13_2.ods**	±0.35%	±0.17° (±0.13°)
Quadrature current, 3-point tracking	**testbrg61-13_4.ods**	±0.12%	±0.044° (±0.04°)
Quadrature current, 3-point tracking C_2 = 4.9 pF . L_{sec} = 8.15 µH. 3 pF - 30 pF ref cap ($L_1 \approx$ 50 nH).	See separate article[18]	**±0.04%**	±0.03°
Quadrature voltage.	**testbrg61-14_2.ods**	±0.35%	±0.14° (±0.11°)
Quadrature voltage. 3 pF - 30 pF ref cap ($L_1 \approx$ 50 nH).	**testbrg61-14_3.ods**	**±0.03%**	±0.14° (±0.10°)
Phase shift	**testbrg61-14_5.ods**	±0.32%	±0.12° (±0.10°)
Herzog	**testbrg61-1214.ods**	±0.38%	±0.11° (±0.10°)
Load side voltage sampling C_2 = 8.7 pF. 8 pF - 48 pF ref. cap. with 56 pF in parallel.	**testbrg61-1215.ods**	±0.28%	±0.30° (±0.30°

The best possible phase performance (indicated in brackets) is an estimate of what can be achieved if the optimum upper calibration frequency is chosen. Most of the 2-point tracking bridges are similar in this respect, and there is effectively no practical difference between a number of methods. Generally, those methods that do not carry a generator power-factor penalty are to be preferred when extreme accuracy is not required. 3-point tracking gives the best results; but the additional circuit complexity is unwarranted for typical working bridges, and particularly if a conventional diode detector is to be used.

The amplitude performance is limited by the characteristics of the reference capacitor. It is generally best when the inductance of the lower voltage-sampling arm is minimised. This is demonstrated by the results for bridges using a 3 pF- 30 pF beehive trimmer rather than a physically-large variable capacitor.

The results tabulated above are a demonstration of what can be achieved, but not necessarily of what has to be achieved. In practice, anything better than about ±0.5° and ±0.5% (±0.25 Ω in a 50 Ω system) is fine for a working impedance-monitoring bridge.

18 **A Self-evaluating precision reference bridge**. Section 8. D W Knight. http://g3ynh.info/zdocs/bridges/ .

19. The utility of the Faraday shield

The application of the current transformer to the field of RF measurement was patented by Josef Stanek of Siemens and Halske (Germany), the US Patent [# **2134589**] being awarded in 1938. The Faraday shield was included in this invention, and its purpose was explained as follows:

"The metallic coating of the insulating sheath is electrically connected to one terminal of the measuring instrument, preferably to that terminal which .. is grounded. This arrangement serves the following purpose. In the case of high-frequency, a transformer is also to be regarded as a condenser, the primary conductor .. forming the one and the secondary conductor forming the other electrode.. Therefore a capacitive displacement current could flow from the primary conductor to the secondary circuit and impair the measurement. The grounded coating however carries off this displacement current and makes it ineffective."

Since that passage was written, the need for the shield has become an article of faith among radio engineers; and others have gone on to say that the purpose of the shield is not to minimise the transmission-line mismatch but to provide electrostatic screening. In section **11** however, we showed that the shield upsets the forward and reverse symmetry of the transformer phase performance, and in section **18b** we showed that it can slightly degrade the frequency-tracking; i.e., at a subtle level, perhaps not relevant in 1938, it can cause the type of problem that it is supposed to prevent. Moreover, it does help to minimise the through-line mismatch; but since that can also be done in other ways, the utility of the shield is open to question.

An unshielded version of the test bridge was assembled as shown in the photographs below:

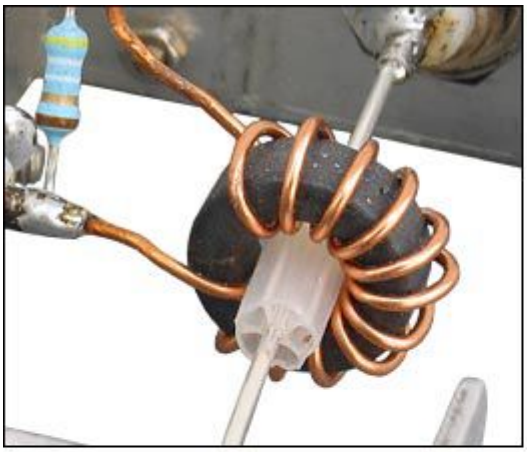

The through-line is a 0.9 mm diameter silver-plated wire, and the transformer core is spaced away from it by means of a stub of polyethylene honeycomb insulator as used in 75 Ω UHF TV-antenna

cable. To prevent the polyethylene from melting during the soldering to the BNC sockets, the heat was shunted away by attaching to the wire a small pair of pliers with a rubber band around the handles. Sliding the insulator away from the point being soldered also helped.

In a jig designed for shielded transformers, it is obvious that the the through-line is a lot longer than it needs to be. That does not pose a problem analytically, but it raises the point that doing without the shield is an aid to miniaturisation. In fact, the transformer core could simply be placed on the back of the load-port socket, in which case the mismatch of the load-side line would be negligible.

The investigation was begun by acquiring two datasets as listed below:

No Faraday shield	No compensation. 12 turns, FT50-61, R_i = 50 Ω .	C_{ieff}
testbrg61-12_8.ods	50 Ω reference load.	12.1 pF
testbrg61-12_9.ods	75.5 Ω reference load.	1.4 pF

An obvious feature of the data for the uncompensated bridge with the 50 Ω load connected is that that the apparent secondary capacitance is higher than for a shielded bridge. This might seem anti-intuitive to those who see the shield as a distributed capacitance across the coil, but since the average characteristic resistance of the through-line is now somewhere around 300 Ω, equations **(14.3)** or **(15.1)** tell us that at least some of this increase must be due to the mismatch. Other features are that the stray capacitance across the voltage sampling network is reduced, and the value of the upper voltage sampling capacitor C_2 has to be increased by about 0.7 pF in order for the R_v data to reproduce the known value of L_i (8.97 μH). The increase is, of course, partly due to stray capacitance between the line and the summing point (i.e., the voltage-sampling network end of the transformer secondary).

In the case of the uncompensated bridge with the 75 Ω load, agreement with the model developed in section **2** is not so good. One reason for that is that the bridge with the 50 Ω load has a phase crossover frequency of 15.3 MHz and the data only go up to 14.5 MHz, whereas with a 75 Ω load, the apparent secondary capacitance is reduced and the data go up to 30 MHz . With this extra coverage, it can be seen that the quadrature balance data are somewhat more divergent from theory at high frequencies than for shielded bridges. Also, the value of L_1 returned from the in-phase balance data is too large by about 30%, the reduced χ^2 is about 6, and the graph of residuals shows a distinct curvature.

In fact, we should expect the data do deviate from the model; and we should expect the deviation to be worse with a 75 Ω load than it is with a 50 Ω load because the ratio of voltage to current is increased with increasing load impedance, i.e., the relative output of the current transformer goes down. This gives greater influence to the principal suspect, which is the stray capacitance between the line and the detector port. If C_2 appears to have increased by 0.7 pF, then this capacitance must be of the same order. Hence a more accurate model for the unshielded bridge is as in the diagram below.

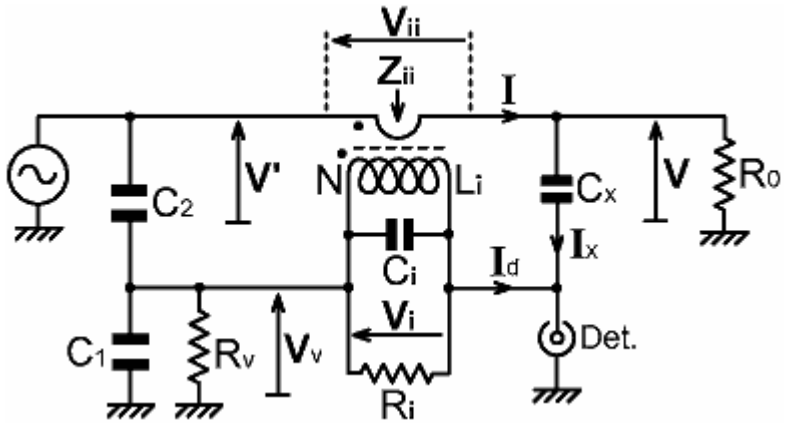

Since the voltage at the detector is zero when the bridge is balanced, the stray capacitance C_x passes its current into a virtual earth. Therefore C_x is effectively across the load, and as we know from equation **(14.1)**, one of its effects will be to reduce the apparent secondary capacitance. In this sense its presence is beneficial, because it reduces the mismatch of the through-line, but there is a greater issue (N times greater it will transpire) regarding the current injected into the detector port.

In the absence of C_x, the bridge balances when $\mathbf{V_V} = \mathbf{V_i}$. When C_x is included however, the balance point is skewed such that the voltage $\mathbf{V_V} = \mathbf{V_i}$ produces a current $\mathbf{I_d}$ that is equal and opposite to the injected current $\mathbf{I_x}$. The magnitude of the voltage difference needed to counteract $\mathbf{I_x}$ depends on the source impedance of the Thévenin-equivalent generator producing it. This impedance is the sum of the output impedances of the voltage sampling network and the current sampling network, these being:

$$\mathbf{Z_v} = R_v \,//\, \mathbf{j}X_{C1} \,//\, \mathbf{j}X_{C2}$$

and

$$\mathbf{Z_i} = R_i \,//\, \mathbf{j}X_{Li} \,//\, \mathbf{j}X_{Ci}$$

Thus we can draw an equivalent circuit that allows us to determine the balance condition.

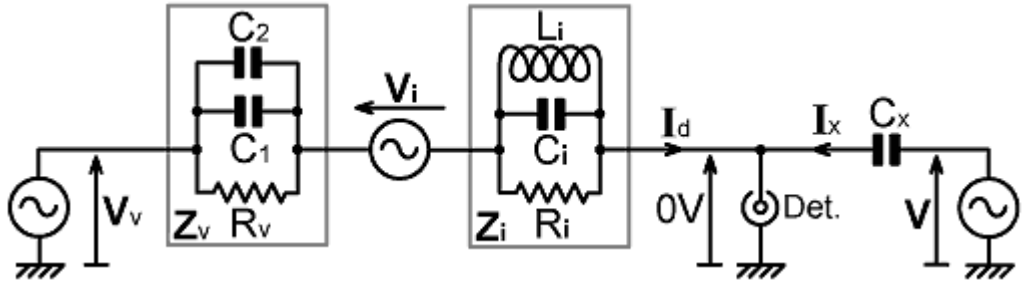

The balance condition is $\mathbf{I_d} = -\mathbf{I_x}$. Written explicitly this is:

$$\frac{\mathbf{V_V} - \mathbf{V_i}}{\mathbf{Z_v} + \mathbf{Z_i}} = \frac{-\mathbf{V}}{\mathbf{j}X_{Cx}} \qquad (19.1)$$

Expressions for $\mathbf{V_V}$ and $\mathbf{V_i}$ were given in section 2. Modified to allow for the capacitance C_x in parallel with the primary load, these become:

$$\mathbf{V_v} = \mathbf{V} \left[1 + \frac{\mathbf{Z_i}}{N^2 (R_0 \,//\, \mathbf{j}X_{Cx})} \right] \frac{\mathbf{Z_v}}{\mathbf{j}X_{C2}}$$

and

$$\mathbf{V_i} = \frac{\mathbf{V}\,\mathbf{Z_i}}{N (R_0 \,//\, \mathbf{j}X_{Cx})}$$

Substituting these into equation **(19.1)**, cancelling the voltages and rearranging gives the dimensionless balance relationship:

$$\frac{\mathbf{Z_v}}{\mathbf{j}X_{C2}} \left[1 + \frac{\mathbf{Z_i}}{N^2 (R_0 \,//\, \mathbf{j}X_{Cx})} \right] - \frac{\mathbf{Z_i}}{N (R_0 \,//\, \mathbf{j}X_{Cx})} = \frac{-(\mathbf{Z_v} + \mathbf{Z_i})}{\mathbf{j}X_{Cx}}$$

which can be regrouped:

$$\frac{\mathbf{Z_v}}{\mathbf{j}X_{C2}} \left[1 + \frac{\mathbf{Z_i}}{N^2 (R_0 \,//\, \mathbf{j}X_{Cx})} \right] + \frac{\mathbf{Z_v}}{\mathbf{j}X_{Cx}} = \frac{\mathbf{Z_i}}{N (R_0 \,//\, \mathbf{j}X_{Cx})} - \frac{\mathbf{Z_i}}{\mathbf{j}X_{Cx}}$$

Now, multiplying X_{C2} into top and bottom of the last term on the left-hand side, and noting that $X_{C2} / X_{Cx} = C_x / C_2$; and also factoring $\mathbf{Z_i} / N$ from the right-hand side and noting that $1/(\mathbf{a}//\mathbf{b}) = (1/\mathbf{a}) + (1/\mathbf{b})$:

$$\frac{\mathbf{Z_v}}{\mathbf{j}X_{C2}} \left[1 + \frac{\mathbf{Z_i}}{N^2 (R_0 \,//\, \mathbf{j}X_{Cx})} + \frac{C_x}{C_2} \right] = \frac{\mathbf{Z_i}}{N} \left[\frac{1}{R_0} + \frac{1 - N}{\mathbf{j}X_{Cx}} \right]$$

Inverting this expression and rearranging gives:

$$\frac{\mathbf{j}X_{C2}}{\mathbf{Z_v}} = \frac{N \left[R_0 \,//\, \mathbf{j}X_{Cx} / (1-N) \right]}{\mathbf{Z_i}} \left[1 + \frac{\mathbf{Z_i}}{N^2 (R_0 \,//\, \mathbf{j}X_{Cx})} + \frac{C_x}{C_2} \right]$$

and hence:

$$\frac{\mathbf{j}X_{C2}}{\mathbf{Z}_v} = \left[1 + \frac{C_x}{C_2} \right] \frac{N\,[\,R_0 \,//\, \mathbf{j}X_{Cx}/(1\text{-}N)\,]}{\mathbf{Z}_i} + \frac{R_0 \,//\, \mathbf{j}X_{Cx}/\,(1\text{-}N)}{N\,(R_0 \,//\, \mathbf{j}X_{Cx})} \qquad (19.2)$$

Taking the right-most term on its own and expanding it gives:

$$\frac{R_0 \,//\, \mathbf{j}X_{Cx}/\,(1\text{-}N)}{N\,(R_0 \,//\, \mathbf{j}X_{Cx})} = \frac{\mathbf{j}\,R_0\,X_{Cx}/\,(1\text{-}N)}{N\,[\,R_0 + \mathbf{j}X_{Cx}/\,(1\text{-}N)\,]} \left[\frac{1}{R_0} + \frac{1}{\mathbf{j}X_{Cx}} \right]$$

Now factoring 1/ (1-N) from the denominator and cancelling, then multiplying numerator and denominator by the complex conjugate of the denominator, we obtain:

$$\frac{R_0 \,//\, \mathbf{j}X_{Cx}/\,(1\text{-}N)}{N\,(R_0 \,//\, \mathbf{j}X_{Cx})} = \frac{\mathbf{j}\,R_0\,X_{Cx}\,[\,(1\text{-}N)\,R_0 - \mathbf{j}X_{Cx}\,]}{N\,[\,(1\text{-}N)^2\,R_0^2 + X_{Cx}^2\,]} \left[\frac{1}{R_0} + \frac{1}{\mathbf{j}X_{Cx}} \right]$$

Here we can make an approximation by noting that for the test bridge, with N = 12 , R_0 = 50 Ω and C_x no greater than 1 pF (actually 0.33 pF as it turned out), the term $(1\text{-}N)^2\,R_0^2 = 302500$, whereas X_{Cx}^2 , at its lowest (at say 2×10^8 radians/sec), will be >25 million. Hence the error in deleting $(1\text{-}N)^2\,R_0^2$ from the denominator will be <1% at the high end of the HF spectrum and negligible at the low end. Hence:

$$\frac{R_0 \,//\, \mathbf{j}X_{Cx}/\,(1\text{-}N)}{N\,(R_0 \,//\, \mathbf{j}X_{Cx})} = \frac{\mathbf{j}\,R_0\,[\,(1\text{-}N)\,R_0 - \mathbf{j}X_{Cx}\,]}{N\,X_{Cx}} \left[\frac{1}{R_0} + \frac{1}{\mathbf{j}X_{Cx}} \right]$$

And after putting the first factor into **a**+**jb** form (and noting that $\mathbf{j}^2 = -1$):

$$\frac{R_0 \,//\, \mathbf{j}X_{Cx}/\,(1\text{-}N)}{N\,(R_0 \,//\, \mathbf{j}X_{Cx})} = \frac{R_0}{N} \left[1 + \frac{\mathbf{j}\,(1\text{-}N)\,R_0}{X_{Cx}} \right] \left[\frac{1}{R_0} + \frac{1}{\mathbf{j}X_{Cx}} \right]$$

Multiplying out:

$$\frac{R_0 \,//\, \mathbf{j}X_{Cx}/\,(1\text{-}N)}{N\,(R_0 \,//\, \mathbf{j}X_{Cx})} = \frac{1}{N} \left[1 + \frac{(1\text{-}N)\,R_0^2}{X_{Cx}^2} + \frac{R_0}{\mathbf{j}X_{Cx}} - \frac{(1\text{-}N)\,R_0}{\mathbf{j}X_{Cx}} \right]$$

We can now make another approximation, less serious than the previous one, which is that the second term of the series can be deleted because $X_{Cx}^2 >> (1\text{-}N)\,R_0^2$. The error in this case is <0.05% for the test bridge at the high end of the HF spectrum, i.e., truly negligible. Now noting that 1-(1-N) = N and $1/\mathbf{j} = -\mathbf{j}$, we get:

$$\frac{R_0 \,//\, \mathbf{j}X_{Cx}/(1\text{-}N)}{N\,(R_0 \,//\, \mathbf{j}X_{Cx})} = \frac{1}{N} - \frac{\mathbf{j}R_0}{X_{Cx}} \qquad (19.3)$$

Substituting this back into equation **(19.2)** and rearranging the terms gives:

$$\frac{\mathbf{j}X_{C2}}{\mathbf{Z}_v} - \frac{1}{N} + \frac{\mathbf{j}R_0}{X_{Cx}} = \left[\, 1 + \frac{C_x}{C_2} \,\right] \frac{N\,[R_0 \,//\, \mathbf{j}X_{Cx}/\,(1\text{-}N)\,]}{\mathbf{Z}_i} \qquad (19.4)$$

The 1/N term is of course part of the transformer constant in the in-phase balance condition. Since this is a small correction to allow for the difference between **V** and **V'** caused by the insertion impedance, and N is generally >10, the <1% error introduced earlier is <1% of <10%, i.e., <0.1%, and is therefore harmless.

Now, taking the right-most factor on its own and expanding it (also recalling that $\mathbf{Z}_i = R_i \,//\, \mathbf{j}X_{Li} \,//\, \mathbf{j}X_{Ci}$) gives:

$$\frac{N\,[R_0 \,//\, \mathbf{j}X_{Cx}/\,(1\text{-}N)\,]}{\mathbf{Z}_i} = \frac{\mathbf{j}\,N\,R_0\,X_{Cx}/\,(1\text{-}N)}{R_0 + \mathbf{j}X_{Cx}/\,(1\text{-}N)} \left[\frac{1}{R_i} + \frac{1}{\mathbf{j}X_{Li}} + \frac{1}{\mathbf{j}X_{Ci}} \right]$$

One again factoring 1/(1-N) from the denominator and cancelling, then multiplying numerator and denominator by the complex conjugate of the denominator, gives:

$$\frac{N\,[R_0 \,//\, \mathbf{j}X_{Cx}/\,(1\text{-}N)\,]}{\mathbf{Z}_i} = \frac{\mathbf{j}\,N\,R_0\,X_{Cx}\,[\,(1\text{-}N)\,R_0 - \mathbf{j}X_{Cx}\,]}{(1\text{-}N)^2\,R_0^2 + X_{Cx}^2} \left[\frac{1}{R_i} + \frac{1}{\mathbf{j}X_{Li}} + \frac{1}{\mathbf{j}X_{Ci}} \right]$$

Again we can use the approximation that $X_{Cx}^2 >> (1\text{-}N)^2\,R_0^2$. This time however, the <1% error will slightly affect the goodness of fit to the model; potentially incurring a frequency-dependent curvature that will be small but possibly visible above the experimental noise. Thus:

$$\frac{N\,[R_0 \,//\, \mathbf{j}X_{Cx}/\,(1\text{-}N)\,]}{\mathbf{Z}_i} = N\,R_0 \left[\, 1 + \frac{\mathbf{j}\,(1\text{-}N)\,R_0}{X_{Cx}} \,\right] \left[\frac{1}{R_i} + \frac{1}{\mathbf{j}X_{Li}} + \frac{1}{\mathbf{j}X_{Ci}} \right]$$

Multiplying out:

$$\frac{N\,[R_0 \,//\, \mathbf{j}X_{Cx}/\,(1\text{-}N)]}{\mathbf{Z}_i} = N\,R_0 \left[\frac{1}{R_i} + \frac{(1\text{-}N)\,R_0}{X_{Cx}\,X_{Li}} + \frac{(1\text{-}N)\,R_0}{X_{Cx}\,X_{Ci}} + \frac{1}{\mathbf{j}X_{Li}} + \frac{1}{\mathbf{j}X_{Ci}} - \frac{(1\text{-}N)\,R_0}{\mathbf{j}X_{Cx}\,R_i} \right]$$

Now observe that $X_{Cx}\,X_{Li} = -L_i / C_x$. For the test bridge, with N = 12 , $R_0 = 50\ \Omega$, $C_x < 1$ pF and $L_i = 9\ \mu$H , the second conductance term will be <0.00006 Siemens, i.e., it corresponds to a

resistance of >16.7 kΩ in parallel with R_i. It represents a minor frequency-independent adjustment to the apparent transformer efficiency, which will be lost in the uncertainty of the efficiency factor and can therefore be dropped.

If we take C_i to be about 10 pF , and the maximum frequency to be 2×10^8 radians/sec, the third conductance term will be <0.00022 Siemens, i.e., it corresponds to a resistance of >4.5 kΩ in parallel with R_i and can be dropped with the proviso that there will be an additional frequency dependent deviation from the model of <1% in the in-phase response.

Hence:

$$\frac{N\,[R_0 \,//\, \mathbf{j}X_{Cx} / (1-N)\,]}{\mathbf{Z_i}} = N\,R_0 \left[\frac{1}{R_i} + \frac{1}{\mathbf{j}X_{Li}} + \frac{1}{\mathbf{j}X_{Ci}} - \frac{(1-N)\,R_0}{\mathbf{j}X_{Cx}\,R_i} \right] \qquad (19.5)$$

The additional capacitive susceptance term, of course, gives rise to a shift in the apparent value of C_i in exactly the same way as did the other parasitic effects analysed in sections **11** to **14** and summarised in section **15**. To quantify the effect we can introduce a new parameter C_{ix}' to represent the apparent secondary capacitance (the parameter is given a prime because there is another small contribution to be added later). Noting that -(1-N) = N-1 , C_{ix}' is defined by the relationship:

$$\frac{1}{X_{Cix}'} = \frac{1}{X_{Ci}} + \frac{(N-1)\,R_0}{X_{Cx}\,R_i}$$

i.e.:

$$-2\pi f\,C_{ix}' = -2\pi f\,C_i - 2\pi f\,(N-1)\,C_x\,R_0 / R_i$$

Thus:

$$C_{ix}' = C_i + (N-1)\,C_x\,R_0 / R_i \qquad (19.6)$$

Comparing this with equation **(15.1)** (cf. the effect of C_0), we can see that this represents N C_x of shift for the current injected into the detector port, minus C_x of shift for the extra capacitance across the line. Overall, the lack of a Faraday shield has made a significant positive contribution to the apparent secondary capacitance. If C_x is 0.33 pF , $R_0 = R_i$, and N = 12 , it amounts to 3.6 pF. This is in addition to the positive contribution caused by having a through-line characteristic resistance greater than R_0. There is nothing yet to imply that the situation is uncorrectable however.

Substituting equation **(19.6)** into **(19.5)**:

$$\frac{N\,[R_0 \,//\, \mathbf{j}X_{Cx} / (1-N)\,]}{\mathbf{Z_i}} = N\,R_0 \left[\frac{1}{R_i} + \frac{1}{\mathbf{j}X_{Li}} + \frac{1}{\mathbf{j}X_{Cix}'} \right]$$

and substituting this back into equation **(19.4)**:

$$\frac{\mathbf{j}X_{C2}}{\mathbf{Z}_v} - \frac{1}{N} + \frac{\mathbf{j}R_0}{X_{Cx}} = \left[1 + \frac{C_x}{C_2} \right] N R_0 \left[\frac{1}{R_i} + \frac{1}{\mathbf{j}X_{Li}} + \frac{1}{\mathbf{j}X_{Cix}'} \right]$$

Now we can see that the term $\mathbf{j}R_0 / X_{Cx}$ is also in a form that causes it to contribute to the apparent secondary capacitance. Moving it to the right hand side and moving **j** to the denominator shows that it is a positive contribution. It becomes part of the secondary admittance series when the denominator is multiplied by $(1+ C_x / C_2)\, N\, R_0$. Hence:

$$\frac{\mathbf{j}X_{C2}}{\mathbf{Z}_v} - \frac{1}{N} = (1 + C_x/C_2)\, N\, R_0 \left[\frac{1}{R_i} + \frac{1}{\mathbf{j}X_{Li}} + \frac{1}{\mathbf{j}X_{Cix}'} + \frac{1}{\mathbf{j}\,(1+C_x/C_2)\, N\, X_{Cx}} \right] \qquad (19.7)$$

Now we can define a new parameter C_{ix}, without the prime, such that:

$C_{ix} = C_{ix}' + C_x / [\, (1+C_x/C_2)\, N \,]$

Also notice that $(1+ C_x / C_2) = (C_x+C_2) / C_2$. Hence:

$C_{ix} = C_{ix}' + C_x C_2 / [\, (C_x+ C_2)\, N \,]$

The new contribution to the apparent secondary capacitance is 1/N times the capacitance of the series combination of C_x and C_2. For the test bridge it amounts to about 0.03 pF, and so it is not very important, but it might as well be included for completeness. Combining this result with equation **(19.6)** gives:

$C_{ix} = C_i + [\, (N-1)\, C_x R_0 / R_i \,] + C_x C_2 / [\, (C_x+ C_2)\, N \,]$	**19.8**

and substituting this into equation **(19.7)** gives:

$$\frac{\mathbf{j}X_{C2}}{\mathbf{Z}_v} - \frac{1}{N} = (1 + C_x / C_2)\, N\, R_0 \left[\frac{1}{R_i} + \frac{1}{\mathbf{j}X_{Li}} + \frac{1}{\mathbf{j}X_{Cix}} \right]$$

$\mathbf{Z}_v$ is, of course, $R_v // \mathbf{j}X_{C1} // \mathbf{j}X_{C2}$, and so, noting that $X_{C2} / X_{C1} = C_1 / C_2$, the first term can be expanded giving:

$$\frac{-X_{C2}}{\mathbf{j}R_v} + \frac{C_1}{C_2} + 1 - \frac{1}{N} = (1 + C_x / C_2)\, N\, R_0 \left[\frac{1}{R_i} + \frac{1}{\mathbf{j}X_{Li}} + \frac{1}{\mathbf{j}X_{Cix}} \right]$$

(19.9)
Balance condition

Equating reals:

$$\frac{C_1}{C_2} = \frac{(1 + C_x / C_2)\, N\, R_0}{R_i} - 1 + \frac{1}{N} \qquad (19.10)$$

Upon deletion of the factor $(1+C_x / C_2)$, this expression is the same as equation **(2.1)** for the shielded bridge. Hence, apart from the approximations made earlier, the introduction of C_x merely causes a small reduction in the apparent transformer efficiency (about 3% for the test bridge).

If we modify equation **(19.10)** by including the transformer efficiency factor k', we obtain a more general expression for the transformer constant introduced in section **5a**:

$$K_T = \frac{C_1}{C_2} = \frac{(1 + C_x / C_2)\, N\, R_0}{k'\, R_i} - 1 + \frac{1}{N} \qquad (19.10a)$$

Transformer constant

Equating imaginaries:

$$\frac{-X_{C2}}{Rv} = (1 + C_x / C_2)\, N\, R_0 \left[\frac{1}{X_{Li}} + \frac{1}{X_{Cix}} \right]$$

The frequency dependent apparent secondary inductance is now slightly different from the the quantity L_i' introduced in section **2**, because it involves C_{ix} instead of C_i, but since the apparent value of C_i is disturbed by almost every parasitic reactance in the system, there seems little point in generating a new definition. Hence, by analogy with what was done previously, we will use:

$X_i = 2\pi f L_i' = X_{Li} // X_{Cix}$

Hence:

$$\frac{1}{2\pi f\, C_2\, R_v} = \frac{(1 + C_x / C_2)\, N\, R_0}{2\pi f\, L_i'}$$

i.e.:

$L_i' = C_2 (1 + C_x / C_2)\, N\, R_0\, R_v$

i.e.:

$$L_i' = (C_2 + C_x)\, N\, R_0\, R_v \qquad 19.11$$

Notwithstanding a few small approximations, which are slightly more serious than the approximations used in deriving the perturbation series for the other parasitic effects (equation **15.1**); the only difference between this and the quadrature balance condition for a shielded bridge (equation **2.2**) is that C_2 has been replaced by $(C_2 + C_x)$.

As can be noted from all of the derivations in the preceding sections, the secondary coupled inductance L_i is a strongly conserved parameter; and so for a given transformer, the quantity $(C_2 + C_x)$ can be determined from the original model as the value to which "C_2" must be adjusted to reproduce the value of L_i obtained when a Faraday shield is present. For the test bridge illustrated above, "C_2" for the fit had to be increased by about 0.7 pF, but this difference should not be identified as C_x. If removing the shield introduces stray capacitance between the through-line and the detector port, then there must be an almost equal amount of stray capacitance between the through-line and the summing point (i.e., the other end of the transformer winding). Hence we should expect the difference to be the sum of C_x and the additional stray capacitance across C_2, i.e., if the shift is 0.7 pF, then C_x is 0.35 pF.

And so, after the analytical challenge of finding the balance condition, it transpires that the spreadsheet template for data analysis can be modified to include unshielded bridges simply by labelling "C_2" as "$C_2 + C_x$", multiplying the first term of the transformer constant by $1 + C_x / C_2$ (equation **19.10a**), and amending the series for apparent secondary capacitance. Deleting the shield-protrusion capacitance term from equation **(15.1)**, then combining it with **(19.8)** gives:

$$C_{ieff} = C_i' + C_{is} - \frac{L_h}{R_i^2} - \frac{L_2}{N R_v R_0} + \frac{L_0}{R_i R_0} - \frac{C_0 R_0}{R_i} + \frac{(N-1) C_x R_0}{R_i} + \frac{C_x C_2}{N (C_x + C_2)} \quad (19.12)$$

Sec. Load | VS network | Through-line | Direct pickup

Note incidentally, that the introduction of the 'direct pickup' capacitance C_x also provides a model for very-near-field coupling between the generator and detector. It explains an effect that was observed during the process of experimental optimisation, which was that the phase crossover frequency of the prototype bridge increased slightly when a nickel-plated connector and an RG58 cable at the receiver input were replaced by a silver-plated connector and a Belden 9880 cable (section **8**).

So now we return to the question of whether or not it is necessary to use a Faraday shield. To that, the answer is probably 'yes' if the circuit designer makes no attempt to correct for the apparent secondary capacitance, and probably 'yes' if the transformer has a large number of turns or a low value for R_i. This can be understood by differentiating the penultimate term of equation **(19.12)** above:

$$\partial C_{ieff} / \partial C_x \approx (N-1) R_0 / R_i$$

Then again, there are effects, such as the inductance of the secondary load resistor, that can make the apparent secondary capacitance negative; and given the practice of describing bijou inductorettes as 'resistors', we might be glad of something to push it the other way. An issue therefore is: 'how severe is the curvature introduced by the approximations used in deriving the model?', i.e., 'how correctable is the direct pickup effect?' An attempt to answer that question was made by correcting the bridge in various ways and analysing its performance using the method described in section **16**. The datasets for experiments carried out on the test jig are given in the spreadsheets listed below. The results for a working bridge using quadrature-current-injection neutralisation are discussed in a separate article (reference is given in the table).

No Faraday shield 1.6 MHz to 30 MHz	R_0 = 50 Ω , R_i = 50 Ω . Inductance balance coil fitted.	Max. |Z| error.	Max. φ error ( ) → best possible
testbrg61-1210.ods	Capacitor across load port [a].	±0.43%	±0.19° (±0.11°)
testbrg61-1211.ods	Herzog compensation[b].	±0.14%.	±0.11° (±0.10°)
testbrg61-13_1.ods	Phase-shift compensation[c].	±0.63%	±0.66° (±0.47°)
testbrg61-14_1.ods	Quadrature voltage compensation[d].	±0.35%	±0.05° (±0.05°)
see separate article[19]	Current injection, 3-point tracking.	±0.04%	±0.033° (±0.025°)

Notes:

a) By placing a trimmer capacitor across the load port, adjusting R_v and C_2 at 2 MHz and adjusting the inductance balance coil and the trimmer at 24 MHz, the bridge gave a phase error less than ±0.2° and a magnitude error less than ±0.5% over the 1.6 MHz to 30MHz range. Significant improvement could have been obtained by moving the upper calibration frequency to 27 or 28 MHz. The amplitude performance is not as good as was obtained from the shielded version of the bridge (section **18a**) but is nevertheless perfectly acceptable.

b) Using Herzog's compensation method, calibrating at 2 MHz and 26 MHz, the phase error was within ±0.11° and the magnitude error within ±0.14%. The amplitude performance is better than that obtained from the shielded version (section **18e**), possibly indicating partial cancellation of system non-idealities.

c) The phase shift compensation method (section **18d**) did not work properly for this test. In particular, neutralisation could only be achieved by having less Ω/turn across the auxiliary winding than across the main secondary. This was not known until the resistance was measured at the end of the test run. Increasing the auxiliary winding to 2 turns would probably have fixed the problem, but the experiment was not repeated. The interesting point about this result however, is that neutralisation can be achieved with the secondary and auxiliary loading ratios reversed. The reason is that the vector sum $\mathbf{V_a} + \mathbf{V_i}$ has its smallest lead in relation to the primary current when both windings have the same Ω/turn. The phase swings positive again when if the resistance shunting the auxiliary winding is further reduced.

d) Quadrature voltage compensation (section **18c**), using a 2-turn winding with a 250 Ω pot. across it, gave a phase error within ±0.05° and magnitude error within ±0.35%. The remarkable phase performance in this case is possibly (but not necessarily) due to cancellation of system non-idealities, i.e., it might be difficult to reproduce (but then again, it might not).

19 **A Self-evaluating precision reference bridge**. Section 8. D W Knight. http://g3ynh.info/zdocs/bridges/ .

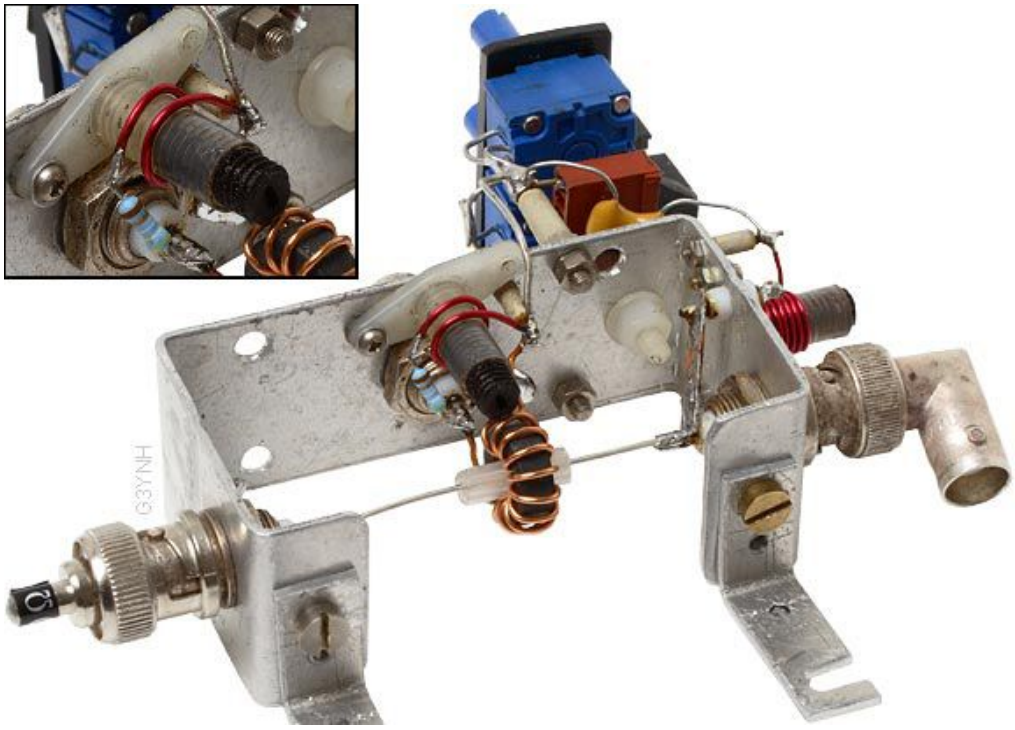

Unshielded bridge with Herzog HF compensation coil in series with the secondary load resistor. Phase error better than ±0.11°, magnitude error better than ±0.14%, from 1.6 MHz to 30 MHz (**testbrg61-1211.ods**).

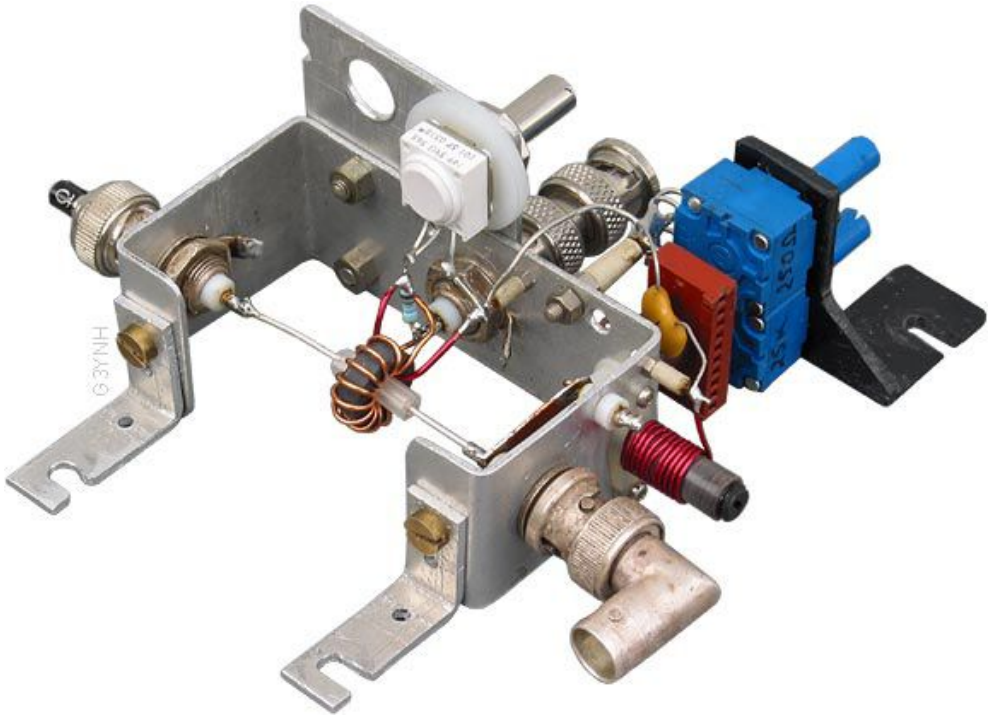

Unshielded bridge with phase-shift neutralisation (see section **18d**). The auxiliary voltage is provided by a 1 turn winding shunted by a 100 Ω Cermet variable resistor (**testbrg61-13_1.ods**). The auxiliary load resistance, measured after the test, was 3.34 Ω .

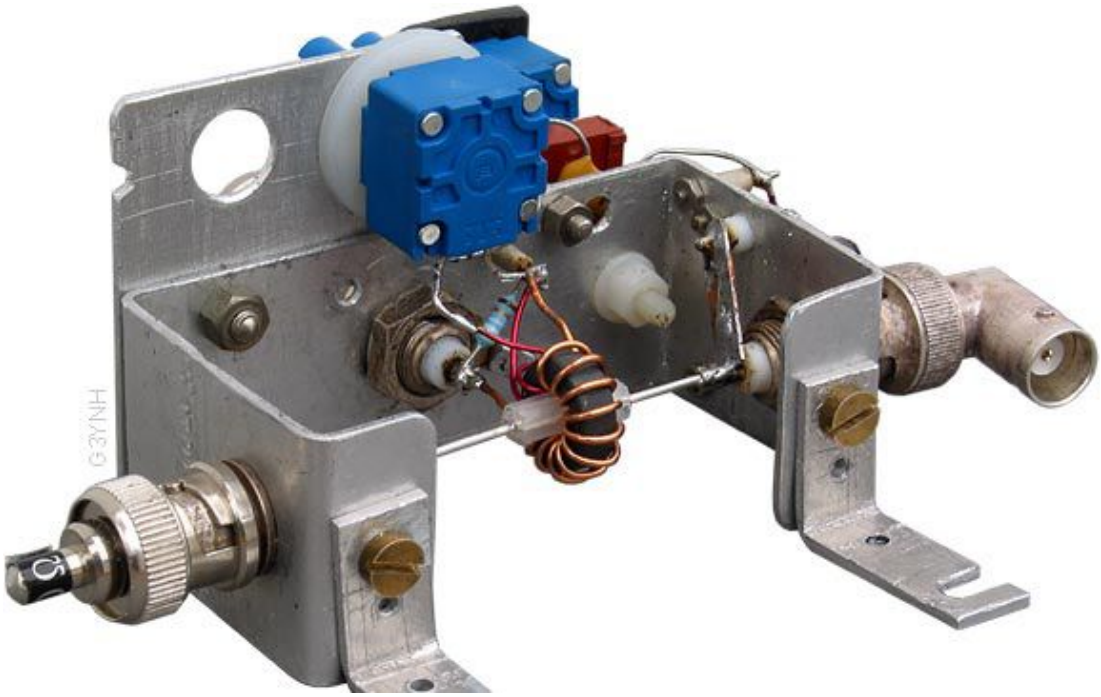

Unshielded bridge with quadrature voltage compensation. A 2-turn lightly-loaded winding produces an output at approximately +90° relative to V_i. A 250 Ω cermet pot. across the winding adjusts the output level, the resulting quadrature voltage being added to the current transformer output. Maximum phase error of this bridge is ±0.05° over the 1.6 MHz to 30 MHz range, close to the ±0.03° performance limit for type 61 ferrite and 2-point frequency tracking (**testbrg61-14_1.ods**).

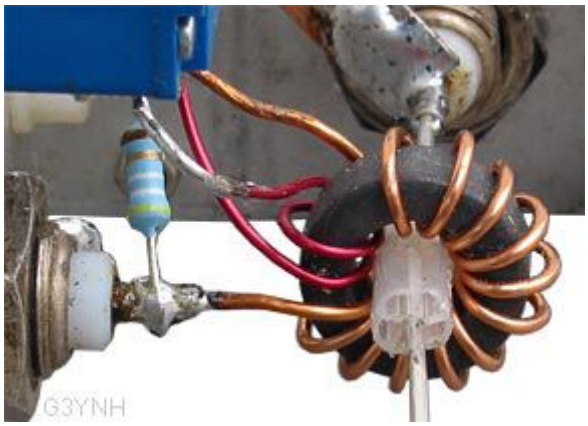

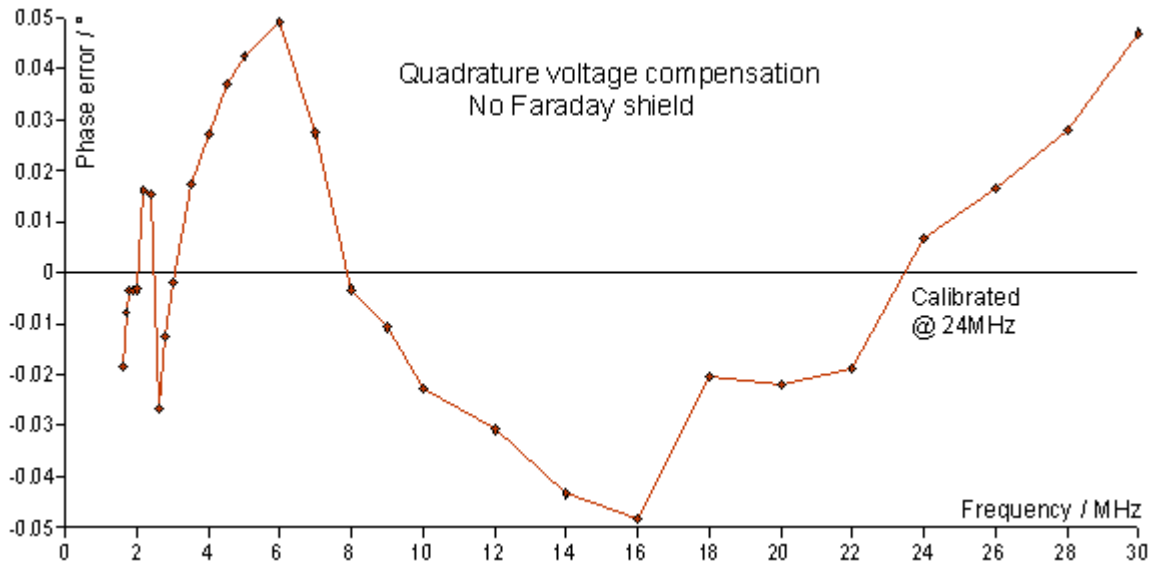

The greatest potential for phase accuracy is, of couse, given by the 3-point tracking scheme described in section **18b**. Rather than evaluating this method on the test jig; a working bridge was constructed in order to improve the circuit layout and minimise the inductance of the lower voltage-sampling arm. The result was a bridge with no Faraday shield showing a maximum phase error of ±0.03° and a maximum amplitude error of ±0.04% over the 1.6 MHz to 30MHz range; i.e., more than two orders of magnitude better than most of the impedance-monitoring bridges reported elsewhere prior to this work. The device is described in detail in a separate article. A Faraday shielded version gave practically identical results.

In summary we may note that, although the unshielded bridge has a larger effective secondary capacitance than its shielded counterpart, the correction process is no less effective. Whether the shield is redundant however, must remain moot. The following points should be considered when making a decision:

- The shield eliminates the direct pickup signal, improving the phase performance of uncorrected bridges and bridges with a low transresistance (i.e., a low value for R_i / N).

- The shield reduces the average through-line characteristic resistance.

- The circuit model for the unshielded bridge requires additional parameters, which are difficult to determine unless measurements are also made on a shielded version; i.e., the shielded bridge is easier to simulate.

- The shield gives rise to asymmetry in forward and reverse phase performance (a problem that might be solvable by using a two-hole core and earthing the shield at its mid point). Since forward-power bridges do not normally require neutralisation however, this is probably not important.

- The shield increases the physical length of the transformer assembly.

20. Final comments

The test procedures, theory and data-analysis techniques described in this article were developed without prior knowledge of the experimental conclusions. Consequently, the test-jig used was a Heath-Robinson affair and had plenty of scope for improvement. The temptation to redesign it from scratch part-way through the work was resisted in the interests of comparability between the various results.

A particular suspicion arose during the course of the work, to the effect that the parasitic inductances of the components in the lower voltage-sampling arm were limiting the achievable magnitude performance. This network has several equivalent-series-inductances; that of the variable capacitor, that of the padding capacitor, and that of the pair of variable resistors in series. These do not combine into a single frequency-independent equivalent series inductance for the whole arm, and consequently cannot be balanced-out perfectly by a single coil in the upper voltage-sampling arm. In the working bridge described in the article to follow, this shortcoming is addressed by miniaturisation and attention to layout, and results in substantial improvement.

A fairly obvious improvement to the experimental technique can also be had by building the bridge into a metal box and screwing the lid down tightly before calibrating and testing. This makes the bridge immune to the positions of the operators hands and the various tools and cables lying around, thereby improving the accuracy of calibration and reducing the amount of scatter in the evaluation data. The bridge described in the follow-on article is essentially a boxed version of the test bridge used here, and suggests an altogether better way of doing things in the event that anyone should wish to repeat or extend this work.

Whenever a mathematical derivation is carried out for the first time, the resulting exposition is not usually the most elegant. During the work described here, the pressure was to deal with the insurgence of an ever-increasing number of subtle effects, all of which had somehow to be crammed into the model. The resulting analysis template is consequently a bit of a mess. It did its job however, which was to establish and quantify all of the factors that affect bridge resistance and reactance balance to a level of about 1 part in 1000 or better. With hindsight, i.e., by knowing in advance all of the things that are important, it is possible to simplify the analysis by factoring it into separate parts, and to dispense with the need for certain approximations and difficult-to-estimate parameters. The work stands however, there is little point in repeating the data analysis; and the true test of its worth is to see whether it can inform the design of future bridges.

By following the working given in section **19**, it is possible to write down a general balance condition for bridges that have been neutralised and corrected for voltage-sampling network inductance, i.e.:

$$\frac{C_1}{C_2} + 1 + \frac{\mathbf{j}X_{C2}}{R_V} - \frac{1}{N} = (1 + C_x / C_2)\, N\, \mathbf{Z_0} \left[\frac{1}{k'\, R_i} - \frac{\mathbf{j}}{X_{Li}} \right] \qquad (20.1)$$

This is obtained from equation **(19.9)** by substituting $\mathbf{Z}_0$ in place of R_0, inserting a transformer efficiency factor (k'), and deleting the term for apparent transformer-secondary capacitance. There is no need to include the inductances of the voltage-sampling capacitors, because the inductance-balance correction cancels them out. Likewise, there is no need to include a long series of terms to account for the numerous causes of high-frequency phase error, because a phantom neutralisation term cancels them all out. The result, as is evident from the neutralisation experiments, is an extremely accurate model; which even accounts for the differences between Faraday-shielded and unshielded transformers (when a Faraday shield is used, $C_x = 0$). It separates cleanly into frequency-independent expressions for resistance and reactance balance provided that $\mathbf{Z}_0$ is purely resistive, and it can be used for circuit component-value calculations insofar as k, L_i and various

stray capacitances can be estimated.

Equation **(20.1)** might look like an obvious conclusion of this work, or even the outcome of a naive derivation based on the idea that capacitors don't have inductance and coils don't have capacitance. It contains a subtle distinction however, which unravels the problem of bridge evaluation by perturbation analysis. The trick (being discovered in one of the author's 'why didn't I think of this before' moments) is that the bridge can perfectly well be balanced when the load impedance is not purely resistive. Hence we can generalise the balance condition by replacing R_0 with $\mathbf{Z}_0 = R_0 + \mathbf{j}X_0$. The point of the perturbation analysis is to convert deviations of C_1 and R_V from their calibration settings, into equivalent deviations of load resistance and reactance in the event that the calibration is left untouched. All that is needed for that is the rate of change of R_0 with respect to C_1 (i.e., $\partial R_0 / \partial C_1$) and the rate of change of X_0 with respect to R_V (i.e., $\partial X_0 / \partial R_V$). With the reactance error X_0 appearing explicitly in the balance equation, the required derivatives are easily obtained without the need for further approximations; and it transpires that there is no need to try to estimate the strays across C_1. This simplified method of bridge evaluation is developed and used in the follow-on article.

DWK